Computational *ab initio* approaches for area-selective atomic layer deposition: methods, status and perspectives

Fabian Pieck, Ralf Tonner-Zech[a]*

Abstract

Area-selective atomic layer deposition (AS-ALD) has emerged as a transformative technique in nanotechnology, enabling the precise deposition of materials on designated substrates while preventing unwanted growth on adjacent surfaces. This capability is critical for applications in microelectronics, catalysis, and energy technologies. Computational methods, particularly density functional theory (DFT), are indispensable for uncovering the mechanisms underlying AS-ALD, providing insights into surface interactions, selectivity mechanisms, and precursor design. This review introduces the theoretical background of computational techniques applied to AS-ALD and provides a detailed overview of their applications. Special emphasis is placed on the use of *ab initio* methods to explore surface chemistry, optimize precursor and inhibitor properties, and improve selectivity. A comprehensive overview of the literature is given with an analysis of research questions targeted, and methods used. By consolidating the state of knowledge and identifying future challenges, this work aims to guide researchers in further leveraging computational approaches to drive innovations in AS-ALD processes.

Keywords

AS-ALD, computational modelling, density functional theory, first principles, area-selective atomic layer deposition,

---

[a] Dr. Fabian Pieck, Prof. Dr. Ralf Tonner-Zech

Wilhelm-Ostwald-Institut für Physikalische und Theoretische Chemie, Leipzig University, Linnéstr. 2, 04103 Leipzig, Germany
e-mail: ralf.tonner@uni-leipzig.de, ORCID: 0000-0002-6759-8559
e-mail: fabian.pieck@uni-leipzig.de, ORCID: 0000-0001-6912-2725

1 Introduction

1.1 What is AS-ALD and why is it important?

"There is plenty of room at the bottom." The famous statement by Feynman emphasizing the not yet realized potential of nanotechnology is also true for the ongoing downscaling of devices in microelectronics.[1] While the gate length in transistors was 50 µm in the mid-1960s, the smallest features in currently produced chips are approaching 1 nm.[2] The result is requiring an unprecedented accuracy in fabrication which still mostly relies on "top-down" techniques like etching, using elaborate and very expensive setups.[3] This creates the possibility for "bottom-up" techniques to become competitive. One of the major approaches here is atomic layer deposition (ALD) which uses self-limited surface chemistry to produce thin films with precise thickness.[4–10] Here, a key feature of ALD is the separation of the reactive species in the gas phase which is achieved by pulsing only one reactive species in the reaction chamber at a time (Fig. 1.a). Once all species are added, one ALD cycle is completed, while repetition of ALD cycles leads to material deposition. Over the last decades, efficient ALD processes have been developed for a large range of materials on a diverse set of substrates.[11]

Increasingly, the demand is not only for well-defined thicknesses but also for selectivity in deposition. This results from the requirement to deposit material on one growth surface (GS) while a neighboring non-growth surface (NGS) is left clean (Fig. 1.d). One key application for this area-selective ALD (AS-ALD) process is the fully self-aligned via (FSAV) - a key component in microelectronic circuits (Fig. 2.).[12] Ideally a via connects two metal lines in different layers of the microelectronic circuit while being perfectly aligned to the top and bottom line as shown in Fig. 2. However, creating vias with top-down approaches can lead to edge-placement errors (Fig. 2.b).[1,13,14] These errors can promote electron tunneling resulting in a loss of device functionality. As a solution, edge-placement errors can be prevented by the high deposition accuracy of AS-ALD processes and the introduction of FSAVs (Fig. 2.c,d).[8] In 2021, TSMC demonstrated the use of AS-ALD to achieve such a via with the goal of interconnect expansion beyond 3 nm nodes.[12] As a different target application, the possibility to deposit material in complex 3D structures is providing opportunities for AS-ALD, e.g., in modern memory devices.[15]

Beyond microelectronic technology, (AS-)ALD is used in fields like catalysis, solar cells or battery research.[9,16–21] Furthermore, AS-ALD has been combined with top-down patterning approaches, e.g. in the case of TiO_2 where the selective deposition is used for tone inversion and resist hardening.[22] The major challenge in AS-ALD is achieving (near-)perfect selectivity for a high number of ALD cycles. Usually, this is determined by the ratio of material deposited on the GS in comparison to the material deposited on the NGS (Fig. 1.g). A more detailed discussion is found in section 0. This goal can be achieved through a variety of routes which can be categorized as: (i) intrinsically selective (Fig. 1.d), (ii) area-activating (Fig. 1.e) and (iii) area-deactivating (or inhibitor-based, Fig. 1.f) approaches. All these approaches rely on an in-depth understanding of deposition and surface chemistry to analyze and improve the selectivity for a given process. For example, the precursor can chemically modify the inhibitor layer and thus lead to growth on the

NGS. Or the co-reactant modifies the NGS to make it susceptible for the precursor in the next ALD step. Therefore, the chemical interactions between all components are crucial for achieving selectivity: precursor, co-reactant, surface and inhibitor or activator.

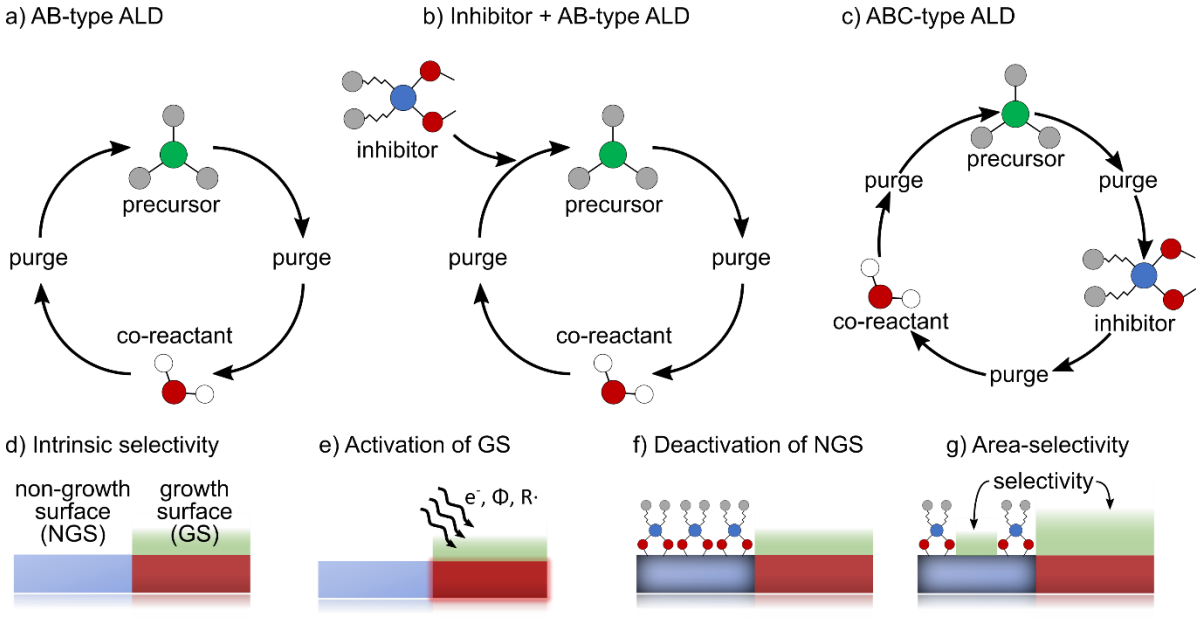

Fig. 1. Schematic illustration of the AS-ALD process. This can be done via an AB-type ALD process (a) without or (b) with an initial inhibitor deposition or (c) an ABC-type process including inhibitor redosing. Selectivity can be obtained based on (d) intrinsic selectivity, (e) activation of the growth surface, (GS) or (f) deactivation of the non-growth surface (NGS). Here, selectivity is defined as (g) the relative deposition on GS in contrast to the NGS.

Thus, a microscopic understanding of the chemical interactions in the system is crucial for optimization of the AS-ALD process and achieving the best possible selectivity. This is where computational approaches play a key role. Computational chemistry as a research field uses methods from theoretical chemistry to solve research questions in the chemical sciences. While a more detailed discussion of the methods used in AS-ALD modelling is presented in section 0, a brief overview is provided as orientation for the reader at this point supported by Fig. 3. Computational methods can be categorized in static and dynamic approaches. Static approaches solve the underlying equations for one point in time while dynamic approaches describe the development of a system over a given period. Another distinction concerns the description of the interaction between the fundamental components of the chemical system (nuclei and electrons). This can either be a description using classical mechanics (using Newton's equations of motion) or quantum mechanics (using the Schrödinger equation). The quantum mechanical approaches describe electrons explicitly and typical examples are density functional theory (DFT) and wavefunction-based methods (e.g., Hartree-Fock (HF)). Molecular dynamics (MD) approaches can then either use classical potentials to describe the interactions of nuclei (classical MD) or quantum-mechanical potentials (*ab initio* or AIMD). More recently, machine learning (ML) has been used as a new paradigm to generate interaction potentials (MLP). Approaches spanning more than one regime of time scales and system sizes shown in Fig. 3. are termed multiscale modelling.

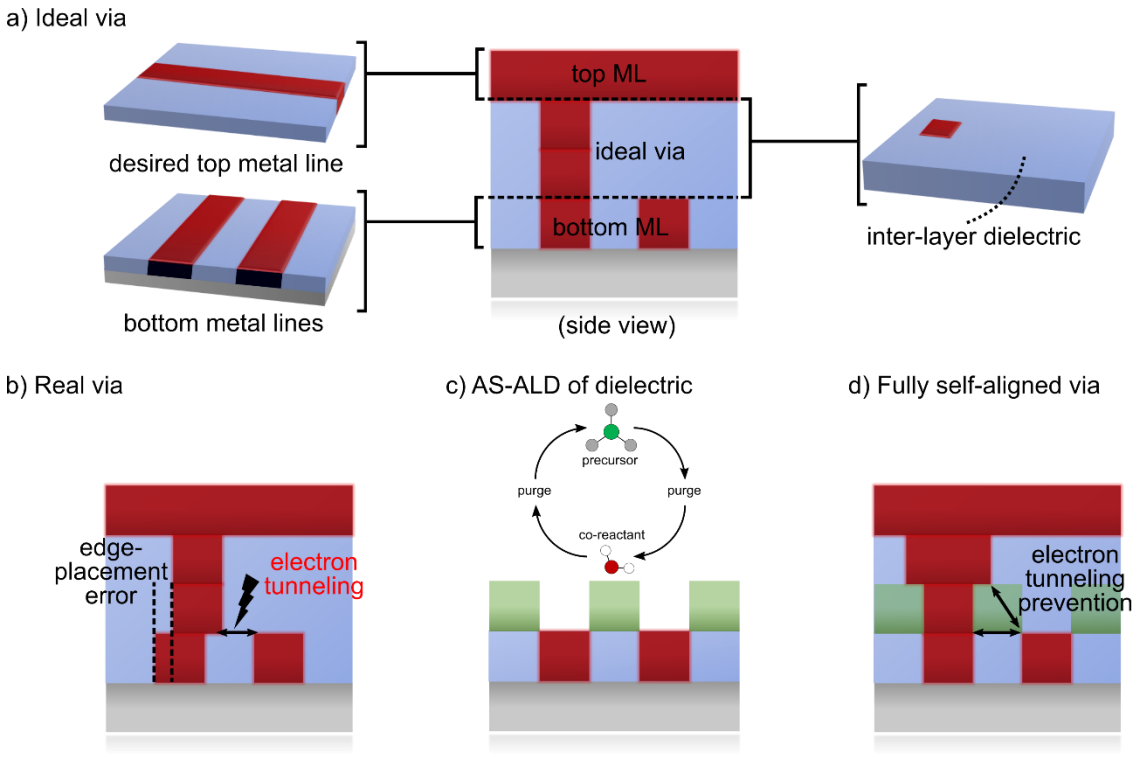

Fig. 2. An ideal via perfectly aligns with the top and bottom metal lines (red) (a). Insufficient alignment results in an edge-placement error (b). The fully self-aligned via can be achieved via a dielectric-on-dielectric deposition (green on blue) with AS-ALD (c) prior to the via buildup (d).

While MD approaches can tackle nanosecond timescales at best, real ALD processes take place on timescales of seconds or minutes. To capture this theoretically, the above-mentioned approaches are not suitable. Here, methods for solving sets of rate equations can be used. Most prominent in ALD is the stochastic approach of using a Monte Carlo (MC) ansatz to solve kinetic rate equations (kinetic MC or kMC). This approach can then use input from quantum mechanical approaches (reaction barriers and energies) which effectively makes it a multiscale (more precisely two-scale) approach. If no information about barriers is available, a stochastic approach of surface adsorption can be applied which uses information like van-der-Waals volume of adsorbates and surface reactive sites to provide the change in surface coverage during the ALD process. These MC approaches are currently in increasing usage in AS-ALD modelling.

AS-ALD is experimentally carried out in a reactor which is mostly neglected in the modelling. Although the gas phase chemistry is much less important in ALD compared to chemical vapor deposition (CVD) and similar approaches, the flow mechanics can be important, e.g., for fast surface reactions which are diffusion-limited.[23] Modelling these phenomena requires approaches that do not rely on the chemical structure of the system anymore but instead solve coupled rate equations, like computational fluid dynamics (CFD) or finite-element (FE) methods. The coupling of such large-scale approaches to kMC, AIMD or DFT in a multiscale ansatz has been a long-standing goal (not only) of the ALD community and some progress is visible.[24]

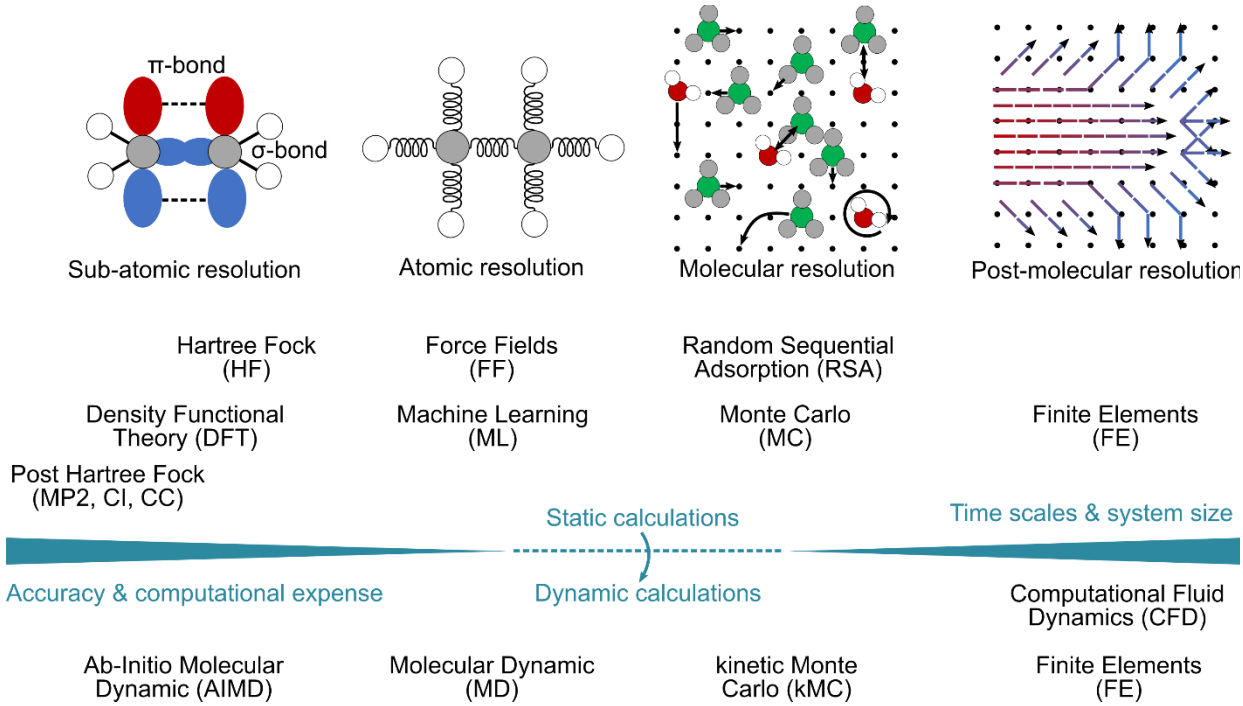

Fig. 3. Overview of modelling approaches used for AS-ALD divided into static and dynamic calculations and sorted by typical time scales and system sizes. Accuracy increases to the left.

The most heavily used (quantum chemical) computational method in AS-ALD modelling is DFT. It provides a detailed description of the electronic structure and chemical reactivity but is efficient enough to handle systems of a few hundred atoms. This enables the *ab initio* description of surface chemistry which determines selectivity.

This review now aims at summarizing the computational work in the field of AS-ALD with a focus on *ab initio* methods. It provides an overview for the non-specialist of which methods are available and which questions in AS-ALD can be targeted with those methods. A comprehensive overview of the literature is given together with a perspective on current developments and a "wish-list" of developments for the future. This will enable experts and non-experts alike to judge the suitability of using computational methods in their research in the field of AS-ALD. The aim is thus to broaden the already expanding scope of computational methods in this field and motivate researchers to use them where suitable. In the spirit of a previous review on computations in (non-area-selective) ALD by Elliott, the emphasis is that the threefold aim of computational work to validate, explain and predict should be the target:[25] Validating the accuracy of the computational methods, explaining experimental findings and ultimately moving on to predicting new chemistry in AS-ALD and thus contributing to further innovations in this field.

1.2 Scope of this review

The focus of this review is a comprehensive overview for the use of *ab initio* methods to deliver insight for AS-ALD with some notes on methods that are based on results from these methods (e.g., kMC). Reviews on other theoretical approaches (classical mechanics and coarse graining,

classical nucleation theory, CFD, etc.) can be found elsewhere.[26,27] Also the literature on other deposition processes like area-selective CVD is not covered.[28] Note, that some of the AS-ALD principles explicated within this work, have been summarized before.[6,8,9,29] Since modelling for such complex chemical phenomena requires close interplay to experimental studies, this fruitful interaction has also been covered before.[30–33] Of course, the knowledge gained in this field often builds on insights gained from previous work on (non-area-selective) ALD. In this context several reviews are available, e.g., on the history of ALD,[34] the principles of ALD,[35–38] or on precursor design.[39,40] The modelling aspects of ALD have also been summarized comprehensively.[25,41–45] A very helpful database of manuscripts and reviews in the field of ALD has been compiled and is continuously updated.[11] Recently, AS-ALD has become the focus of perspectives and overview articles. One perspective shows several crucial aspects for inhibitor selection in area-deactivation approaches and especially outlines for the first time clearly the importance of interaction between inhibitor and precursor.[46] The surface chemistry perspective has been chosen in a more recent review on selection criteria for inhibitor-based AS-ALD.[47] Also, the upcoming application of AS-ALD in industry has been summarized outlining the key role of modelling here.[48] Shong et al. published a perspective on theoretical design strategies for precursors in AS-ALD showcasing what theory can bring to the field.[49]

What is still lacking is a comprehensive review of computational approaches to the field of AS-ALD outlining the perspectives and challenges which is the goal of this review.

1.3 Approaches to AS-ALD

In setting the stage, the different approaches to achieving selective deposition are briefly summarized (Fig. 1.) and it is outlined which key challenges they represent for computational modelling.

1.3.1 Intrinsically selective AS-ALD

In this approach, the different reactivity of two substrates with regard to the precursor is used to achieve selectivity. It has also been called “substrate-specific ALD”[50]. This can be achieved using chemically different surfaces (e.g., Cu and SiO_2[51]), different surface terminations of the same material (e.g., H-Si and HO-Si[52,53]) or different facets (e.g., Pt(100) and Pt(111)[54]). It has long been known in the ALD community that growth depends on surface type and termination.[50,55,56] The Parsons group then first used this concept specifically to achieve selective ALD growth between two substrates.[57–59] Among others, the Chen group extended the concept considerably until today.[48] The key advantage of intrinsically selective AS-ALD is that no new chemical species is introduced. This is beneficial for complex application environments where contamination and simplicity of production plays a key role.[48] The disadvantage is the limitation in terms of suitable material combinations. Furthermore, it is important to control the surface termination for selective reactivity.[56] Often, this approach is combined with selectivity-enhancing post-treatment (section 1.3.4). A variation of this idea uses different diffusion coefficients on GS and NGS to achieve selectivity (section 4.8).[25] The difference in surface properties like electric

resistivity has also been exploited.[60] The main computational challenges for intrinsically selective AS-ALD are:

(i) Tune the differences in precursor reactivity on GS and NGS
(ii) Find the optimal combination of surfaces
(iii) Identify a suitable set of surface terminations or facets

In all cases, the goal of the computational approaches is to maximize the difference in thermodynamic and kinetic driving forces for the surface reactions of the precursor and/or the co-reactant between GS and NGS. Some theoretical studies argue with thermodynamic differences, most use differences in reaction barriers to explain selectivity differences (Tab. 2).

1.3.2 Area-activating AS-ALD

In this approach, the GS is activated by some pre-treatment to make it more reactive towards the precursor and/or co-reactant. This approach has first been put forward by Mackus et al.[61] The pre-treatment mostly comprises:

(i) Plasma or electron-beam exposure (also termed "direct-write" ALD)[61,62]
(ii) Chemical treatment (e.g., creating reactive sites at the surface)[63]

After the pre-treatment step, the approach is essentially inherently selective AS-ALD since the selectivity is determined by the relative reactivity of the precursor/co-reactant with the GS and NGS. Computational approaches can thus be used to:

(i) Understand the surface structure after the activation step
(ii) Tune precursor differences in reactivity on activated GS and NGS

This approach has similar advantages to the intrinsically selective ansatz since it does not introduce a new chemical species. However, the activation step must be compatible with envisioned production setups and surface roughness or inhomogeneities can be an issue.

1.3.3 Area-deactivation or inhibitor-based AS-ALD

In this approach, a new chemical species is introduced to enhance selectivity: the inhibitor (Fig. 1.b,c). The core idea of an inhibitor-based approach is to block the NGS, while the GS is not blocked. While approaches using polymer films exist,[6] most current approaches use molecular inhibitors comprised of a surface-anchoring head group and a deposition-blocking tail group (Fig. 4.). If a long chain is used as tail group, the resulting structures are called self-assembled monolayers (SAMs, often the term is also used for the monomers). If a short chain is used, the term small-molecule inhibitor (SMI) is established in the literature. As is obvious from Fig. 4., the two inhibitor classes have strong similarities in their approach to block the surface. Indeed, both classes were proposed in the same seminal work by Chen, Kim, McIntyre and Bent in 2004.[64] Prior to this work, SAMs were only used in microcontact printing for patterned deposition of ZnO[65] and TiO_2.[66] Although the term SMI does not yet appear, the concept of varying the chain length to change the blocking property has already been established in this key paper[64] and the methoxy-substituted "short chain SAM" $Si(CH_3)(OMe)_3$ proposed was used for successful AS-ALD much later.[67] Also, the major blocking mechanisms (Fig. 5.) had already been outlined

in this study: reactive surface site deactivation (Fig. 5.b) (here: bonding to HO-Si and Si-O-Si groups) as well as steric blocking (Fig. 5.c,d). The targeted usage of small molecules (in contrast to SAMs) for the blocking of NGS has been put forward by Mameli et al. inspired by work from Yanguas-Gil, Libera and Elam.[68,69] The main challenges for computational approaches here are:

(i) Find an optimal inhibitor that blocks NGS but not GS

(ii) Identify a precursor that reacts with GS but does not decompose or penetrate the inhibitor layer

(iii) Understand the factors governing stability of the inhibitor layer

Chemically, this is the most complex approach but its tunability to various material combinations (including the possibility to block several NGSs with one inhibitor[70] or the usage of precursors as inhibitors[71]) lead to strong research activity here. Given the major role of surface chemistry in determining selectivity in this approach, computational approaches are especially useful for these inhibitor-based approaches (section 3.4).

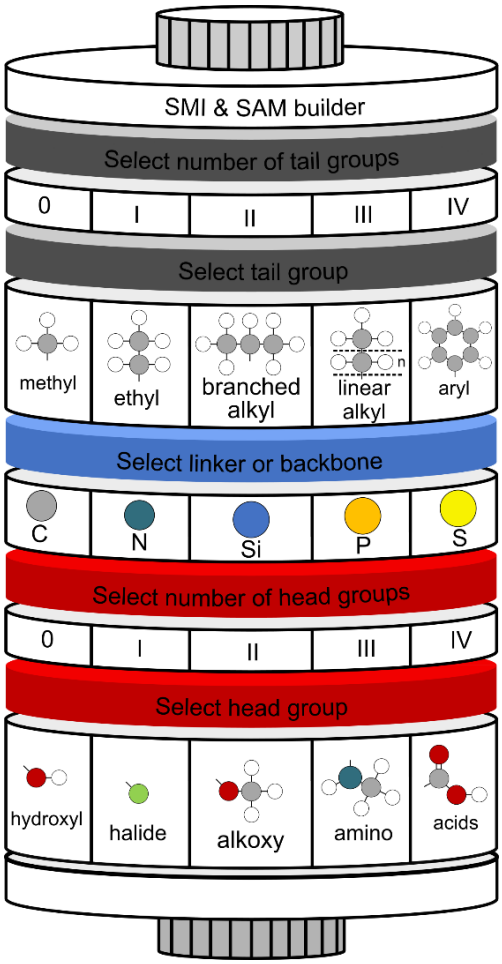

Fig. 4. Schematic illustration of the structure of small molecule inhibitors (SMI) and molecules forming self-assembled monolayer (SAM) in use for AS-ALD.

1.3.4 Post-treatment to improve selectivity

Selectivity achieved by any of the approaches outlined is never perfect. Yet, many applications – especially in the field of microelectronics – require very high selectivity. Thus, several ways to improve it have been put forward. [8] These include:

(i) Repeated application of the inhibitor as multiple exposure approaches, or even ABC-type ALD cycles where the inhibitor is reapplied in every ALD cycle (Fig. 1.c)

(ii) (Repeated) chemical etching or plasma treatment steps to remove unwanted material on the NGS (also implemented as atomic layer etching, ALE, approaches[72])

Although these approaches sometimes rely on surface chemistry, they are often not suitable as a target for computational approaches due to the time and length scales involved. An exception is ALE which will not be covered here.[73] Accordingly, computational approaches to post-treatment steps will not be considered further.

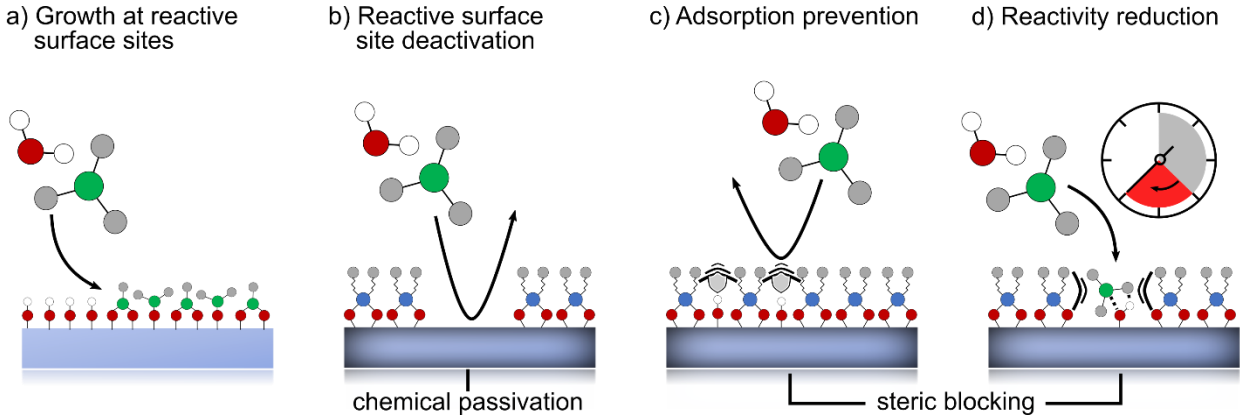

Fig. 5. Illustration of AS-ALD blocking mechanisms. In (a) an unprotected surface is shown as comparison, where reactive sites lead to material deposition. Blocking is achieved by (b) passivating these reactive surface sites (also called chemical passivation[74]), (c) preventing precursor and co-reactant adsorption to a reactive site or (d) slowing down the reactivity at the reactive sites favoring the desorption of all adsorbates. As (c) and (d) are caused by steric repulsion, these effects are usually combined under the term steric blocking.

1.4 Important concepts

Several concepts are central to discussing AS-ALD and will thus be introduced here.

1.4.1 Nomenclature

Since some of the established nomenclature in AS-ALD research is not always used in the same manner, the choices for this review are initially outlined. It has been discussed before that in AS-ALD the "substrate" is the more accurate term than the "surface". The reason is that the surface changes its chemical composition during the process. Thus, while initially an SiO_2 surface is found for the ALD reaction of Al_2O_3, the surface transitions towards an Al_2O_3 surface step by step. Therefore, "substrate" is used here to express the general surface site exposed during the ALD cycle. The term "surface" is used only when it clearly refers to a clean and chemically uniform entity. ALD consists of two half-cycles of reactions (Fig. 1.a). It is common practice to use the

word “precursor” for the adsorbate carrying the (non-oxygen) element to be deposited, while “co-reactant” is used for the second adsorbate. While arguments have been put forward that this expression can be misleading,[75] the established nomenclature precursor and co-reactant will be used here. The term co-reactant also applies to the plasma in such ALD experiments. To avoid the clumsy term “precursor and/or co-reactant”, often only precursor is used in the text. In inhibitor-based approaches, the resulting substrate termination is often called the “blocking layer”. Here, the expression “inhibitor layer” is used instead to avoid confusion with two terms for the same aspect.

1.4.2 Thermodynamic and kinetic driving forces

A successful thermal ALD process usually requires a thermodynamic driving force, i.e., being exergonic as shown by a negative Gibbs free reaction energy ΔG_r (eq. 1.1) for all reaction steps. Exceptions are the growth of metastable materials[76] and ALD processes using continuous energy input (e.g., plasma ALD).[77]

$$\mathrm{A} + \mathrm{B} \rightarrow \mathrm{C}\,, \Delta G_r < 0 \qquad 1.1$$

The thermodynamic signature is closely connected to the so-called “ALD window” (Fig. 6.) which determines the temperature window where a certain ALD process is successful (Fig. 6.c).
The ALD growth reaction (Fig. 6.c) always competes against unwanted side reactions like condensation (Fig. 6.a) unreactive diffusion of adsorbates (precursors/co-reactants) (Fig. 6.b), decomposition (Fig. 6.d) or desorption (Fig. 6.e). This can be the result of a higher thermodynamic driving force for these side reactions either by more negative enthalpy (ΔH) or higher entropy gain (ΔS, contribution to ΔG_r is temperature-dependent, eq. 1.2).

$$\Delta G_r = \Delta H + T \cdot \Delta S \qquad 1.2$$

One goal of a computational investigation is thus to determine ΔH, ΔS and ΔG_r for a set of ALD reactions. As a first approximation, the reaction energy (ΔE_r) is often used instead of ΔG_r. These electronic energies result directly from *ab initio* computations and neglect zero-point vibrational energy, temperature and pressure effects (T = 0 K, p = 0 bar). This approximation must be used with care in ALD modelling due to the elevated temperatures and low pressures which can both affect the entropy contribution strongly. The common approach to move from ΔE_r to ΔG_r is the rigid-rotor harmonic oscillator (RRHO) approximation which is rooted in statistical thermodynamics. This approach introduces efficient approximations for translational (trans), rotational (rot), vibrational (vib), and electronic (elec) contributions to H and S (eq. 1.3, eq. 1.4). Here, the electronic energy (E_{QM}) based on an *ab initio* calculation is one major contribution to the enthalpy. In practice these terms are often formulated as corrections to the inner energy U. In these cases, enthalpy is derived based on $H = U + k_B T$.

$$H = H_{trans} + H_{rot} + H_{vib} + H_{elec} + E_{QM} \qquad 1.3$$

$$S = S_{trans} + S_{rot} + S_{vib} + S_{elec} \qquad 1.4$$

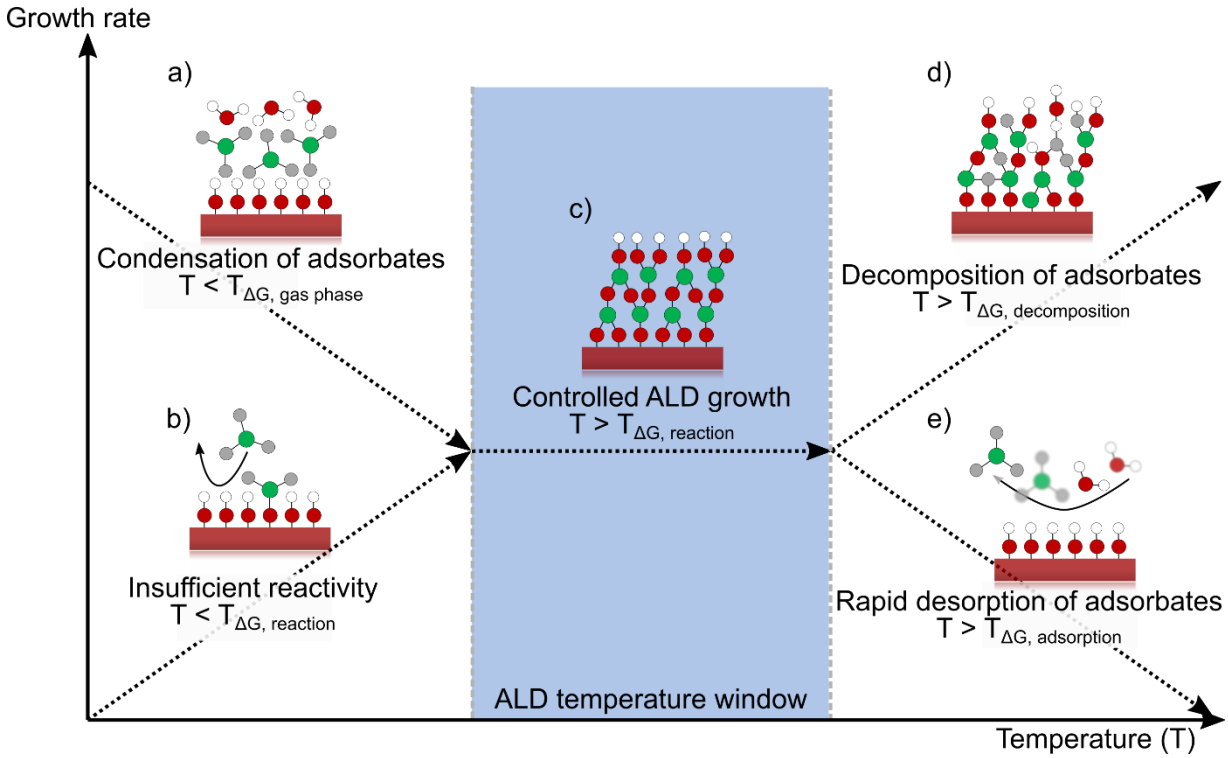

Fig. 6. Schematic representation of the ALD window. At low temperatures (T), condensation of adsorbates (precursor or co-reactant) (a) or incomplete reactivity (b) dominates, as the energy required to maintain adsorbates in the gas phase (ΔG, gas phase) or to overcome reaction barriers (ΔG, reaction) is insufficient. At the optimal T range (c), reaction barriers are effectively surmounted, enabling successful ALD deposition. At too high T, undesired outcomes such as adsorbate decomposition (d) or rapid desorption (e) occur, as the supplied energy surpasses the thresholds for side reactions (ΔG, decomposition) or adsorption (ΔG, adsorption).

Within the RRHO approximation, every component of eq. 1.3 and eq. 1.4 is formulated based on its partition function and the ideal gas law. In consequence, only the harmonic vibrational frequencies of the system and E_{QM} have to be calculated by *ab initio* methods. With more complex approaches even anharmonic corrections to the vibrational terms can be included.[78] However, due to the computational expense of this method this is mostly unfeasible for surface chemistry questions. The reaction barrier is the second major factor determining the ALD reactivity and even more so the selectivity in AS-ALD. If transition state theory (TST) is assumed to be applicable, the reaction rate k of the chemical reactions in the ALD process can be determined directly from the reaction barrier $\Delta G^{\ddagger}$ via the Eyring equation (eq. 1.5). The prefactor A can then either be determined from experience (or assumed to be the same for all competing reactions) or it can be computed via TST (qq-TST).[79,80] There are possibilities to move beyond the TST picture by capturing effects like reaction probability, but they are usually out of scope for investigations of ALD chemistry.

$$k = A \cdot \mathrm{e}^{-\frac{\Delta G^{\ddagger}}{RT}} \qquad 1.5$$

Determining relative reaction rates is crucial for AS-ALD since the competing reactivity on GS and NGS is the defining factor for selectivity. Results of thermodynamic computations are thus important for screening of several possible AS-ALD reactions but not sufficient to determine

selectivity.[81] One approach used in catalysis to avoid the computation of reaction barriers is making use of the Bell-Evans-Polanyi (BEP) principle. It states that there is a correlation between thermodynamic driving forces and barrier heights for a set of similar reactions (i.e., a more thermodynamically favorable reaction (strong negative ΔE) has a lower barrier (moderate $\Delta E^{\ddagger}$)) and thus allows to approximate reaction barriers by assuming the same prefactor (eq. 1.5) and the same position of the transition state on the reaction coordinate for all reactions considered. For (AS-)ALD, it has not been checked systematically, if the BEP is a good approximation. Initial findings that the Hammond postulate, which gives similar statements, is true for SAM decomposition were reported already by Xu and Musgrave.[82] There are AS-ALD studies assuming the BEP to hold.[83]

1.4.3 Selectivity

The crucial factor determining a successful AS-ALD process is selectivity. This means a measure of how much material *m* is deposited on the GS relative to the NGS. Most commonly selectivity is defined as

$$S = \frac{m_{\mathrm{GS}} - m_{\mathrm{NGS}}}{m_{\mathrm{GS}} + m_{\mathrm{NGS}}}. \qquad 1.6$$

The equation has originally been proposed by Gladfelter for selective CVD[84]. It has been derived for rate constants initially and Gladfelter showed that it can be used with coverages of GS and NGS.[84] In the AS-ALD literature, however, several other approaches were developed to quantify the selectivity by quantities that are experimentally accessible. Mostly, "amount of material grown" is used instead of coverages (which are hard to determine experimentally). This amount is then determined as thickness, which is experimentally obtainable: (i) via the relative intensity of X-ray photoelectron spectroscopy (XPS) signals[85], energy-dispersive X-ray spectroscopy (EDS) mapping[86] or as „substrate-normalized concentration"[87]; (ii) via ellipsometry[88]. Ultimately, the selectivity is calculated as[46]

$$S_x = \frac{R_{\mathrm{GS}} - R_{\mathrm{NGS}}}{R_{\mathrm{GS}} + R_{\mathrm{NGS}}}. \qquad 1.7$$

Here, S_x is the selectivity after *x* number of ALD cycles and *R* is the atomic composition of the deposited material on GS and NGS, respectively. Hence, the value ranges between 0 (no selectivity) to 1 (perfect selectivity). Comparison to computational data is possible, e.g., through the theoretical determination of relative reaction rates. Similar to the ALD window discussed above, a "selective ALD window" has been proposed.[33] The typical reason behind selectivity in AS-ALD is nucleation delay on the NGS due to the mechanisms discussed below in more detail.[89] However, selectivity can also be achieved via substrate-dependent diffusion (section 4.8).[89]

1.4.4 Selectivity loss

Ideally, the AS-ALD process stays selective for an unlimited number of cycles. In reality, several factors influence the loss of selectivity during deposition (Fig. 7.):

(i) Finite nucleation delay (i.e., the number of ALD cycles where no growth happens) on NGS and unwanted start of growth (Fig. 7.a)

(ii) Disintegration of inhibitor layer in area-deactivation processes due to desorption or chemical reactions (Fig. 7.b)

(iii) Penetration of inhibitor layer by precursors and reaction with unpassivated surface groups (Fig. 7.c)

(iv) Overgrowth of inhibitor layers (Fig. 7.d)

The mechanisms of blocking and unwanted growth on the NGS have been analyzed under ALD conditions with experimental approaches.[90–96] An analytical model has been proposed fitting experimental data to a set of parameters with the goal to gain insights into possible selectivity-reducing mechanisms.[97] It will be shown that computational approaches can complement and complete this picture. The onset of "loss of selectivity" has been defined by Parsons for a value of $S < 0.9$ (eq. 1.7).[97]

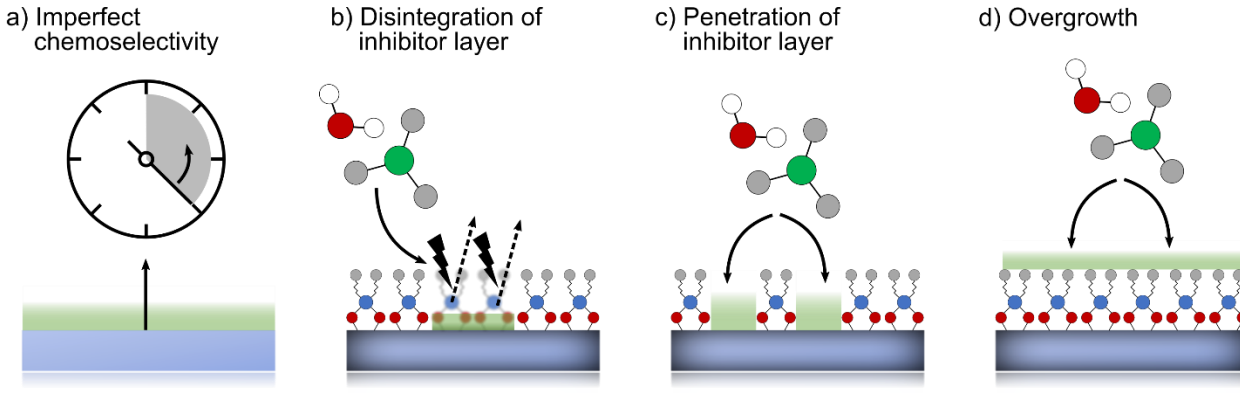

Fig. 7. Mechanisms resulting in a loss of selectivity. (a) Imperfect chemoselectivity leads to limited nucleation delay in intrinsically selective AS-ALD. The usage of inhibitors is limited by (b) the disintegration of the inhibitor layer due to reactions with precursor or co-reactant, (c) penetration or (d) overgrowth of the inhibitor layer.

2 Computational methods for AS-ALD

This chapter outlines the main computational methods used in the modelling of AS-ALD. This introduction is targeted at a non-specialist audience. For further detailed information, reviews and textbooks on the topic are available.[98–100] An overview of the methods presented and how they are connected and related is given in Fig. 3. in the introduction.

2.1 Density functional theory

DFT is the most heavily used method not only in AS-ALD but in computational materials modelling in general.[101] This is due to the accurate description of electronic structure while maintaining a moderate computational effort. This consideration of "accuracy" vs. "cost" (= computational resources and time required) is the decisive criterium in computational modelling.

2.1.1 Theory

The foundation of DFT is formed by the two theorems formulated by Hohenberg and Kohn in 1964.[102] Their core idea was to use the electron density ρ as the central quantity in formulating their theory of electronic structure in contrast to using the wave function (section 2.2). Previous approaches by Thomas and Fermi have already been formulated in 1927 but due to the use of classical terms for electron-electron interaction and the kinetic energy of the electrons, covalent bonding could not be described accurately. The first Hohenberg-Kohn theorem states that the total ground energy E_0 of a system is a unique functional of the electron density:

$$E_0[\rho_0] = T[\rho_0] + V_{\mathrm{ee}}[\rho_0] + V_{\mathrm{ne}}[\rho_0] \qquad 2.1$$

Here the contributions are the kinetic energy of the electrons $T[\rho_0]$, the potential energy from electron-electron repulsion $V_{\mathrm{ee}}[\rho_0]$ and the potential energy from electron-nuclear attraction $V_{\mathrm{ne}}[\rho_0]$. A functional is a function where the argument is again a function (while the argument in a function is a scalar quantity). Since the electron density is a function of the cartesian coordinates (i.e., it varies at different points in 3D space), this makes the energy a functional of ρ. This theorem allows to compute the energy and all properties of a system just by knowing the electron density. The second theorem is the DFT variant of the variational principle (see section 2.2.1). It states that only the exact ground state density ρ_0 results in the ground state energy E_0 and every other density delivers higher energies. This gives an idea of how to search for the ground state density: just check if the energy lowers upon changing a test density. These theorems however do not lead to a practically useful method since there is no systematic way to vary a density. This goal was achieved a few years later by Kohn and Sham (KS).[103] They formulated the energy functional as in eq. 2.2.

$$E_{\mathrm{KS}}[\rho] = T_{\mathrm{KS}}[\rho] + J_{\mathrm{ee}}[\rho] + E_{XC}[\rho] + V_{\mathrm{ne}}[\rho] \qquad 2.2$$

They realized that the quantitatively most important term in the energy functional (eq. 2.1) is the kinetic energy of the electrons $T[\rho]$. If an error is introduced here, it results in a large numerical error in the energy. Their core idea was now to approximate this kinetic energy $T[\rho]$ by the kinetic

energy $T_{\mathrm{KS}}[\rho]$ of a model system which contains independent electrons (i.e., the electron-electron interaction V_{ee} in this system is zero) but – by definition – delivers the same density as the real system to be solved. The clue is that the kinetic energy for such a KS model system can be computed exactly by using orbitals φ (= one-electron wavefunctions) as shown in eq. 2.3. T_{KS} is a pretty good approximation to the actual kinetic energy *T*.

$$T_{\mathrm{KS}} = -\frac{1}{2}\sum_{i}^{N}\int \mathrm{d}\vec{r}\ \varphi_i^*\,\nabla^2\,\varphi_i \qquad 2.3$$

Two more terms in eq. 2.2 can be accurately formulated: the electron-nuclear attraction (V_{ne}, called the 'external potential' in DFT language) and the classical Coulomb interaction between the electrons (J_{ee}). The only terms to be approximated now are: the difference between the kinetic energy of the KS system and the actual real system ($T - T_{\mathrm{KS}}$) and the electron-electron interaction terms which arise from the quantum nature of electrons: the "exchange" term (E_X) as a result of the Pauli principle and the "Coulomb" (E_C) term resulting from the fact that electrons are not point charges (which is captured by *J*) but have a probability distribution in space which depends on all other electrons. These last three terms are summed up in the exchange-correlation functional (E_{XC} in eq. 2.2). DFT is an exact theory up to this point and the approximations arise since the exact form for E_{XC} is unknown (it is even "unknowable"[104]). Furthermore, although DFT is a theory based on electron density, orbitals are reintroduced in the KS-approach (which underlies the vast majority of all published DFT data). Although this introduces a degree of arbitrariness which was heavily discussed in the literature previously, it allows to use the molecular orbital picture for interpretation of DFT results as done for HF theory.[105] In practice, KS- and HF-orbitals have very similar shapes and lead to similar bonding interpretation. More care has to be taken when discussing the meaning of (virtual) orbital energies.[106]

2.1.2 Exchange-correlation functionals

The choice of the exchange-correlation functional (often simply called density functional, DF) determines the accuracy of DFT computations to a certain extent. There is no systematic way to improve a functional but depending on the "ingredients" used for their development, several classes of functionals can be distinguished (Fig. 8.). These classes have been put in a hierarchy which is most often illustrated by referring to the biblical picture of "Jacob's ladder" (in this context climbing from the "earth" of HF to the "heaven" of the exact DF; in the original version the top is given as "chemical accuracy" which however is an ambiguous term) which results in the functionals being classified into "rungs" of this ladder. The simplest DFs belong to the rung of local density approximation (LDA). They only depend on the electron density at a certain point and the corresponding energy ε_{XC} (eq. 2.4).

$$E_{XC}^{\mathrm{LDA}} = \int \mathrm{d}\vec{r}\ \rho(\vec{r})\ \varepsilon_{XC}(\rho(\vec{r})) \qquad 2.4$$

This does not mean that the electron density is described uniformly throughout the whole chemical system, but instead at every point in space (usually determined on a 3D integration grid), the LDA energy functional is evaluated and summed up. This means that LDA is specifically good at describing slowly varying electron densities (e.g., simple metals) but not great for molecules and chemical bonding. Nowadays, it is mostly used in solid state physics for metals and should not be used for other chemical systems.

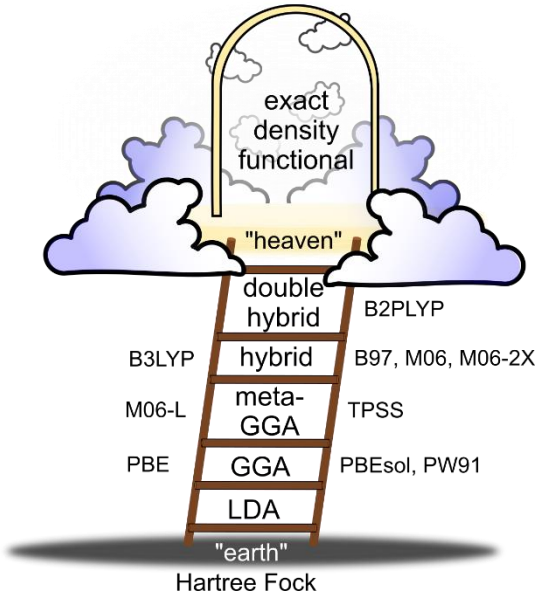

Fig. 8. The hierarchy of density functionals sorted in rungs of a "Jacob's ladder" (following J. Perdew).

The next rung are the DFs of the generalized gradient approximation (GGA) type. If the energy is expanded as functional of the electron density in a Taylor series, the step after LDA is to incorporate the first derivative of the electron density. After some removal of unphysical properties of the resulting gradient expansion approximation, the class of GGA functionals results. They are the most used class of DFs in material science due to the efficient algorithms for computing them paired with a good to very good accuracy for many systems.[101] The GGA functional developed by Perdew, Burke and Ernzerhof (PBE)[107] has become the quasi-standard in material science. This is partly due to the good performance but also partly due to early claims that it is "parameter-free". The only parameter-free DF thus is the exchange functional for the LDA by Dirac. But since the parameters in PBE are derived from physical boundary conditions to a (pretty unphysical) model system (the homogeneous electron gas) it was more appealing to many scientists compared to the fitting of parameters on accurate molecular data as is done, e.g., for BP86. In large benchmark studies, there is no notable performance difference.[108,109]

The third rung – the next step in the Taylor series – leads to the class of meta-GGA functionals (e.g., TPSS, M06-L). Although they are used in molecular chemistry increasingly, they have not been applied to AS-ALD up to now. In contrast to the step from LDA to GGA, an increase in accuracy is not guaranteed. However, they form the basis for many modern DFs. The fourth rung

leads to the hybrid functionals which include a fraction of "exact exchange" in the exchange functional. This term stems from using the HF expression for the exchange energy with the density from the DFT approach and leads to considerable improvement in accuracy, especially for main group chemistry, reaction barriers and optical properties. However, for the periodic boundary condition (PBC) calculations mostly used in AS-ALD, the large increase in computational cost (approx. 10x compared to GGA) often leads to these computations not being feasible.

In the last decade, several further DFs have been developed which partly combine features of several rungs, introduce exact exchange in smarter ways (range-separated DFs, local hybrid DFs) or become dependent on the unoccupied orbitals (rung 5, double hybrid DFs). However, in AS-ALD modelling none of these more modern DFs is in use up to now. Large-scale benchmark studies in molecular chemistry[108–110] as well as surface science[111,112] can deliver guidelines on how to choose the best DF for the given research question in AS-ALD. But often, the implementation of more exotic functionals is limited in the available computational codes. The lack of accurate benchmark data in AS-ALD makes it also hard to evaluate the different DFs for their accuracy. Thus, currently, there is hardly any study not using the PBE functional (Tab. 1 and Tab. **2**). If several DFs are used, quite large deviations can be found.[113]

2.1.3 Typical DF errors and London dispersion interaction

Currently used DFs show some major inaccuracies.[114] One well-known issue is the gross underestimation of band gaps of semiconductors by GGA functionals which can be traced back to the delocalization error (called the self-interaction error for one-electron systems).[115] Connected to the same underlying cause is the over-delocalization (GGAs) and over-localization (hybrid DFs) of electron densities. This can lead to errors in dissociation energies and especially reaction barriers but is mostly relevant for electron transfer phenomena.[114]

The second issue is the inadequate description of static correlation effects. This can be understood as the result of one Slater determinant (see section 2.2) not even being qualitatively adequate for a description of the chemical system. Typical examples are open-shell transition metal compounds or open-shell singlet states in biological systems but also bond dissociation curves creating open-shell fragments.[114] This issue is mostly not relevant for AS-ALD modelling up to now. It might become more pressing when more deposition modelling of metal ALD is carried out.

The third, and for AS-ALD most pressing, issue is the failure of many DFs to describe London dispersion interactions. This interaction can be described as the attractive part of the van-der-Waals potential, and it is also often referred to as van-der-Waals forces (although this term is discouraged by experts) or dispersion attraction.[116] The classical physical picture behind this interaction can be drawn as an attraction of induced dipoles. DFs of the first three rungs typically do not describe this interaction since it is intrinsically an electron correlation effect which is not well captured by approaches using one Slater determinant as KS-DFT or HF (see section 2.2.1). This leads to the result, that, e.g., the potential energy curve of the benzene dimer is completely repulsive for PBE and B3LYP.[117] In recent years, it became clear that the failure to describe these interactions leads to large errors in interaction energies especially for non-covalently bound systems (e.g.,

physisorbed precursors).[116] But also for covalently bound systems, dispersion attraction plays a major, stabilizing role.[118]

Several approaches were developed to capture these effects in the framework of DFT.[119] DFs can be parametrized to incorporate these effects in a mean-field approach (e.g., the Minnesota family of functionals),[120] or the non-local electron-electron interactions underlying the dispersion attraction can be incorporated directly into the functionals which leads to the vdW-DFs (e.g., optB88, vdW-DF)[121]. The by far most used approach, also in AS-ALD, is the addition of a correction term to the KS-DFT energy by a semi-empirical scheme. The most common approaches have been initially developed by Grimme (DFT-D)[122,123] and by Tkatchenko and Scheffler (DFT-TS)[124]. In these approaches, the stabilizing dispersion term is approximated by the pairwise interaction energy of atoms (A and B) in the systems which are then summed up (eq. 2.5). This interaction energy is determined from the polarizability of the atoms in the system expressed via the C_6-parameters (the term stems from the perturbation theory approach to intermolecular interaction) considering the decay behavior of this interaction with distance (r^{-6}). In addition, parameters (s_n) and so-called damping functions are used to tune the interaction energy to every functional.

$$E_{\text{disp}}^{\text{DFT-D}} = -\frac{1}{2}\sum_{A\neq B}\sum_{n=6,8} s_n \frac{C_n^{AB}}{r_{AB}^n} f_{\text{damp}}(r_{AB}) \qquad 2.5$$

The DFT-D approach relies on tabulated, pre-computed C_6 parameters which are either constant (DFT-D2), dependent on the chemical environment (DFT-D3) or additionally on the charge of the atom (DFT-D4). The DFT-TS approach computes these C_6 parameters on-the-fly but requires a Hirshfeld partitioning of the electron density which is based on a promolecular density and thus also requires atom-dependent parameters. In practice, both approaches (DFT-D3 or D4 compared to DFT-TS) deliver very similar chemical insights. The usage of DFT-D3 together with the PBE functional has become the de facto standard in computational material science and thus also in the modelling of AS-ALD if PBC are used.

2.2 Wavefunction-based methods

Solving the Schrödinger equation (eq. 2.6) is the goal of wavefunction based methods. Thereby, the Hamilton operator $\hat{H}$ of the system is known and the wavefunction is approximated to calculate the energy *E* of the system.

$$\underbrace{\left(\hat{T}_{\text{n}} + \hat{T}_{\text{e}} + \hat{V}_{\text{nn}} + \hat{V}_{\text{ee}} + \hat{V}_{\text{ne}}\right)}_{\hat{H}} \Psi = E\Psi \qquad 2.6$$

The operator $\hat{H}$ contains all the terms describing the interactions between the particles in a chemical system. Except for very specific environments, these are nuclei and electrons. Thus, $\hat{H}$ contains the kinetic energy of nuclei ($\hat{T}_{\text{n}}$) and electrons ($\hat{T}_{\text{e}}$), and potential energy terms of the interactions between nuclei ($\hat{V}_{\text{nn}}$), electrons ($\hat{V}_{\text{ee}}$) and between electrons and nuclei ($\hat{V}_{\text{ne}}$). In most computations, the Schrödinger equation for the electrons can be solved for a stationary

arrangement of nuclei since the latter are much heavier and move thus much slower. This so-called Born-Oppenheimer approximation leads to $\hat{T}_{\mathrm{n}} = 0$ and $\hat{V}_{\mathrm{nn}}$ being constant and the following $\hat{H}$ is used:

$$\hat{H} = \hat{T}_{\mathrm{e}} + \hat{V}_{\mathrm{ee}} + \hat{V}_{\mathrm{ne}} \qquad 2.7$$

The wavefunction for a multi-electron system cannot be written explicitly and the most common approach is the "orbital approximation". This means the wavefunction of the system Ψ is written as a product of one-electron wavefunctions (molecular orbitals) φ. It turns out that a specific type of product is needed – the Slater determinant (eq. 2.8) – to account for the indistinguishability of electrons and the Pauli principle.

$$\Psi = \frac{1}{\sqrt{N}} \begin{vmatrix} \varphi_1(1) & \cdots & \varphi_N(1) \\ \vdots & \ddots & \vdots \\ \varphi_1(N) & \cdots & \varphi_N(N) \end{vmatrix} \qquad 2.8$$

Nearly all published work in AS-ALD which are based on wavefunction methods uses the Born-Oppenheimer as well as the molecular orbital approximation (Tab. 1 and Tab. **2**).

2.2.1 Hartree-Fock

The most complicated term in eq. 2.7 is the electron-electron interaction ($\hat{V}_{\mathrm{ee}}$). In principle, the electrons move in a correlated fashion, that means their movement depends on all other electrons at every point in time. However, it is often enough to capture this correlated movement in an approximate manner. In the so-called mean-field approximation, the Schrödinger equation is solved for one electron by considering the other electrons as a background field (instead of computing the interaction with every single one of the other electrons explicitly). The result of this approximation are the HF equations (eq. 2.9) where one Schrödinger equation for each electron exists (the one-electron Hamiltonian is now called the Fock operator $\hat{F}$ and the one-electron wavefunction is the molecular orbital) which implicitly depends on all other One-Electron-Schrödinger equations through the HF potential (the above-mentioned mean-field). These interdependent equations have then to be solved in an iterative manner – the self-consistent field (SCF) approach.

$$\hat{f}_i \varphi_i = \varepsilon_i \varphi_i \qquad 2.9$$

To make this approach practically useful, another approximation is needed. The (unknown) molecular orbitals are expanded in a set of known basis functions. This is called the basis set approximation or the linear combination of atomic orbitals (LCAO) to give molecular orbitals (MO). The HF equations then transform into matrix equations (Roothaan-Hall equations, eq. 2.10) which are much easier for a computer to solve. Here, the matrix $\boldsymbol{C}$ contains all coefficients of the basis functions for every molecular orbital while $\boldsymbol{S}$ contains the overlap between the different basis functions.

$$\boldsymbol{FC} = \boldsymbol{SC\varepsilon} \qquad 2.10$$

If the basis set is infinite, eq. 2.10 would not be an approximation. In practice, the basis set needs to be finite which results in an error introduced by this approach. For AS-ALD, either atomic orbitals are used as basis sets (see section 2.8.1 on molecular approaches) or plane-wave basis sets (see section 2.8.2). HF is historically very important and conceptually very close to KS-DFT. In practice, it is less accurate than DFT but as "costly" and thus not used anymore. However, it is the starting point for the electron correlation methods discussed next.

2.2.2 Electron correlation methods

The energy computed via the HF method deviates from the exact energy of the system by the energy correlation term E_{corr}:

$$E_{\mathrm{corr}} = E_{\mathrm{exact}} - E_{\mathrm{HF}} \qquad 2.11$$

Capturing this term, which is associated with the explicit interaction of electrons beyond the mean-field approximation, requires moving beyond HF. This is done by approximating the multi-electron wavefunction by more than one Slater determinant. Either by generating substituted determinants as a sum (configuration interaction, CI) or with an exponential approach (coupled cluster, CC). Furthermore, the Rayleigh-Schrödinger perturbation theory approach can be used which leads to Møller-Plesset perturbation theory of *n*-th order (MP*n*). Discussing the details of these approaches is beyond the scope of this review, especially given their negligible usage in AS-ALD. The interested reader is referred to textbooks on the topic.[98,125]

However, two major approaches shall be discussed which are important methods to benchmark the accuracy of DFT computations. Although they are not used in AS-ALD yet, it is known from other communities that benchmarking is important and it should be extended in AS-ALD.[111,126,127]

The most economical way to capture the correlation energy is MP2. This approach only requires orbital energies and a further set of integrals. Modern MP2 implementations combine smart approximations to these integrals (e.g., density fitting, Cholesky decomposition, Tensor network)[128,129] are close to the efficiency of (hybrid) DFT computations and thus competitive for molecular approaches. Unfortunately, when using PBC, MP2 is very costly and hardly used.[130]

The second method of relevance is DLPNO-CCSD(T) and related methods.[131,132] CCSD(T) stands for CC with singles, doubles and perturbative triples which refers to the number of electrons moved from occupied to virtual orbitals when creating the additional Slater determinants (eq. 2.8). While this approach is only applicable to small molecules, modern implementations with clever approximations are applicable to systems with hundreds of atoms and thousands of electrons. DLPNO stands for domain localized pair natural orbitals which summarizes the approximations used. In a nutshell, the approach makes use of the fact that electron correlation is large when electrons are close to each other and weak otherwise. Thus, the correlation energy of electrons which are far apart is computed with "cheaper" methods (MP2). Also, molecular orbitals are transformed via unitary transformations (a mathematical operation that does not change the energy) to localize them on parts of the system and thus further speed-up the computations.

2.3 Electronic structure analysis

Many results of *ab initio* investigations are not easily accessible for interpretation. While energies can be interpreted in a straightforward manner, this is not the case for the electronic structure: wavefunction, electron density and derived properties do not directly correspond to chemical concepts. The field of electronic structure analysis (ESA) now aims at deriving quantities that make the connection between the delocalized electronic structure resulting from an orbital-based computation and local chemical concepts like Lewis structures, chemical bonds or charge distributions. The field of ESA is vast[133] and only a few methods have been used for AS-ALD up to now. However, the potential is large and thus some methods are briefly presented that can deliver insights in the field.

2.3.1 Atomic partial charges

The most often used ESA-based property in AS-ALD are atomic partial charges.[50,134,135] The idea is to derive the charge state of an atom in a molecule. This necessitates the partitioning of the electronic structure and summing up all the electron density belonging to one atom. This can be done in three ways: (i) assigning orbitals to atoms, (ii) dividing the electron density into basins belonging to one atom or (iii) fitting charges to the electrostatic potential of the molecule. Many methods have been developed for every approach since the seminal work by Mulliken.[136,137] Notably, it cannot be checked if any one method is superior a priori since no experimental charges can be measured for comparison. The methods derive their value from being robust (trends not changing with computational parameters, e.g., the basis set), consistent (reproduce known chemical trends) and insightful. In the end, a method is useful if it helps to understand the chemical system. Atomic partial charges can be used in AS-ALD to understand the charge-transfer upon adsorption of precursors or inhibitors to the surface. They are also helpful to understand trends in bond polarity, e.g., among a set of precursors.

2.3.2 Orbital analysis

In the MO approach typically used for *ab initio* computations, a set of occupied and (typically) delocalized orbitals results – the canonical orbitals. In KS-DFT, these are the KS orbitals which can be interpreted in a similar manner.[105] Visualizing these orbitals can help to understand the electronic distribution in a chemical system and show bonding and antibonding interactions. However, these analyses are often infeasible for AS-ALD once the substrate is considered. For computations with PBC, mostly plane wave basis sets are used which do not allow such an analysis in a straightforward way. One way to derive a similar picture is using the partial density of states (pDOS) approach. Here, the contribution of certain atoms in a system to the periodic equivalent of an orbital (the band) are analyzed, which has been used in AS-ALD a few times.[86,134] This analysis can give an idea about bonding interactions in a qualitative manner. The localization of orbitals can also be used to provide such a qualitative view on bonding interactions.[138] Orbital analysis can be used to better understand precursors themselves or the chemical interactions of a precursor with a substrate. However, other approaches are better suited in many cases.

2.3.3 Electron-density analysis

The electron density can be analyzed in a similar way to the orbitals. In most cases, a topological analysis of the density is used, which is a kind of a functional analysis approach. The most prominent ansatz here is the atoms-in-molecules (AIM) approach developed by Richard Bader.[139] AIM delivers atomic basins, bond paths and many derived quantities (e.g., partial charges). It is rarely used for surface chemistry and thus has not been used in AS-ALD up to now. A simpler approach is visualizing charge-density differences. In this case, the electron density of a precursor-substrate complex is taken, and the electron density from the separated precursor and substrate is subtracted. Thus, one derives the density changes induced by the bonding interaction. This approach is very common in surface science and has also been used in AS-ALD.[140] Yet, it has the disadvantage that the resulting figures often do not allow a straightforward analysis regarding the most important interactions.

2.3.4 Energy-based analysis

The driving force for chemical reactions is energy lowering. Thus, the idea to analyze energy comes naturally. The bonding energy can be decomposed into several sub-terms. Such methods are called energy decomposition analysis (EDA) methods. Many different approaches have been developed here.[141,142] They all have in common that they split up the (experimentally measurable) bonding energy into sub-terms which are not experimentally accessible. However, these sub-terms can be connected to chemical concepts like Pauli repulsion, orbital interaction, electrostatic interaction, dispersion attraction, etc. Thus, these methods deliver a quantitative analysis of the bonding in a chemical system and allow discussion of the origin of a certain bonding arrangement as well as discussion of trends among similar systems. The EDA has been applied recently to AS-ALD using its extension to PBC – the energy decomposition analysis for extended systems (pEDA).[143,144] It is promising to gain further insights into the driving forces for precursor/inhibitor-surface interactions as well as selectivity mechanisms in the future.

2.4 Molecular dynamics

Static computations solve the electronic Schrödinger equation (eq. 2.6) for a given arrangement of nuclei. Structural optimization then determines the best arrangement of nuclei for a given chemical system by successively computing eq. 2.6 while systematically changing (optimizing) the positions of nuclei. This requires the Born-Oppenheimer approximation and leads to a potential energy surface. If the question is how a system changes over time, e.g., for the process of a precursor interacting with a substrate, MD approaches are applied. Here, the focus is on the dynamics of nuclei since the dynamic behavior of electrons (quantum dynamics) requires different theoretical approaches[145] and is not relevant for (most parts) of AS-ALD. When the changes of a system over time are described with MD, Newton's equations of motion are typically used:

$$F = m\frac{\mathrm{d}v}{\mathrm{d}t} \qquad 2.12$$

Where the force F acting is given as the mass of the system m multiplied by the acceleration (derivative of the velocity v w.r.t. time t). The approach now is to define starting conditions with a specific arrangement of atoms and assign velocities to these atoms in order to compute the forces acting on the atoms. The forces after a certain timestep are then computed with different algorithms. The choice of the timestep (typically in the order of the fastest molecular vibration in the system, ca. 0.5-1 fs) and the choice of the algorithm (velocity verlet, leapfrog, etc.) is important for the accuracy of the resulting MD. When this approach is applied many consecutive times, the result is a MD trajectory which describes the behavior of the chemical system over the simulated time (in the order of picoseconds for AIMD). Further crucial choices for the MD algorithm are the ensemble (the decision which state functions are kept constant: pressure p, temperature T, number of particles N, volume V, energy E) and the thermostat (Nosé-Hoover, Anderson, etc.) which helps to keep these values constant. There are many details to be considered when actually carrying out an MD computation which are beyond the scope of this short description and can be found in the literature.[146] What is crucial for AS-ALD modelling is the question of how to treat the electrons in this MD approach. There are currently three major approaches to describing intermolecular interactions (the potential).

2.4.1 Classical MD

The interactions between atoms is treated with classical mechanics. Thus, the electrons are not considered explicitly but in an indirect fashion. To carry out a classical MD computation, a force field is required. This is a set of parameters which describes the interactions between the atoms. Typically, it consists of bonded parameters (potential energy functions for distance, angle and dihedral angle changes) and non-bonded parameters (electrostatic and van der Waals forces). For each atomic species in the system (atom type and connectivity, e.g., the C atom in C_2H_6 has a different parameter than in C_2H_2), and for every resulting pair of atoms, parameters have to be provided. As one can imagine, this leads to huge parameter sets for systems relevant for AS-ALD. Moreover, deriving these parameter sets and evaluating their accuracy is far from trivial. However, the choice of the specific force field is crucial for the reliability of the computational results and has to be tailored to the system. Choosing the wrong force field gives bogus results. The main advantage of classical MD is that rather large systems (1000s of atoms) and timescales (ns, cutting-edge computations even µs) can be treated. The major drawback of this approach for AS-ALD is that connectivity changes (bond making, bond breaking) usually cannot be described since the approach relies on the connectivity of the atomic species. Reactive force fields try to remedy this issue but are still hardly used for surface chemistry.[147] Also in this approach, the combination of atoms modelled has to be incorporated in the parametrization to make it applicable.

2.4.2 *Ab initio* MD

In this approach, electrons are explicitly considered, and the interatomic interactions are either based on pre-computed potential energy surfaces or computed “on-the-fly”. The pre-computing approach has the advantage that very high accuracy methods can be used,[148] but the same

drawback as force fields that a potential for every pair of atoms is needed. Thus, most AIMD approaches use efficient electronic structure methods (nearly exclusively DFT) to compute the electronic structure at each timestep (or apply some tricks to do it every few timesteps). This approach allows us to investigate chemical reactions relevant for AS-ALD since bond formation processes can be described. The most relevant parameter here is the simulation temperature (for the most often used canonical ensemble where *N*, *V* and *T* are constant). This temperature cannot directly be connected to an experimental temperature but instead scales the velocities of the atoms – higher temperature means higher kinetic energy. At low temperatures, typically only chemical changes without bond breaking are observed, e.g., conformational changes. The reason is that only reaction barriers of the order of $k_B T$ (ca. 2.5 kJ·mol^{-1} for $T = 298$ K, k_B being the Boltzmann constant) can be overcome in MD simulations. High simulation temperatures lead to the observation of reactions with higher reaction barriers in the MD run. However, at very high temperatures the kinetic energy of the system is so large that unphysical atomic movements can result. The main issue here is that in a simplified view on TST the internal energy of the system must rearrange to focus enough of this energy into the "productive" vibrational mode which is connected to the transition state of the reaction. From experiment, this process is known to take picoseconds or longer. Thus, the probability of observing the crossing of a reaction barrier in a picosecond-long trajectory is quite low. Yet, the solution of generating many trajectories is impeded by AIMD's biggest drawback: the immense computational cost due to the many necessary DFT computations. This limits the system size (100s of atoms) and the simulation time (picoseconds) and still requires major high-performance computing (HPC) systems to be used for a few, short (10 ps) trajectories. Also, the low number of achievable trajectories usually prevents statistically meaningful statements (i.e., "the probability ratio of these two reactions is 12% vs. 88%") or the use of techniques like autocorrelation functions to derive properties (e.g., vibrational spectra).

2.4.3 ML potentials

MLP promise to combine the efficiency of classical MD with the accuracy of AIMD and are thus currently intensively investigated.[149,150] As in all ML-based approaches, a large dataset is required to parametrize an ML model. This model "learns" how the interactions between the atoms must be described and can then subsequently be used to run an MD computation. There are many practical aspects to be considered in acquiring the dataset and in setting up the model which is discussed in specialized literature.[151] Currently, the development is very fast and first "black-box" approaches appear which can be used without expert knowledge on ML.[152,153] While the experience with these approaches is not yet comprehensive enough to make a general statement about the accuracy of the resulting MD simulations, it is a very promising approach for the modelling of AS-ALD if dynamical behavior of the system plays an important role.

2.5 Monte Carlo approaches

While MD follows the development of a system over time step-by-step, MC approaches are intrinsically stochastic. That means that probability and randomness are the core idea here. How can this lead to insights into physical systems? In probability theory there are ways to determine quantities by "smart sampling" and evaluating the remaining errors with the help of statistical analysis. The major advantage is that only part of the phase space of a system need to be evaluated. In electronic structure theory, this means that not all integrals are solved in a systematic manner (as is done in CC, CI or MP2) but instead "randomly" some of these integrals are solved and the remaining error evaluated. This approach is called quantum MC (QMC) and is one of the most accurate approaches to solving the electronic structure problem.[154] However, for AS-ALD, this is not relevant.

Instead, the stochastic description of molecular movement is very important in a process which relies on adsorbates being deposited on a surface from the gas phase in a non-directional manner. Thus, several of the following methods are heavily used in AS-ALD. It is important to notice that these MC approaches share with classical MD simulations that the electronic structure of the system is no longer considered. Furthermore, as the explicit movement of atoms is also not included in MC approaches, they represent a higher abstraction level of the underlying physics (Fig. 3.). As neither the electronic structure nor the movement of atoms is explicitly described, MC simulations highly rely on the quality of the input data describing the possible structures (systems states) and reactions (system transitions). The main advantage of these approaches is that they are very fast and lead to macroscopically measurable quantities (i.e., coverage).

The MC approaches presented in this review can be classified based on their strategy to gain insight into AS-ALD. The most complex approach uses elemental reactions and their rate constants to describe the system as complete as possible.[155–157] Overall, such kMC simulations provide the most insightful picture but at the highest computational cost. The simplest MC approach presented here is neglecting thermodynamic and kinetic information. By so called random sequential adsorption (RSA) simulations, the question of adsorbate packing and density is addressed.[71,74,113,158,159] A third group of MC simulations is located between RAS and kMC in terms of complexity and insights, as they can be considered simplified kMC or more complex RAS simulations.[15,160–163] As a side note, similar to DFT and HF, a mean-field approximation is possible in the kinetic modeling of a system assuming uncorrelated adsorbates. Such methods are referred to as (mean-field) microkinetic modelling.[164–166] Since they are not yet used in AS-ALD, we will not further discuss them.

2.5.1 Random sequential adsorption

This approach uses simplified models to represent the molecules, for example the sum of their atomic van-der-Waals radii or even simple geometric shapes like ellipsoids or circles. The substrate is reduced to a regular 2D lattice sometimes even without PBC. The algorithm then determines an adsorption spot for sequentially incoming molecules considering a random factor (which gives the method its name). In case no overlap with a neighboring molecule is present at

the selected lattice point, the incoming molecule is placed at this spot and the algorithm is repeated. Usually, the judgment on the overlap is based on the 2D shape of the considered molecules. This algorithm has a history[167–170] in other fields and has recently been adapted to AS-ALD.[71,74,113,158,159] For AS-ALD, the main goal of an RSA simulation is to derive surface coverage, hole size and density, as well as inhibitor density. These insights can help to judge inhibitor blocking efficiency and mechanisms: Good selectivity in combination with a high surface coverage is hinting towards steric blocking while good selectivity with a high inhibitor density is hinting towards chemical passivation as the major blocking mechanism.[74] Still, both effects are contributing to the overall blocking efficiency. For conducting reasonable RSA simulation, the technical parameters of the simulation cell size, boundary conditions, and rotational degrees of freedom of incoming molecules must be sampled, as they considerably impact the final surface coverage. While RSA simulations are extremely fast, the main downside is their limited accuracy, which is caused by the strong approximations of neglecting any reaction events such as conformer changes beyond rotations, desorption, diffusion or reactions as well as neglecting inter-molecular interactions beyond steric blocking.

2.5.2 Monte Carlo

As RSA simulations proved to be a simple and yet insightful tool, several extensions to expand their use cases are available. These expansions include diffusion events[158] in the form of lattice point hopping and the combination of adsorption and reaction events[159]. As an attempt to judge the precursor penetration of an inhibitor layer, Kim et. al. combined an RSA algorithm for the formation of an SMI inhibitor layer with a second RSA algorithm for the precursor adsorption on the inhibited surface.[15,160–162] In contrast to RSA simulations, MC simulations going beyond the early steps within an AS-ALD process are rarely present within the literature. A recent example is the MC approach developed by Carroll et. al.[163] This ansatz focuses on material growth or, more precisely, the analysis of lateral overgrowth in AS-ALD processes. As a side feature, information on material stoichiometry and growth per cycle are also obtained. This algorithm uses a 3D lattice to describe multiple adjacent surfaces. All central atoms of the precursor or co-reactant (Al and O for Al_2O_3 ALD), as well as all ligands (i.e. CH_3 or OH), can occupy a single lattice point on this grid. Material deposition is modeled by random selection of reaction sites (lattice points), while individual reactions are accepted based on predefined rules. As for RSA, reactions are assumed to be irreversible, and diffusion events are neglected. Still, this approach is significantly more complex since the user can add additional constraints to fine-tune the (lateral) growth. These constraints are considered based on encoded rules for adsorbate-adsorbate interactions influencing packing, orientation, and multi-site bonding of adsorbates. In addition, rules for adsorbate-surface interactions (attractive or repulsive) influencing the adsorbate position and orientation or even enabling additional reactions at the GS-NGS interface are present.

2.5.3 Kinetic Monte Carlo

While the previously presented MC algorithms provide insights and guidance for AS-ALD, they lack one important component: time. This is evident as kinetic information is not included. Yet, realistic large-scale modeling of AS-ALD necessitates knowledge of the rate constants *k* of all elemental steps (from state *i* to *j*) included in the MC simulation which is done in kMC.

$$k_{ij} = \frac{q^{\ddagger,\mathrm{vib}}}{q_i^{\mathrm{vib}}} \frac{k_\mathrm{B} T}{h} \mathrm{e}^{-\frac{\Delta E_{ij}^{\ddagger}}{k_\mathrm{B} T}} \qquad 2.13$$

The rate of a chemical reaction is connected to the reaction barrier $\Delta E_{ij}^{\ddagger}$ via eq. 2.13. In practice, the ratio of the partition functions *q* is often approximated to be unity. Especially the selectivity in AS-ALD is determined by the relative values of the reaction barriers of SMIs and/or precursors on GS and NGS. If there are several possible chemical reactions in a system, the (coupled) rate equations need to be solved to derive product distributions.[27,171,172]

$$k_{\mathrm{tot}} = \sum_j k_{ij} \; ; \Delta t = \; -\frac{\ln\left(o_2\right)}{k_{\mathrm{tot}}} \qquad 2.14$$

The kMC approach is a stochastic way to solve these coupled rate equations. It requires as input the reaction energies and barriers for all relevant reactions in a chemical system. These parameters can be based on *ab initio* computations[157] (e.g., adsorption energies) but can also be determined to fit experimental data[155] or simply represent reasonable assumptions[171]. The modeling is then carried out on a lattice representing the surface. The type and complexity of this lattice (e.g., is off-lattice adsorption allowed?) determines the quality of description of the AS-ALD process. Then, similar to the MC simulations, several cycles of kMC runs are carried out, and using a random factor in the algorithm, the product distribution is derived as a function of time. For example, in the Bortz-Kalos-Lebowitz (BKL)[173] algorithm, the time steps are derived from the total rate constants of all currently possible events and a random number o_2 (eq. 2.14). The complexity of the model can be improved by further chemical interactions like the repulsion of adsorbed species towards incoming molecules. The advantageous description of surface processes by kMC is through their consideration of reaction barriers in addition to the adsorption processes from the stochastic modeling. This makes it a very promising method to evaluate the AS-ALD process beyond the nucleation stage. The added complexity, however, makes the computations much more demanding than simple MC simulations but still much less complex than DFT computations. The major drawback is that the DFT modeling of the relevant chemical reactions in the deposition must be complete. If one crucial reaction barrier is missing, the kMC algorithm will convey the wrong picture. Accordingly, only very few studies are found in the literature.[155–157]

2.6 Beyond atomistic modelling

As stated above, ALD happens in a reactor. Since time scales of seconds and length scales of centimeters are unavailable by atomistic modeling this cannot directly be modeled. However, as outlined in the introduction, gas flow might be an important factor in understanding certain AS-

ALD processes. We briefly outline major approaches here. CFD approaches uses numerical methods to solve macroscopic equations of fluid dynamics, and this is also applicable to gas flow in 3D. The nonlinearity of gas flow yields quite complex equations, making HPC resources indispensable. Moreover, interaction with the surface can be incorporated. The results are time-dependent concentration of gas components which can then be used as input for microscopic modelling. FE methods are used to numerically solve a set of coupled differential equations. The system is decomposed into several geometrically simple sub-systems (finite elements) which can then be solved efficiently. Multiscale modeling refers to methods combining several computational approaches suitable for different time and length scales. Exemplified for AS-ALD, thermodynamics properties and reaction barriers from DFT can be utilized as input for kMC simulations, whose product distribution can feed a CFD reactor model. The Christofides group applies this approach to ALD, and recently also to AS-ALD.[24] Here, the coupling of the "scales" is the crucial aspect since information from one scale is not trivially included as information in the next scale. A second challenge is the coupling from large scales back to the microscopic scales, i.e., the results from flow analysis on CFD level back to the DFT computation. Other communities, e.g., theoretical heterogeneous catalysis, have been working on this problem for decades.[174]

2.7 Machine learning

ML is a subfield of artificial intelligence (AI) where statistical methods are used to enable computers to perform tasks they were not explicitly programmed for. It is a part of data-based science and thus fundamentally different from the other methods outlined above which are based on physical principles and solving the resulting equations. Thus, ML-approaches require a large set of (reliable) data to be trained on. For a given problem, a model is trained on these data sets which then fulfills the targeted task. This very fast developing field is summarized in recent reviews.[175–178] Beyond the usage of ML for creating interatomic potentials as outlined in section 2.4.3, this family of approaches can also be used to extract information from large datasets and interpolate data. For instance, ideal experimental ALD parameters have been predicted in the past.[179] Overall, the usage of ML techniques is still rare in AS-ALD. The major bottleneck for widespread usage of ML in AS-ALD is the lack of large datasets for training ML models from experimental as well as from the computational side.

2.8 Modelling environments

One major decision in *ab initio* modelling of AS-ALD is how to treat the substrate. While the chemistry of precursors is clearly modelled with molecular approaches, this is not so clear for molecule-surface interactions. Two major approaches evolved which are both in use in the AS-ALD literature. The general idea of both approaches is illustrated in Fig. 9..

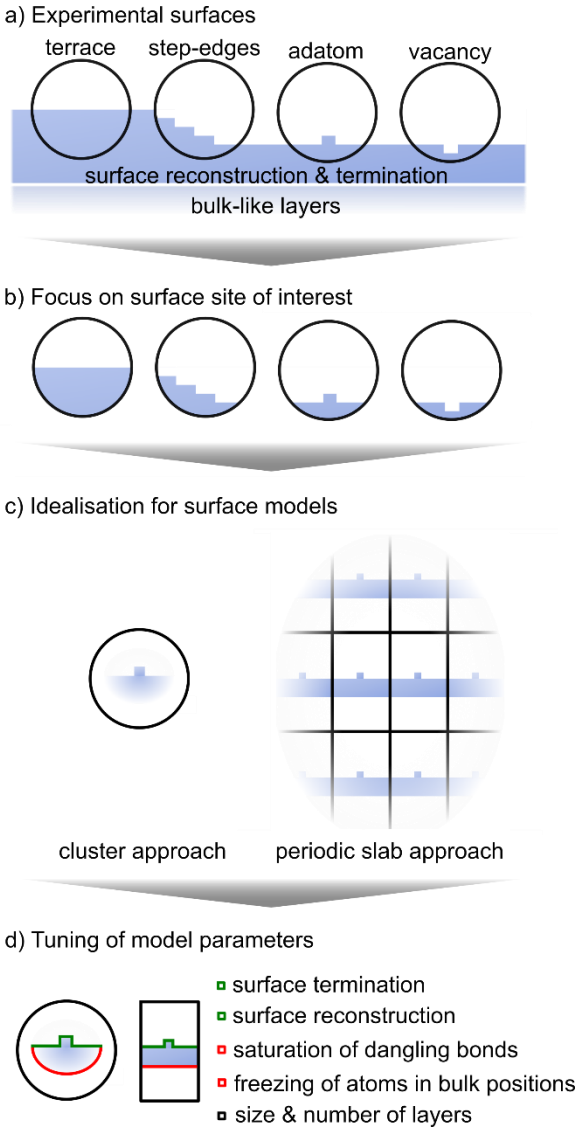

Fig. 9. Decision tree for the modeling of surfaces. The feature-rich experimental surface (a) has to be reduced to a feature of interest (b). This feature can then be modelled by either a cluster or slab approach (c). Based on the selected approach, tuning of computational parameters (d) is the necessary final step.

2.8.1 Cluster approach

The surface can be modelled by cutting out a small cluster containing the reactive site (Fig. 9.). The adsorbate then interacts with this active site in the computations. This approach is computationally very efficient and does not need large HPC resources. Furthermore, it allows – in principle – the usage of more accurate methods than DFT (e.g., MP2, CCSD(T)) since computational codes of molecular chemistry can be used. In AS-ALD modelling, it is mainly used to compute adsorption structures of precursors and SMIs.

The pioneering modelling of ALD chemistry by Musgrave et al. had been started by using this modelling approach.[180] They established the cluster approach to model the silicon surface (Si_9H_{12})

and benchmarked DFT approaches (B3LYP/D95(d,p)/LanL2DZ) against accurate wavefunction based methods (QCISD(T)/DZVP) – an approach that has been picked up later on.[181] Due to the limited computational resources, early modeling of (AS-)ALD often had to use size-reduced ligands and model systems and also had to compromise on technical accuracy aspects like basis set size. Nevertheless, in many cases a good agreement to experimental data could be achieved.[53,85] Modern AS-ALD modelling nearly exclusively models the exact chemical system that is used experimentally. This is important since steric effects by bulky ligands can be a major factor in selectivity.

The challenges are associated with the many detailed decisions necessary to set up the cluster model correctly. Cluster size, partial freezing of edge atoms, saturating atoms at the edges (which atoms, which bond lengths), how to deal with the frozen atoms in thermochemistry calculations are just some of the decisions to be made. Yet, the major drawback is its neglect of the surface periodicity. First, it cannot capture the full electronic structure of the solid (molecular orbitals instead of band structure) which is especially relevant for conducting surfaces (for which the approach is nowadays hardly used anymore). Second, while structures are often quite reliable, energies can strongly depend on the size of the cluster and usually deviate from slab results.[182] Especially reaction barriers are often found to be very high compared to extended slab modelling.[71,160] Third, the possible reactions with the surface are limited to the atoms included in the cluster and pathways might be missed which need neighboring atoms (an example is the reaction of benzylazide on Si(001)[183,184]). Lastly, the investigation of coverage-dependent reactions is not possible. However, in studies by Chabal et al., frequently a good agreement between cluster and slab approaches was found for precursor adsorption on differently terminated Si(001) surfaces.[53] The cluster approach is thus suitable for efficient screening of surface chemistry but not the method of choice for accurate in-depth investigations of AS-ALD.

2.8.2 Slab approach

The atomic and electronic structure of solids is best described with the help of a unit cell and PBC.[185,186] This approach can be adapted to AS-ALD by modelling the surface as a slab consisting of several layers in the unit cell using PBC (Fig. 9.). For technical reasons (the plane-wave basis sets typically used require 3D PBC), the slab is repeated in the third dimension with a vacuum layer to separate it from the next periodic image. Also in this approach, several parameters have to be chosen appropriately for the results to be meaningful: number of layers in the slab, vacuum thickness, frozen layers, etc.[187] The surface model is of utmost importance: setting up the unit cell and deciding about the surface termination requires experimental knowledge of the substrate under AS-ALD conditions. This is well-known for some surfaces (e.g., Si(001))[188] but much less clear for amorphous (e.g., SiO_2, Al_2O_3) or complex substrates. In this case, setting up a good surface model requires in-depth investigations.[189] Also, the change in surface termination during the AS-ALD process is rarely known. Considering the periodicity of the surface has the advantage of delivering an accurate description of the electronic structure and avoiding finite-size effects. Different coverages can be simulated on an equal footing, and structures and energies are less

dependent on the model chosen (if the parameters are well-converged). The main drawbacks are the considerably larger computational cost (10-100x) compared to molecular cluster computations and the lack of accurate methods beyond DFT. In conclusion, slab computations are the preferred choice for AS-ALD modeling.

2.9 Accuracy

The accuracy of a method determines its applicability. Especially when predictions are the goal of computational approaches, accuracy must be sufficient to allow conclusive statements on the modelled properties. Some general statements can be made based on the extensive computational chemistry literature. DFT approaches are very accurate for the prediction of atomic structures. This has been extensively shown by comparison to structural data from experiment.[190] Although they are slightly less accurate for transition state structures, the lack of experimental data does not allow a quantitative comparison. Reaction energies are more sensitive to the density functional chosen and can deviate by tens of $kJ \cdot mol^{-1}$ from experimental data.[108,110,120] Main group chemistry is much more accurately modeled than transition metal chemistry. And thermochemistry is more accurate than reaction barriers. For AS-ALD modelling, GGA-type functionals are chosen which show a balanced description throughout typical ALD chemistry requirements (structures, energies, barriers). More accurate descriptions for main group chemistry are usually achieved with hybrid functionals.[109] In all cases, the inclusion of dispersion correction schemes enhances the accuracy of structures and energies.

In contrast to DFT, the accuracy of wavefunction-based methods can systematically be improved. While MP2 is often comparable to (hybrid) DFT approaches in accuracy, CCSD(T) is much more accurate for energies. If large basis sets (at least triple-zeta quality) are used, they often approach "chemical accuracy" (i.e., $<4\ kJ \cdot mol^{-1}$ error). There are two ways to determine the accuracy of a computational method: (i) comparison to a theoretical benchmark method (e.g., CCSD(T)) or (ii) comparison to experimental data. Usually, the first approach is done in molecular chemistry since benchmark data are available. In surface chemistry, and thus also AS-ALD, the lack of available benchmark methods leads to the second approach being more favorable. Unfortunately, not many accurate experimental data are available in AS-ALD which would allow to quantify the errors in structures and energies made by the (DFT) modeling. Assessing the accuracy of other methods (kMC, AIMD, etc.) has the same drawback of lack of benchmarking data. Some exceptions exist: Recent thermodynamic measurements for ZrO_2 showed semi-quantitative agreement for the DFT approaches it compared to.[191] It was shown that the surface model in the theoretical description is important for this comparison and that inclusion of dispersion interaction treating methods might change the results qualitatively. These kinds of measurements are crucial for further establishing the accuracy of DFT and other modeling approaches for ALD and AS-ALD.

3 Computational insights for AS-ALD

This section now summarizes the contributions that computational modeling can make to the field of AS-ALD. It is interesting to note that it is often stated that ALD needs multiscale modelling to be understood.[192] However, the microscopic aspects (e.g., surface chemistry) can be treated quite independently from the macroscopic aspects (e.g., gas flow) which explains the success of many DFT-based approaches in ALD.[25,39,42,43,193–199] This is all the more the case for AS-ALD modeling, where selectivity is mostly determined by the local reactivity of precursors and inhibitors on GS and NGS. Although recent approaches exist to extend to multiscale modeling,[24] the necessity in the framework of modelling AS-ALD is still an open question. As outlined in the introduction, the focus here is thus on the insights gained by *ab initio* modelling of the key aspects of AS-ALD. A comprehensive overview of studies in AS-ALD that contain computational investigations is found in Tab. 1 for inhibitor-based approaches and in Tab. 2 for intrinsically selective approaches. This includes studies which focus on a theoretical investigation of certain aspects as well as the vast majority of studies where experimental data are either explained by computations or where predictions from computations are checked experimentally. Notably, the details on the computational approaches are often found only in the supporting information of the studies cited.

Tab. 1 Inhibitor-based AS-ALD: Computational studies sorted chronologically.[a]

Approach	ALD process	Precursor	Co-reactant	GS	NGS	Inhibitor	Research question[b]	Computational Model	Computational Method[c]	Code[d]	Targets[e]	Comments	Year	Ref
SAM	Al_2O_3	TMA	H_2O	-	-	OTS-based SAMs (models)	3a, 3c, 3d	Cluster SAM: CH_3CH_2OH, $CH_3CH_2NH_2$, and $CH_3CH_2CH_3$; Test against CH_3-$(CH_2)_4OH$	XC: B3LYP BS: 6-311++G(d,p)	G98	TD (G) TS RR	First computational study on AS-ALD, SAM terminal group determines stability, Hammond postulate valid, correlation to bond energies, precursor interaction with SAM local	2004	[200]
SAM	PbS	Pb $(tmhd)_2$)	H_2S	-	SiO_2	ODTS	1a, 3a	Cluster Si: $Si_9H_{12;}$ SiO_2: $Si_9H_{10}(OH)_2$; SAM and ligand truncated	XC: B3LYP BS: D95(d,p), LanL2DZ(Pb)	G03	TD (E) TS	precursor reacts with NGS, not SAM, >80 cycle, precursor penetrates SAM Exp.: SE, WCA, XPS, AES	2010	[181]
SMI	SiO_2	BDEAS	O_2 plasma	SiO_2	Al_2O_3	Hacac	2a	Slab Hydroxylated Al_2O_3(0001) [4L] SiO_2(001) [18L]	XC: PBE-D3 BS: 400eV K: Γ-only	VASP	TD (E) TS	SMI binds to NGS, not GS, Hacac in chelate mode, physisorbed precursor, surface acidity correlation, Exp: FTIR, SE	2017	[69]
SAM	Al_2O_3	TMA	H_2O	SiO_2	TiO_2	ODPS	3a, 3b, 3c	Molecular model: propyl for ODPS Slab for MD	XC: B3LYP-D2 BS: 6-311G** MD: UFF, NVT ensemble	Q-Chem LAMMPS	TD (E) TS	Precursor physisorbs on SAM, no decomposition, no penetration, more physisorption at high p (MD) → less selectivity Exp.: AFM, FE-SEM, WCA, XPS	2017	[201]
SMI	Ru, Pt, Al_2O_3, HfO_2	TMA, MeCpPt Me_3	H_2O, O_2	Si-H	SiO_2	DMADMS, DMATMS	2a, 2b, 2c 1a, 3a, 3c	Cluster Si: Si_9H_{14} SiO_2: $Si_9H_{12}(OH)_2$ SMI-covered SiO_2: Si_9H_{12}-O_2-$Si(CH_3)_2$	XC: B97-D3 BS: def2-SVP	G16 MC	TD (G) TS	Ads on NGS, not GS, exp. agreement for Pt, Ru; Al_2O_3 and HfO_2 can be deposited → incomplete passivation by SMI, precursor-inhibitor Exp.: WCA, XPS, FE-SEM	2018	[71]
SAM	Al_2O_3, ZnO, MnO	TMA DEZ, $MnCp_2$	H_2O			SAM	1e, 3a	Molecular model MeOH, MeSH, MeCOOH	XC: M06-2X, M06-L BS: TZP	AMS	TD (G) TS	Precursor interaction with and ALD growth on SAM models Exp.: SE, AFM	2019	[202]
SMI	Al_2O_3	TMA, DMAI	H_2O	SiO_2	Co, Cu	ET	4a 1a, 2b, 3a, 3b	Cluster Si(111): $Si_{26}H_{26}$ Co/Cu: MC model	XC: B97-D3 BS: def2-SVP, LanL2DZ ($Si_{surface}$)	G16 MC	TD (G) TS C	DMAI dimerization decisive for selectivity in contrast to TMA monomer – agree to exp. Exp: WCA, SE, XPS	2020	[160]
SMI	SiO_2	BDEAS	O_2 plasma		Al_2O_3	Hacac	2a, 2c (MC) 3a, 3c, 3d	Slab Al_2O_3(0001) [4L] partially hydroxylated	XC: PBE-D2, PBE-D3, optPBE-vdW BS: 400 eV K: 2x2x1	VASP MC	TD (E) TS IR	chelate/monodentate adsorption of SMI, monodentate decisive for selectivity loss - SMI desorption and SMI-precursor interactions, Exp: IR	2020	[113]
SMI	ZrO_2	TEMAZ	O_2, H_2O	SiO_2	Cu	3-hexyne	2a, 2b	Slab Cu(111), Cu(110), Cu(100) Cluster a-SiO_2: $Si_{27}O_{60}H_{12}$	XC: PBE-vdWsurf BS: NC-PP, 85 Ry K: 2x2x1	QE Phonopy	TD (G)	Chemisorption of SMI on NGS, physisorption on GS, selectivity loss through oxidation of NGS (XPS) after 10 cycles Exp.: XPS, FM	2020	[203]
Inhibitor layer	Pt	MeCpPt Me_3	O_2		Si	CF_x	1a, 1b 3a, 3b, 3e	Slab Si(001) [8L] F_3C-Si(001)	XC: BEEF-vdW BS: 400eV K: 2x2x1	QE	TD (G)	T-dependence in exp. explained by entropy, co-reactant penetrates Si, but not precursor, Exp.: XPS, WCA, SE, AFM, TEM, GIXRD	2020	[204]

Inhibitor layer	ZnO	DEZ	H_2O	Si	Si/indicone	Indicone	1a, 1b, 1e 2a 3a	Cluster Si(001): $Si_{15}H_{16}(OH)_4$ molecular models for polymer	XC: B97-D3 BS: def2-SVP	G16	TD (G) TS	alucone decomposition (b-H elimination), ZnO blocking mechanism, Exp.: SE, QCM, GIWAXS, XPS, AES	2020 [205]
SAM	ZnO/TiO_2	DEZ/ TDMAT	H_2O	EUV patterned Cu, SiO_2	Non-patterned Cu, SiO_2	Stearate hydroxamic acid derivatives	2c 3a	Slab SAM packing Cluster SAM reactions	Packing: XC: PBE-D3, BS: 420 eV Reactions: XC: PBE0, BS: def2-TZVPD //def2-SVP	VASP Q-Chem	TD (E) ESA	Packing density of SAM as function of head group, sterics, H-bonding, vdW, photochemistry of SAM layer	2021 [138]
SMI	SiO_2	BDEAS	O_2 plasma		Al_2O_3	Hacac, alcohols	2c 2a	Slab Hydroxylated slabs Al_2O_3(0001) [4L]	XC: PBE-D3 BS: 400eV K: 2x2x1	VASP	TD (E) MC (RSA)	RSA gives effective gap sizes of SMI layer at full coverage, optimize inhibitor packing by combining several SMIs	2022 [158]
SMI	Al_2O_3	TMA, DMAI, TDMAA	H_2O		Al_2O_3	Hacac	2a	Slab Hydroxylated slabs Al_2O_3(0001) [4L]	XC: PBE-D3 BS: 400eV K: 2x2x1	VASP	TD (E)	Exp.: IR for blocking mechanism supported by computation, steric shielding vs. chemical passivation	2022 [206]
SMI	TiO_2	TDMAT	H_2O		TiO_2	TMPMCT	2a 2c	Slab TiO_2(101) anatase [2/3L]	XC: PBE-D3+U BS: 500 eV	VASP MC	TD (E) TS	SMI hydrolysis creates more space – denser SMI – better blocking, Ti precursor-inhibitor Exp: WCA	2022 [15]
SMI	Al_2O_3	TMA, TEA	H_2O	Cu	SiO_2	alkoxysilanes, MTMS, DMDMS, TMMS, TMES, TMPS	2a, 2b 3a, 3c (mol. model)	Slab SiO_2 [3L] Cu(111) [4L] Molecular model	XC: PBE-D3 BS: 480 eV (def2-TZVPP for molec. calc) K: 3x3x1	VASP G09	TD (G) TS	SMI doubly bonded, blocking via chemical passivation, possible cross-linking of SMIs, entropy decisive for trend, Research data published ExP. WCA, SE, XPS, IR	2022 [67]
SMI	SiO_2	BDEAS	O_3	SiO_2	Al_2O_3	Hacac	2a, 2b, 2c 3a	Slab Al_2O_3(0001) [n.a.] β-SiO_2 (0001) [n.a.]	XC: [n.a.] BS: 50 Ry K: 2x2x2 (SiO2)	QE PWscf kMC	TD (E) TS	Multiscale: DFT and kMC data. Steric effects included. Later extended to AIMD, kMC and CFD[24] plus ML [207]	2022 [157]
SMI	SiO_2	BDEAS	O_2 plasma	SiO_2	ZnO	ethylbutyric acid, pivalic acid	2a, 2b, 2c 3b 5a	Slab ZnO($10\bar{1}0$) [4/6L] H-ZnO($10\bar{1}0$) [4L] H-SiO_2(0001) [6L]	XC: PBE-D3+U BS: 400 eV K: G-only AIMD	VASP	TD (E) TS	Improved selectivity due to theory-optimized SMI → good packing and strong NGA-binding, coverage-dependent energies (TD, TS), multiple binding modes of SMIs, Exp: LEIS, XPS	2023 [208]
SMI	Ru	Carish	O_2, H_2O	Ru (with O_2)	Ru (with H_2O	$Ru(EtCp)_2$	1a, 1b, 2a, 2b, 3c 3a	Slab Ru(0001) [4L]	XC: PBE-D3 BS: 400 eV K: 3x3x1	VASP MC	TD (E)	EtCp on surface blocks precursor, H_2O converts EtCp to HO-Cp →increased SMI density, less unoccupied sites, better blocking, precursor-inhibitor for Ru , Exp: TEM, WCA, FE-SEM, XPS, EDS	2023 [209]
SMI	SiN_x	Si_2Cl_6	NH_3	SiN_x	SiN_x-tBu	TBC	1a, 2a 3a, 3c	Cluster $Si_9N_7H_{21}$	XC: M06-L BS: def2-SVP	G09	TD (E) TS	Inhibitor leaves *t*-Bu group at NGA which blocks precursor, co-reactant removes *t*-Bu group via β-H elimination	2023 [210]

SMI	Al_2O_3	TMA, DMAI	H_2O	SiO_2	Cu	MSA	2a, 2b, 2c 3e	Slab SiO_2(0001) [3L] Cu(111) [4L]	XC: PBE-D3 BS: 450 / 480 eV K: 3x3x1 / 6x6x1	VASP	TD (E) TS	SMI chemisorbs on GS and NGS, much higher barrier on GS, full coverage possible, Surface oxidation considered Exp.:AES, XPS, WCA	2023	[87]
SMI	TiN	TDMAT		SiO_2	Ru, Co	aniline	1a 2a, 2b, 2c 3a	Slab Ru(0001) [4L] Co(0001) [4L] SiO_2(0001) [4L]	XC: PBE-D3 BS: 400eV K: 2x2x1	VASP RSA	TD (E) TS	Physisorption on GS, catalytic decomposition and 2 adsorption modes on NGS lead to good packing, starting point for IR prediction with clusters (B3LYP-D3/LanL2DZ/6-31G**)[211]	2023	[159]
SMI	Ru	EBECH-Ru	O_2	SiO_2	TiN, SiN	aldehydes (hexanal, decanal, undecanal)	2a, 2b	Cluster SiN: $Si_9N_7H_{21}$ SiO2: $Si_9O_7H_14$ SMIs: formaldehyde, benzaldehyde, hexanal	XC: B97-D3 BS: def2-SVP	G16	TD (E) TS	Large barriers found, slightly smaller for GS, 2nd reaction site needed for SMI on GS Exp.: WCA, XPS	2024	[212]
SMI	Ru	Carish	O_3	Cu	SiO_2	DMADMS, TDMAS	2a, 2e 1a, 1b 3a	Slab SiO_2(0001) [4L] partially and fully hydroxylated Cu [n.a.]	XC: PBE-dDsC BS: 400eV K: [n.a.] MC with R	VASP	TD (G)	DMADMS leaves two Me groups at surface, TDMAS has $N(Me)_2$ group → β-hydride elimination → imino group plus H → less steric hindrance, precursor-inhibitor Exp: WCA, SE, FE-SEM, XPS	2024	[162]
SMI	SiO_2	BDEAS	O_2 plasma		Al_2O_3	HAc, Hacac, Hthd	2a, 2c	Slab Al_2O_3(0001) [4L] partial OH	XC: PBE-D3 BS: 400 eV K: 2x2x1	VASP RSA	TD (E) TS	blocking mechanisms: HAc better due to smaller size – denser packing – higher chem. passi-vation, Hthd better due to bulkiness – better steric shielding Research data published Exp: in-situ IR, in-situ SE	2024	[74]
SMI	ZnO	DEZ	H_2O	HO-SiC	Cu	Mono-, di-, tri-propargylamine	2a, 2c	Molecular model Cu atom-SMI Slab for GFN-xTB: Cu(100) [4L]	XC: M06 BS: 6-31G(d,p) GFN-xTB, ReaxFF	G16 AMS	TD (G) TS	SMI bonding to the NGA, cross-linking of SMIs	2024	[213]
SMI	Al_2O_3	TMA, TEA	H_2O	Cu	SiO_2	TMPS	2a, 2b, 2c 3a, 3b, 3c 5a	Slab a-SiO_2 [4L] (2 amorphous models)	XC: PBE-D3 BS: 550 eV / TZ2P K: 2x2x1	VASP AMS	TD (G) TS ESA	Amorphous NGA model necessary for blocking mechanism, decomposition of SMI layer, TMA more reactive than TEA, reactivity reduction Research data published	2024	[214]
SMI	HfO_2	TDMAHf	H_2O	TiN	Cu; SiO_2	DES	2a, 2b, 2c 3a, 3d	Slab SiO_2(0001) [3L] Cu(111) [4L]	XC: PBE-D3 BS: 480 eV K: 3x3x1 / 6x6x1	VASP MC	TD (E) TS	SMI blocks two NGS, decomposes on Cu – both fragments block, on SiO_2 ethyl fragment blocks, Exp.: WCA, XPS, FT-IR, SE, FE-SEM, AES	2024	[215]
SMI	Ru	TRuST	H_2, O_2	Mo	SiO_2	DMATMS (precursor-inhibitor)	1a, 1b, 5b	Slab Mo(110) [4L] a-MoO_3 [4L] SiO_2(001) [4L]	XC: PBE-D3, U for MoO_3 BS: 400-500 eV K: 3x3x1 / 5x5x1	VASP	TD (E) TS	Surface reduction by H_2, O_2 only on MoO_3, not on SiO_2, precursor adsorption on Mo, not on MoO_3 Exp.: WCA, FE-SEM, SE, XPS, HR-TEM, EDS, AFM	2024	[216]

SMI	Al_2O_3	DMAI	H_2O	SiO_2	Cu, CuO_x	pyridine, aniline, pyrrole	2a, 2c, 5a	Slab Cu(111) [4L] CuO(111) [5L]	XC: PBE-D3, U for CuO BS: 360 / 440 eV; K: 6x6x1	VASP	TD (E)	Upright SMI blocks worse than flat-lying SMIs, same trend on Cu and CuO Exp.: WCA, SE, AES	2024	[217]

[a] SiO_2 and Al_2O_3 are α-modifications if not stated otherwise. X-[surf](facet) is used as notation for X-terminated [surf](facet) surface.
[b] abbreviations used for research questions tackled by the computational studies:
1 Precursor-surface interactions: precursor adsorption on clean GA (1a), on clean NGA (1b); precursor coverage (1c), precursor screening (1d); ALD growth reactions (1e)
2 Building the inhibitor layer: inhibitor adsorption on clean GA (2a), on clean NGA (2b); inhibitor coverage (2c), inhibitor screening (2d)
3 Selectivity-determining processes: Precursor adsorption on SMI (3a), Precursor penetration of SMI-layer (3b), Precursor decomposition of SMI-layer (3c), inhibitor desorption (3d), inhibitor decomposition (3e), precursor on ALD layer (3f)
4 Gas phase properties: dimerization (4a), gas phase decomposition (4b)
5 Surface state: intrinsic surface properties (e.g., OH density) (5a), intentional modification (5b)
[c] XC: density functional, BS: basis set, K: k-mesh, MC: Monte Carlo, kMC: kinetic Monte Carlo, MD: molecular dynamics
[d] program package used: Gaussian98 (G98), Gaussian03 (G03), Gaussian16 (G16), Vienna ab initio simulation package (VASP), Amsterdam Modelling Suite (AMS)
[e] abbreviations used for the target properties of the computational studies: thermodynamics (TD using energy (E) or Gibbs energy (G)), reaction barriers (TS), spectroscopy modelling (IR), electronic structure analysis (ESA)

Tab. 2. Inherently selective AS-ALD: Computational studies sorted chronologically.[a]

Approach	ALD process	Precursor	Co-reactant	GS	NGS	Research question[b]	Computational Model	Computational Method[c]	Code[d]	Targets[e]	Comments	Year	Ref
Surface termination	Co	(*t*Bu-allyl)Co(CO)$_3$		H-Si(111)	HO-SiO$_2$	1a, 1b	Cluster H-Si(111): $Si_{18}H_{23}$ HO-SiO$_2$: $H_{10}Si_6O_5(OH)_4$	XC: PBE BS: pVDZ	NWChem	TD (E) TS ESA	Precursor reacts only with Si-H which acts as hydrogen donor, analogy to heterogeneous catalysis Exp: IR, AFM, XPS, RBS	2012	[50]
Surface termination	TiO$_2$	TiCl$_4$	H$_2$O	Si(100), HO-Si(100)	H-Si(100)	1a, 1b	Slab Si(100) [6L] Clean, H, or OH termination	XC: PBE BS: 500 eV K: 3x3x1	VASP	TD (E) TS	Precursor chemisorbs on GS, not on NGS, high barrier, endothermic reaction, more favorable ligand loss for OH-termination, Exp: XPS	2013	[85]
Facet selective and inherent	Al$_2$O$_3$	TMA	H$_2$O	Pd, Pt, Ir Cu-OH	Cu	1a, 1b, 1e	Slab Pd, Pt, Ir (111) [3L] Pd, Pt, Ir (211) [9L] Cu(111) [4L], Cu(211) [12L]	XC: PW91 BS: 340 eV K: 3x3x1, 4x4x1 (Cu) Transl. entropy loss	VASP	TD (G) TS	Dissociative chemisorption of precursor with complete hydration on Pd, Pt, Ir. Cu needs OH to be reactive, step edges more reactive, Exp: WCA, QCM, QMS, STM	2014	[218]
Surface termination	HfO$_2$, Al$_2$O$_3$, TiO$_2$	TDMA-Hf, TMA, TiCl$_4$	H$_2$O	HO-Si(100)	H-Si(100)	1a, 1b	Slab H-Si(100) [6L] HO-Si(100) [6L]	XC: PBE BS: 500 eV K: 3x3x1	VASP	TD (E) TS	Trend in exp. selectivity in line with reaction barriers and thermochemistry from DFT Exp: XPS	2014	[53]
Surface termination	Al$_2$O$_3$	TMA	H$_2$O	Si(001)	H-Si(001)	1a, 1b, 1e	Slab Si(001)(2x1) [6L] H-Si(001)(2x1), fully covered, with 1 dangling bond	XC: PBE BS: 500 eV K: 3x6x1 ab initio TD	VASP	TD (G) TS	H$_2$O and TMA on Si, defects (dangling bond), B-doping, H-termination modify selectivity	2016	[193]
Facet selective	CeO$_2$	Ce(thd)$_4$	O$_3$	Pt(111)	Pt(100)	1a, 1b 3f	Slab Pt(100), Pt(111) [3L] CeO$_2$(111) [6L]	XC: PBE (+U for Ce) BS: 340 eV K: 3x3x1	VASP	TD (E)	Precursor fragment has TD preference: GS > ALD layer >> NGS Exp: QCM, TEM, XPS	2017	[54]
Activated	H-In$_2$O$_3$	InCp	H$_2$O/O$_2$	activated H-Si (SiO$_2$)	H-Si	1a, 1b	Slab H-Si(001) [4L] SiO$_2$ [6L]	XC: PBE-D3 BS: 400 eV K: 1x1x1	VASP	TD (G) TS	Computation show faster reaction with OH-groups on GS, no modelling of activation step, Exp.: EBID for activation, XPS, SEM	2017	[219]
Site selectivity	NiO$_x$			Pt (low coordination)	Pt (terrace)	1a, 1b	Slab Pt(111) [5L] Pt(100) [5L] Pt(211) [10L]	XC: PBE BS: 400 eV K: 3x3x1	VASP	TD (E)	Preferred adsorption to low-coordination sites: Pt(111) < Pt(100) < Pt(211), Exp.: TEM, SE, XPS, IR, EXAFS	2018	[220]
Edge selective	MO$_x$ (M = Fe, Co, Ni)	MCp$_2$ (M = Fe, Co, Ni)	O$_3$	Pt-edge	Pt(111), Pt(100)	1a, 1b	Slab Pt(111) [5L] Pt(100) [5L] Pt(edge) [8L]	XC: PBE BS: 400 eV K: 3x3x1 microkinetic analysis	VASP	TD (E) TS	Reactivity: edge > 111 > 100 for all precursors, selectivity T-dependent, activity: NiCp$_2$ > FeCp$_2$ > CoCp$_2$, Exp.: SE, FTIR	2019	[221]
Activated	ZnO	DEZ	H$_2$O	activated H-Si (SiO$_2$)	H-Si	1a, 1b	Slab H-Si(001) [4L]	XC: PBE-D3 BS: 400 eV	VASP	TD (G) TS	Computation show faster reaction with OH-groups on	2019	[88]

							SiO_2 [6L]	K: 1x1x1			GS, Exp.: EBID (activation), TEM, EDX, SE, SEM	
Surface termination	Ru	T-Rudic	H_2O or O_2	H-Si	SiO_2	1a, 1b, 1e	Cluster H-Si(001): $Si_{49}H_{52}$ HO-Si(001): $Si_{49}H_{40}(OH)_{12}$	XC: B97D3 BS: LanL2DZ, def2SVP	G16	TD (E)	Precursor has TD preference for GS, kinetic preference assumed (BEP), Exp: AES, SEM, XPS, XRD, XRR, SE	2021 [83]
Surface termination	SiO_2	DIPAS	O_3	SiO_2	SiN	1a, 1b, 1d	Cluster SiO_2: $Si_9O_7H_{14}$ SiN: $Si_9N_7H_{21}$	XC: M06-2X BS: def2-TZVP	G16	TD (E) TS	DFT for precursor screening: DIPAS largest chemisorption barrier difference (GS-NGS) Exp: WCA	2021 [222]
Inherent	MnO_x	$Mn(EtCp)_2$	H_2O	Pt, Cu	SiO_2	1a, 1b	Slab Pt(111) [4L] Cu(111) [4L] HO-SiO_2 [13L]	XC: PBE [vdW] BS: 400 eV K: 3x3x1	VASP	TD (E) TS ESA	Selectivity is negatively correlated to EN differences of M-O bond (TD), Exp.: SE, SEM, AFM, EDS, XPS	2021 [86]
Inherent	Al_2O_3	TMA	H_2O	SiO_2	Pt	1a, 1b	Slab SiO_2(0001) [1 nm], Pt(111) [1 nm]	XC: PBE, optB86b BS: [n.a.]	VASP	TD (E)	TD of precursor on GS much stronger, "plasma energy window"	2021 [223]
Surface termination	SiO_2	BDIPADS	O_3	SiO_2	SiN	1a, 1b, 1e	Cluster SiO_2: $Si_9O_7H_{14}$ SiN: $Si_9N_7H_{21}$	XC: M06L BS: def2-SVP	G16	TD (E) TS	Lower barrier and TD driving force on GS vs. NGS for adsorption and ligand decomposition, Exp.: WCA, XPS, SE, TEM, EDS	2022 [224]
Inherent	Ta_2O_5	$Ta(OEt)_5$	O_3	basic oxides (Al_2O_3, HfO_2)	acidic oxides (MnO_2, SiO_2, Ta_2O_5)	1a, 1b, 1e	Slab SiO_2(001) ([4L] HfO_2 ($1\bar{1}1$) [3L] Al_2O_3(0001) [3L]	XC: PBE-D3 BS: 400 eV DDEC6 charges Stat. TD	VASP Chargemol VASPKIT	TD (G) TS ESA	Surface acidity a good descriptor for selectivity, H-transfer decisive for precursor decomposition, Exp.: XPS, TEM, AFM, MS, QCM	2022 [135]
Inherent	TaO_x	$Ta(tBuN)(NEt_2)_3$	H_2O	SiO_2, TaN	Cu	1a, 1b, 1e	Slab HO-SiO_2(001) [4L] Cu [n.a.]	XC: PBE_D3 BS: [n.a.] Stat. TD	VASP VASPKIT	TD (G) TS	EtOH cycle to reduce CuO_x to Cu, precursor lower reactivity on reduced NGS than OH-terminated GS Exp: QCM, XPS, TEM, SE	2023 [51]
Surface termination	TiO_2	$TiCl_4$	H_2O	HO-Si(100), HO-Si(111)	H-Si(100), H-Si(111), Cl-Si(100), Cl-Si(111)	1a, 1b	Cluster Si(100): $Si_{15}H_{20}$ and $Si_{35}H_{48;}$ Si(111): $Si_{17}H_{24}$ both with H, Cl, OH-termination and OH defects	XC: B3LYP-D3 BS: 6-311G+(d,p) for Si_{15}, Si_{17}; LanL2DZ//6-311+G(d,p) for Si_{35}	G09	TD (E)	TD-screening of surface terminations, only O-termination and defects react with precursor Exp.: XPS, AFM	2023 [52]
Inherent	Al_2O_3	TMA	H_2O	SiO_2	W	1a, 1b	Slab H-SiO_2(0001) [1 nm], W(110) [1 nm], H-WO_x(010) [1 nm]	XC: PBE, optB86b BS: [n.a.] K: 3x3 (SiO_2, W(110), 3x4 (WO_x(010))	VASP	TD (E)	TD of precursor on GS much stronger, importance of oxide removal on NGA "plasma energy window"	2023 [225]
Site-selective	Al_2O_3	DMAI	H_2O	TiO_2(110)	Si	5a	Slab rutile-TiO_2(110), (100), (101), (001) [8L]	XC: PBE+U BS: 400 eV K: 3x3x3 Stat. TD	VASP	TD (G)	Point defects for patterned ALD, prediction of inhibition for clean TiO_2, selective hydration for O	2023 [227]

											vacancies and interstitials, used in experiment later[226] Exp.: SE, AFM, XPS, STM	
Inherent	Co	$Co(tBu_2DAD)_2$	NH_3	Co, Cu, Pt	SiO_2	1a, 1b, 4b 1e	Slab SiO_2(001) and H-SiO_2(001) [7L] Co(111), Pt(111), Cu(111) [3L]	XC: PBE-D3 (U for Co) BS: 500 eV, K-spacing: 0.003 nm^{-1}	VASP	TD (E) ESA	Co growth on metal surfaces TD favorable. Poor nucleation on SiO_2. Crucial role of reductant NH_3.	2023 [134]
Surface termination	TiO_2	$TiCl_4$ 26 Ti prec	H_2O	HO-SiO_2	TMS-SiO_2	1a, 1b 2a, 2b 3a, 3c, 3d	Slab Si/SiO_2 [n.a.] Gas phase model	XC: PBEsol-D3 BS: DZVP K: G-only	CP2K Phonopy	TD (G) RR	precursor screening, physisorption and chemisorption selectivity, selectivity loss through TMS reaction with $TiCl_4$ and nucleation	2023 [81]
Inherent	Nb, Ta	$M(tBuN)(NEt_2)_3$ (M = Nb, Ta)	H_2O	SiO_2	Cu	1a, 1b, 1e	Slab SiO_2(001) [4L] Cu(111) [3L]	XC: PBE-D3 BS: 400eV K: 3x3x1	VASP	TD (E) TS ESA	sluggish dissocation kinetics on NGA determine selectivity, DFT-informed nucleation model Exp: SE, SEM, AFM	2024 [140]
Inherent	Ru	$Ru(EtCp)_2$	O_2	W	TiN, SiO_2	1a, 1b	Slab HO-SiO_2(001) [6.2 Å] W(110) [6.3 Å]	XC: PBE-D3 BS: 300 eV K: 3x3x1	VASP kMC	TD (E)	Easy decomposition on GS, large barrier on NGA Exp: TEM, AES, QCM	2024 [228]
Surface modification	HfO_2	TDMAHf, $Hf(OtBu)_4$, $HfCl_4$	H_2O	TiN	SiO_2	1a, 1b	Cluster HO-Si(100): $Si_{15}H_{16}(OH)_4$ H_3Si-Si: $Si_{15}H_{16}(OSiH_3)_4$	XC: B97-D BS: def2-SVP and LANL2DZ (Hf, Si)	G16	TD (G)	DIPAS leads to SiH_3-terminated SiO_2 which is then NGS, reactivity profile matches exp Exp.: XPS, XRR, WCA, SEM, AES	2024 [229]

[a] SiO_2 and Al_2O_3 are α-modifications if not stated otherwise. X-[surf](facet) is used as notation for X-terminated [surf](facet) surface.
[b] abbreviations used for research questions tackled by the computational studies:
1 Precursor-surface interactions: precursor adsorption on clean GA (1a), on clean NGA (1b); precursor coverage (1c), precursor screening (1d); ALD growth reactions (1e)
2 Building the inhibitor layer: inhibitor adsorption on clean GA (2a), on clean NGA (2b); inhibitor coverage (2c), inhibitor screening (2d)
3 Selectivity-determining processes: Precursor adsorption on SMI (3a), Precursor penetration of SMI-layer (3b), Precursor decomposition of SMI-layer (3c), inhibitor desorption (3d), inhibitor decomposition (3e), precursor on ALD layer (3f)
4 Gas phase properties: dimerization (4a), gas phase decomposition (4b)
5 Surface state: intrinsic surface properties (e.g., OH density) (5a), intentional modification (5b)
[c] XC: density functional, BS: basis set, K: k-mesh, MC: Monte Carlo, kMC: kinetic Monte Carlo, MD: molecular dynamics
[d] program package used: Gaussian98 (G98), Gaussian03 (G03), Gaussian16 (G16), Vienna ab initio simulation package (VASP), Amsterdam Modelling Suite (AMS)
[e] abbreviations used for the target properties of the computational studies: thermodynamics (TD using energy (E) or Gibbs energy (G)), reaction barriers (TS), spectroscopy modelling (IR), electronic structure analysis (ESA)

3.1 Molecules

ALD approaches use molecular precursors to deposit thin films. Often, also the co-reactant is a molecule (mostly H_2O) or a molecular gas (e.g., O_2, O_3). Even in energy-enhanced approaches (e.g., plasma), the reactive species are created from molecules.[230] In inhibitor-based area-selective approaches, the inhibitor is also mostly a molecular species (Tab. 1). Thus, the modelling of molecular properties and reactivity is crucial for the understanding of AS-ALD processes.

3.1.1 Dimerization

ALD precursors for group 13 elements are Lewis acids and thus have the tendency to form bonds with Lewis bases. This includes the heteroatoms of the ligands or even the alkyl groups and leads to dimerization of the precursor (Fig. 10.).[231,232]

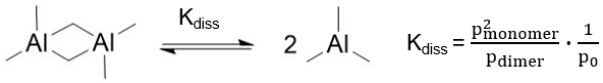

Fig. 10. Dimerization reaction of Al precursors shown at the example of TMA with the equilibrium constant K_{diss} for the dissociation defined via the partial pressures $p_{monomer}$ and p_{dimer} and standard pressure p_0. Reprint with permission from reference [233].

In recent years, it became apparent that the degree of dimerization has a strong influence on the reactivity of the precursor since it (i) reduces the Lewis acidity and thus the surface reactivity of the precursors and (ii) increases the steric bulk which is important for inhibitor-based approaches.[234] Thus, several studies investigated the influence of dimerization on the selectivity in AS-ALD process. The dimerization tendency is typically expressed as dissociated dimer fraction (DDF) and is derived from the equilibrium constant K of the dimerization reaction:

$$K = \frac{4\,DDF^2}{1 - DDF^2} \cdot \frac{p}{p_0}\ ;\ DDF = \sqrt{\frac{K}{4\frac{p}{p_0} + K}} \qquad 3.1$$

Kim et al. found the dimerization of dimethyl-aluminum isopropoxide (DMAI) to be the major factor for the high deposition selectivity compared to trimethylaluminum (TMA) when using ethanethiol as inhibitor.[160] They used DFT approaches (B97-D3/def2-SVP) to compute the dimer dissociation enthalpy of TMA to be 85.4 kJ·mol^{-1} which was found to be close to the experimental enthalpy change of the reaction (ca. 83 kJ·mol^{-1})[235]. Only 2% of the precursor exists as dimers under the ALD conditions modelled (T = 150 °C, p = 1.3 mbar) which corresponds to DDF = 98%. In contrast, DMAI shows a dimer dissociation enthalpy of 267.3 kJ·mol^{-1} which leads to a negligible DDF (10^{-8} %). The authors assumed the same entropy of dissociation and based their conclusions on enthalpy changes (ΔH). The effect of this dimerization on the adsorption of DMAI on Al_2O_3 has very recently been investigated using MLPs.[236] The dimerization energy was computed with DFT approaches (PBE-D3(BJ), 450 eV, VASP) to 239 kJ·mol^{-1} (DMAI) and 94 kJ·mol^{-1} (TMA). The MLP values were ca. 10 kJ·mol^{-1} higher. Already from these examples, it

becomes clear that different DFT approaches can lead to values differing by 10-30 $kJ \cdot mol^{-1}$, depending on the choice of the specific setup (density functional, basis set). This question of "validation" has recently been addressed for precursor dimerization by computing the values at the highly accurate CCSD(T) level with complete basis set (CBS) extrapolation, thus eliminating major error sources. In agreement with previous computational studies, aluminum alkyl precursors were found to be monomeric, while tris(dimethylamino)aluminum (TDMAA) and DMAI are dimeric under typical ALD conditions. The chlorinated aluminum alkyls are partly dissociated depending on temperature and pressure.[233]

The influence of precursor dimerization has not yet been investigated for intrinsically selective approaches where the different reactivity of monomeric and dimeric forms could be used to discriminate between two surfaces, e.g., when one can open the dimer and the other one cannot.

3.1.2 ALD-related molecular properties

ALD precursors have to fulfill a set of properties which have been summarized in the ALD literature.[40,46,67,75,234] The most important factors are: (i) stability against decomposition in the gas phase, (ii) reactivity towards the substrate and (iii) significant vapor pressure under ALD conditions. Precursor stability is not specific for AS-ALD approaches and has been treated in the ALD literature for a range of precursors.[237–240] The (selective) reactivity towards the substrate(s) will be treated in section 3.3.1. This leaves vapor pressure to be discussed here although it is also not specific for AS-ALD. Most computational approaches rely on quantitative structure-property relationships (QSPR)[241] or group-contribution (GC)[242] approaches. They are intrinsically empirical and lack predictive power. *Ab initio* simulations are complicated by the need to properly describe the gas as well as the liquid phase. Recently, a computational workflow based on quantum mechanically derived force fields (QMDFF)[243] was presented which allows the vapor pressure prediction for a range of (AS-)ALD precursors with good accuracy.[244] However, considering the monomer-dimer equilibrium of group 13 precursors (see section 3.1.1) is not yet possible. It can be expected that further development in the field of machine learning will make the prediction of complex properties like vapor pressure more reliable in the future.

3.1.3 Screening

One advantage of computational modeling in AS-ALD is the treatment of large datasets without the need to optimize process conditions for every precursor. Thus, screening approaches have been developed over the years where computational modeling was used to select precursors and/or inhibitors for a given task of selective deposition from a large set of possible candidates. The question of precursor chemistry and precursor choice has been discussed in the ALD literature quite intensively.[39,40,245] Recently, a combination of molecular DFT and ML approaches has been used to predict precursor reactivity for different surface terminations in the framework of AS-ALD.[246] The goal was to extract molecular design descriptors which determine the deposition selectivity. It needs to be seen if more detailed studies support these preliminary findings. Since

the molecular reactivity is hard to correlate to AS-ALD selectivity, most screening approaches focus on the surface chemistry of the precursors which will thus be treated in section 3.3.1.

3.2 Surfaces

3.2.1 Setting up a computational model

Selectivity in AS-ALD stems from the difference in precursor reactivity with GS and NGS, either via an intrinsic reactivity difference or after modification of one surface (activation or inhibition). Thus, the state of the surface is crucial for this selectivity and has been the target of computational modeling. In ultra-high vacuum (UHV) surface science investigations in the last decades, several reliable surface models were derived and used in computational modeling.[247] This is especially true for elemental semiconductors, low-index metal surfaces and binary oxide surfaces. For more complex or less-investigated substrates, it is often necessary to develop a new surface model. But even in the case of established models, the lack of detailed information from the experimental studies on the exact nature of the substrate often impedes an accurate representation. Hence, setting up a suitable model for the surface in AS-ALD is a major challenge and crucially determines the accuracy of the results compared to experiment.[214] The modelling would highly benefit from more studies revealing detailed experimental information about the surface state under ALD condition which is commonly done with UHV surface science approaches.[248] While some promising new developments exist,[249–252] this information is often scarce and leaves some ambiguity in setting up the computational surface model.

3.2.2 Surface state

There are many reports in the AS-ALD literature that the number of nucleation sites is crucial for selectivity. Most prominently, for oxide surfaces, the density of reactive OH-groups at the surface is important. For example, for tungsten ALD, it has been experimentally found that suppressing the formation of hydroxyl groups during the substrate cleaning process of NGS SiO_2 (the so-called piranha clean) extends the selectivity window for the AS-ALD process.[59] Also, suppressing surface oxidation of the silicon substrate (NGS) leads to selective adsorption on the OH-terminated SiO_2 GS.[57] However, in most computational studies, idealized surface models are used.[69] For SiO_2 for example, most often the (0001) facet of its a-quartz modification (Fig. 11.c) is used (Tab. 1 and 2) which leads to a highly ordered pattern of hydrogen bonds at the surface of the slab and an unrealistically high OH density of 9.34 OH nm^{-2} which exceeds the average experimental density of 4.9 OH nm^{-2}.[214,253] Some studies thus used partially hydroxylated cluster models or periodic slabs.

For elemental semiconductors, surface termination also plays a crucial role. In the case of silicon, the bare surface, H, and OH-termination have been investigated. Here, well established computational models exist, and the main question regards the matching of computational model and experimental conditions.[254] For the modeling of metal surfaces, low-index surfaces are usually taken as models for the often-nanocrystalline substrates used in experiments. Here,

frequently the decisive question is whether a native oxide layer exists on the metal surface. Modelling metal oxides is quite challenging and rarely investigated in AS-ALD. Often, neither the stoichiometry nor the surface corrugation are well understood. For Cu and Cu_xO it has recently been found that their reactivity is very similar towards aromatic inhibitor molecules.[217] The reduction of cupric or cuprous oxide was hypothesized to be facilitated by inhibitor deprotonation for methylsulfonic acid (MSA) based on thermodynamic considerations.[87]

3.2.3 Crystalline vs. amorphous models

Even partially hydroxylated models still use a crystalline substrate. Modeling the amorphous nature of oxides has rarely been attempted in AS-ALD (Tab. 1).[69] In a recent study, it was found that considering the amorphous nature of the SiO_2 surface (Fig. 11.a,b) can lead to even qualitative changes in the surface chemistry since the undercoordinated atoms at the surface are more flexible compared to atoms in a crystalline model.[67,214] For the slab approach, a pseudo-amorphous model has to be used which still has a unit cell and periodic boundary conditions but provides a less-ordered arrangement of atoms in the cell. This is typically developed by simulated-annealing approaches to high-temperature MD runs which computationally "melt" the crystalline surface.[255,256]

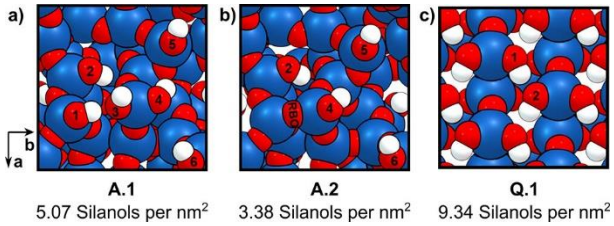

Fig. 11. Unit cells of amorphous a-SiO_2 models (a, b; b contains an reactive bridge oxygen (RBO)) and (c) idealized α-quartz model. The numbers 1–6 denote the oxygen atoms of the surface silanol groups. Color code: Si - blue, O - red, H - white. Reprint with permission from reference [214].

3.3 Intrinsically selective AS-ALD

An overview over computational studies of AS-ALD making use of the intrinsic reactivity differences between GS and NGS is found in Tab. 2. The vast majority of studies in this field use computational approaches to explain the experimentally observed selectivity for a given precursor or a set of precursors. Thereby, precursor adsorption on GS and NGS is mostly investigated with DFT approaches (research question (RQ): 1a, 1b in Tab. 2) with one study using a kMC ansatz in addition.[228] Mostly, thermodynamic as well as kinetic driving forces were investigated but in some cases an analysis was based on thermodynamic driving forces alone[52,54,220,223,225,227–229] or the kinetic driving forces were estimated via the BEP relationship.[83] The slab approach was used in most studies. But for modelling of silicon surfaces, cluster approaches with different terminations (bare, H, OH, NH_2, Cl, SiH_3) are still common until today.[229] Nearly all studies with

slab approaches used the PBE density functional (one used PW91). Cluster approaches mostly relied on hybrid density functionals (B3LYP, M06-2X) with one exception of a GGA functional (B97-D). Some cluster calculations used double-zeta basis sets (def2-SVP, LanL2DZ) while the mostly used triple-zeta basis sets (def2-TZVP, 6-311G+(d,p)) are generally recommended for DFT energy computations.[108] The cutoff energy for slab calculations (which determines the accuracy of the basis set in PBC computations) varied depending on the surface modelled from 300-500 eV while some studies do not report this value. As computational codes, VASP[257–260] is used exclusively for slab calculations, while GAUSSIAN[261] is used for clusters with one exception (NWCHEM[262]). The reporting of electronic energy differences (ΔE) is the standard, while some studies used *ab initio* thermodynamics or statistical thermodynamics approaches to consider the finite temperature and pressure under ALD conditions (ΔG). Only one study combined the DFT investigations with kMC simulations for packing predictions.

3.3.1 Explain precursor differences in reactivity on GS and NGS

Ultimately, the selectivity in intrinsically selective AS-ALD is determined by the chemoselectivity of the precursor (i.e., faster reactivity on the GS) leading to a nucleation delay on the NGS (Fig. 1.d). Thus, reactivity differences on GS and NGS are the focus for computational investigations. The first study by Kwon et al. investigated the selective ALD of Co on silicon.[50] It was shown experimentally that the precursor only reacts with the H-terminated silicon surface (GS) while the OH-terminated surface (NGS) does not react (Fig. 12.). This was explained with catalytic hydrogenation of the precursor by the H-Si(111) surface. The computational study reveals the thermodynamic driving force and the lower reaction barrier for the reaction on the GS (Fig. 12.).

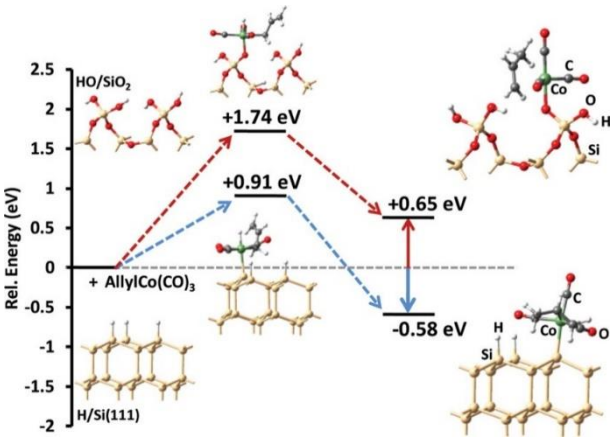

Fig. 12. Computed reaction pathway (PBE/pVDZ) for the ALD reaction of allylCo(CO)$_3$ on the HO-SiO$_2$ and H-Si(111) surfaces. Color code: H, white; O, red; Si, gold; C, gray; and Co, green. Reprint with permission from reference [50].

The study used a cluster model of the silicon substrate, which is still seen in selected works today.[229] As outlined in section 2.8.1, this is generally assumed to be suitable for the local reactivity of precursors when questions of coverage are not relevant. Electronic structure analysis

(ESA) was also carried out here, namely the calculation of atomic partial charges to explain the trends in surface reactivity. As can be seen in Tab. 2, this is quite rarely the case, and most studies focus on the computation of thermodynamic preferences and reaction barrier differences alone. One year later, the same group investigated the reverse selectivity in an AS-ALD process of TiO_2 where the H-terminated Si(001) surface was the NGS and growth took place on the bare and OH-terminated silicon substrate.[85] This time, slab models were used.

That the usage of ESA can be helpful to rationalize findings was shown for AS-ALD of MnO_x on Pt and Cu (GS) vs. SiO_2 (NGS), where selectivity was found to be negatively correlated to electronegativity differences of the M-O bond based on thermodynamic computations.[86] Also, the usage of surface acidity as a descriptor for the selectivity of basic oxides (GS) compared to acidic oxides (NGS) was based on atomic partial charge analysis.[135]

The investigation of different surface terminations for reaching area-selectivity is a major topic in computational studies. In addition to the studies outlined in the previous section,[50,85] the variation of surface termination on silicon and silicon oxide has been analyzed in several studies. Hydrogen-termination of Si(100) and Si(111) has been found to be a good way to create an NGS for ALD of TiO_2 (GS: bare Si or HO-Si[52,53,85]) and Al_2O_3 (GS: bare Si or HO-Si[53,193]), while it acts as GS for metal deposition (ALD of Co,[50] Ru[83]) against SiO_2.

Further selective deposition on two dielectric surfaces was shown for ALD of SiO_2 on SiO_2 and not on SiN using di(isopropylamino)silane (DIPAS)[222] or 1,2-bis(diisopropylamino)disilane (BDIPADS) as precursors[224], ALD of Al_2O_3 on TiO_2 and not on Si,[227] and ALD of HfO_2 on TiN and not on SiO_2.[229] A comparison of various basic (GS) and acidic (NGS) oxide surfaces was investigated for ALD of Ta_2O_5 were surface acidity was found to be a good descriptor of the observed selectivity.[135]

For selective deposition on metals, while not depositing on dielectrics, computational investigations helped to understand the selectivity of MnO_x deposition on Pt and Cu and not on SiO_2,[86] and for Ru deposition on W and not on SiO_2 and TiN.[228] In these cases, thermodynamic preference for the precursor adsorption on the GS was found as well as lower reaction barriers (kinetic preference).

But also the inverse selectivity of ALD on dielectrics and not on metals was analyzed for TMA deposition on SiO_2 and not on Pt[223] or not on W,[225] TaO_x on SiO_2 and not on Cu.[51,140] For the Cu surface, it was found that a co-reactant (ethanol) was important to reduce the oxide layer and decrease reactivity of the NGS to achieve selectivity. The native oxide termination including OH-groups did not lead to a selective deposition.[51] The removal of the oxide layer – here via plasma treatment – was also found to be important to make W an NGS.[225]

3.3.2 Find the optimal combination of surfaces

Screening methods combining DFT calculations and experiments have been employed to identify the largest differences in chemisorption reaction barriers for a class of precursors used in the AS-ALD of SiO_2, targeting growth on SiO_2 (GS) while minimizing growth on SiN (NGS). The experimentally used DIPAS turned out to be the best choice by this measure.[222] For fast screening,

a cluster approach with a minimal cluster of the SiO_2 surface was used here as well as in many other studies. Although it has been shown that the adsorption energies and reaction barriers are not converged with respect to the cluster size using such small clusters,[182] the trends can often be reproduced quite accurately. Screening was also conducted on the surface site using a range of basic and acidic oxides to explain the trend in selectivity based on surface acidity.[135]

3.3.3 Identify a suitable set of surface terminations or facets

Computational approaches can also be used to identify suitable surface terminations for selective ALD. The deposition of Al_2O_3 from TMA and water has been theoretically investigated by Longo et al. with a systematic analysis of the influence of surface termination, surface defects and doping on the deposition selectivity.[193] The ALD conditions were modelled here using *ab initio* thermodynamics which is common in heterogeneous catalysis but has rarely been applied in AS-ALD modelling.

For the ALD of CeO_2 on platinum surfaces, facet-selectivity has been observed and explained by computational modelling.[54] In a slab-based approach, the preference of Pt(111) over Pt(100) for growth could be explained by the different thermodynamic preferences for adsorption of the precursor $Ce(thd)_4$. Notably, this study uses a Hubbard-model type correction for the DFT results (DFT+U) which leads to a localization of the f-electrons and compensates the delocalization error in common GGA-type functionals (see section 2.1.3) for the price of introducing an empirical parameter. The same group reported site-selective adsorption on the same surface where the preference for precursor adsorption on undercoordinated Pt(211) sites was shown compared to the adsorption on (100) and (111) terraces.[220]

In a large-scale study, Lu et al. investigated terraces and step edges on Pd, Pt, Ir and Cu surfaces for the ALD of Al_2O_3.[218] In combination with experimental analysis, they could show that full dissociation of the precursor occurs on Pd, Pt, and Ir while Cu needs hydroxyl-groups to be reactive towards TMA. In addition, a stronger thermodynamic and kinetic driving force was found for the reactivity at step edges of all surfaces, which were modeled by large slabs of the (211) facets.

3.4 Inhibitor-based AS-ALD

Computational studies of AS-ALD using an inhibitor-based approach creating a inhibitor layer on the NGS and allowing ALD on the GS (Fig. 1.f) are found in Tab. 1. Similar to the intrinsically selective approach, most studies combine experimental and computational work here. However, there are quite a few more entirely computational studies addressing key questions in inhibitor-based AS-ALD.[81,157,159,200,209,214,236,263]

Adding another chemical species (i.e., the inhibitor) to the ALD process, leads to more diverse research questions being tackled compared to modelling inherently selective AS-ALD. Most studies address the adsorption structure and energetics of the inhibitor on the NGS (RQ 2a in Tab. 1), while a few also look at the inhibitor adsorption on the GS (RQ 2b). The coverage is studied quite often (RQ 2c) in line with this being one of the key factors for selectivity in this AS-ALD approach. Similar attention is paid to the modelling of precursor chemistry (and sometimes also

the co-reactant). While this might seem surprising at first, it is a clear indicator of the now-established knowledge that only a smart combination of inhibitor and precursor for a given combination of GS and NGS leads to a selective ALD process.[67,234] Most of these studies analyze the interaction of the precursor with the adsorbed inhibitor (RQ 3a) and often compare it to adsorption on the clean surfaces (RA 1a, 1b). The chemical decomposition processes of the inhibitor layer (RQ 3b-e) have been studied much less but increasingly so in recent years.

Thermodynamic as well as kinetic driving forces were investigated in most cases but also for inhibitor-based approaches some studies based their conclusion on thermodynamic driving forces alone.[81,138,158,162,203,204,206,209,264] While the investigation of spectroscopic signatures was done in only one study (IR[113]), there are a few more studies in this research field where ESA was applied, although mostly limited to computing atomic partial charges.

In this research area, the modeling of the surface coverage with kMC or stochastic models is getting more common. However, most studies use DFT-based approaches for a microscopic picture of AS-ALD related chemistry in a single-adsorbate approach. Sometimes, both approaches are combined. Similar to intrinsically selective AS-ALD modelling, the slab approach is used in most studies, however, cluster models are still quite popular for silicon surfaces with different terminations. In early studies, the experimentally used inhibitors were likewise truncated due to limited computational capabilities.[181,200] This is nowadays only done for polymers,[205] or series of compounds.[212]

The majority of slab studies used the PBE density functional (one used BEEF-vdW, one used PBEsol). But especially for cluster studies, other density functionals were also applied (B3LYP, M06(-2X,-L), B97). Several flavors of correcting for missing dispersion interaction were used. Most common is the DFT-D3 correction as in most material science studies. The usage of double-zeta basis sets is still common in cluster computations. The cutoff energy for plane-wave basis sets in slab calculations varied from 400-550 eV. Most slab calculations used the program package VASP, but also other codes (CP2K, QUANTUMESPRESSO, AMS) are reported. For cluster calculations, GAUSSIAN is the dominating code, with AMS or Q-CHEM being used in some studies.

The reporting of electronic energy differences (ΔE) is also the most common approach in this field, but Gibbs energies (ΔG) are reported quite often as well. Surprisingly at first, this was more common in early studies and is now done less regularly. This is explained by slab computations becoming the standard approach for surface reactivity and the much higher computational demand to compute Gibbs energies for this approach (see section 2.8.2).

The major approaches to develop inhibitors are based on SAMs and SMIs as outlined in section 0. Only two computational studies addressed other types of inhibitors: A hydrophobic CF_x layer was modelled with a CF_3-terminated Si(001) surface in a slab model by Kim et al. to gain insight into Pt ALD on protected versus unprotected silicon surfaces.[204] Protection of the same surface by molecular-layer deposited indicone was modelled in the second study by Lee et al.[205] It should be noted that the precursor-inhibitor approach discussed below also leads to a surface modification (OH groups at the SiO_2 surface are replaced by -OCH_3 groups). This suggests that the line between

surface functionalization and inhibitor adsorption is blurry. These works will be discussed together with other SMI approaches below.

The pioneering computational study by Musgrave and Xu appeared in 2004 (focus: decomposition of SAM-layer) while the next study by Prinz and co-workers was published already 6 years later (focus: precursor reactivity with NGS as well as SAM). Beginning in 2017, computational studies (mostly computational parts in experimental publications) appeared more regularly with a significant increase starting in 2020.

3.4.1 Building the inhibitor layer

The core requirement for building the inhibitor layer is the selective interaction of the inhibitor molecule with the NGS and not with the GS. Thus, chemoselectivity of adsorption is crucial here – similar to the chemoselectivity for the precursor in inherently selective AS-ALD.

3.4.1.1 SAMs as inhibitors

The main blocking mechanism for SAMs is steric blocking (Fig. 5.c,d). Thus, a continuous and dense monolayer formation is crucial. In experiment, this ideal monolayer is not straightforward to achieve.[64,265] Surprisingly, very few AS-ALD related studies investigated this building up of the SAM inhibitor layer. In the most extensive and elaborate computational study by Clerix et al., alkanethiolate SAMs with differing chain lengths ($C_{1\text{-}12}$) were investigated on copper.[263] The authors conclude that the type and structure of the surface, the SAM chain length and the resulting coverage determine the phase of the SAM layer and thus the blocking properties. They could show that for longer chain lengths (C_6, C_{12}), lying-down and standing-up phases are found, and the saturation coverage is determined through steric hindrance. Interestingly, they show that the SAM behavior on Cu is different from the well-studied behavior on Au[266] where intermolecular interactions in the SAM layer are decisive. The Cu-SAM interaction still dominates at saturation coverage which is in line with the higher reactivity of the Cu surfaces in other surface chemistry studies.[267–269] The authors also show that short chain-length monomers (C_1, C_2) show no coherent phase on the surface and their ordering is determined by steric hindrance.[138] Indeed, these short chain "SAMs" should better be termed SMIs which show exactly this behavior as discussed in the next paragraphs. Another study by Wojtecki et al. examined the SAM packing density as function of the head group combined with experimental results.[138]

Nevertheless, it is a bit surprising at first that there are so few computational investigations although SAMs have been an intensively researched topic in experimental AS-ALD for a long time.[270] The reason is threefold: (i) SAM layer formation is the crucial step for blocking and this has been investigated in other communities for a long time already,[271] (ii) the investigation of inhibitor layer formation requires extensive computational efforts and know-how,[138] and (iii) the decomposition of the layer is essentially always precursor interaction with the alkane chain of the tail group which has been already modelled in cluster studies.[200–202]

3.4.1.2 SMIs as inhibitors

The shift in the academic AS-ALD community from SAMs to SMIs is also reflected in the computational modelling. The vast majority of studies deal with SMI-based approaches (Tab. 1). The major advantage of SMIs is the direct application from the gas phase while SAMs usually require wet chemical application. The first study in this field by Mameli et al. investigates an SMI where many aspects of computational modelling have been examined over the years: acetylacetone (Hacac).[69] This inhibitor was proposed earlier for AS-ALD in an experimental study by Yanguas-Gil et al.[68]

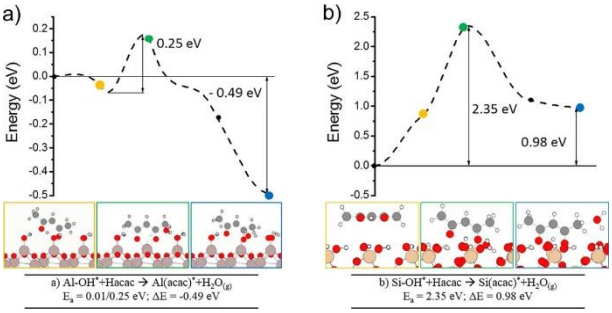

Fig. 13. DFT (GGA/PBE-D3) paths for the acetylacetone (Hacac) adsorption on (a) Al_2O_3 and (b) SiO_2 surfaces. Stationary points are marked by colored dots corresponding to the insets below. Color code: silicon, pink; aluminum, light gray; hydrogen, white; oxygen, red; carbon, gray. Reprint with permission from reference [69].

The computational part of this study reveals that the selectivity in the ALD process stems from the chemoselective adsorption of Hacac on the NGS (Al_2O_3) w.r.t. the GS (SiO_2). Interestingly, this is a common theme in AS-ALD between two dielectric surfaces, the inhibitor chemisorbs on both surfaces. As shown in Fig. 13., the condensation reaction with the surface-OH groups leads to elimination of H_2O and the formation of a bidentate (chelate) binding mode on both surfaces. However, selectivity stems from two factors now. First, a thermodynamic driving force is found on the NGS (ΔE = -47 kJ·mol^{-1}, Fig. 13.a) while the reaction is unfavorable on the GS (ΔE = 95 kJ·mol^{-1}, Fig. 13.b). Second, and more importantly, the reaction barriers vastly differ. While a barrier of only $\Delta E^{\ddagger}$ = 24 kJ·mol^{-1} is found on the NGS, it is 227 kJ·mol^{-1} on the GS. Notably, both reactions start with a weakly bound Hacac species on the surface (Fig. S6 in the SI of ref. [69]). These states are called ‘precursor-states’ in the surface science literature (this term will not be used further to avoid confusion with the ALD usage of the term ‘precursor’),[272] and are often physisorbed, which means they are bound only by London dispersion forces without a significant covalent bonding contribution (other definitions of physisorption exist but this one is supported by quantitative bonding analysis[272]).

The next step in the reaction mechanism is the formation of an intermediate species (yellow dots in Fig. 13.) which shows hydrogen-bonding of the inhibitor to the NGS and physisorption for the GS. Why do these species differ so much although both surfaces are OH-terminated? The reason is the different orientation of the OH-groups which is pointing towards the inhibitor (NGS) or away from the inhibitor (GS). This is one example, where the detailed arrangement of surface atoms is decisive for the selectivity of inhibitor adsorption which has been discussed in detail in

the supporting information of this study. However, it also shows the care that needs to be taken to select appropriate surface models (section 2.8) since other facets in the modelling could show different arrangements of these OH-groups. One feature here, which is also observed in other studies,[214] is the role of the condensation product H_2O which stabilizes the product via hydrogen-bonding. This study thus highlights several key aspects of computational investigations towards the selective inhibitor layer buildup of SMIs: thermodynamic driving force and kinetic preference for SMI on NGS, role of reactive surface groups, surface chemistry steps before and after the rate-determining transition state. Thus, it transpires that for an understanding of selectivity in SMI-based approaches, a detailed analysis of the surface chemistry is crucial.

In a subsequent study on this system, the authors investigated the coverage-dependent adsorption behavior of Hacac which shows a mixture of mono- and bidentate bonding modes. To this end, they applied a stochastic modeling approach, which had been proposed by Khan et al. before, based on work by the Buriak group[71,170] (section 2.5.1), to obtain theoretical saturation coverages. It is also one of the few studies comparing the results from different DFs with the conclusion that they do not differ in predicted trends.[113] The insight that different bonding modes of an inhibitor could be combined to achieve full coverage of the surface was further elaborated by the same group to combine bidentate Hacac bonding with monodentate alcohols as inhibitors. In this study, the authors used their own RSA approach to identify effective gap sizes for designing the best combination of SMIs to achieve full coverage.[158] The idea to combine different SMIs to achieve ideal coverage of the surface has been picked up in other studies later on.[214] For AS-ALD using trimethoxypropylsilane (TMPS), a computational study found a mixture of mono-, bi- and tri-dentate bonding modes on SiO_2 to be the optimal combination to achieve high coverage.[214]

The need to look beyond the mono-molecular picture had been found before by the Lee and Kim groups. In a seminal work, they proposed the usage of 'precursor-inhibitors', i.e. using common ALD precursors as SMIs.[71] The precursor-inhibitor concept has since been extended.[162,209,216] The computational part supporting this idea showed the thermodynamic and kinetic preference for bis(*N*,*N*-dimethylamino) dimethylsilane (DMADMS) (as SMI) adsorption on OH-terminated silicon surface (NGS) over the H-terminated one (GS) (Fig. 14.a).[71] The study used a minimal cluster model of the reconstructed Si(001) surface exposing one surface dimer. Their stochastic modeling approach led to the conclusion that only a fraction of the reactive surface groups (here: HO-Si groups) can be covered by the SMI due to steric hindrance (Fig. 14.b). While the estimated 50% of free OH groups is probably an overestimation because of the prementioned unrealistically high OH density of the a-quartz model, it clearly showed the need to retrieve coverage information of SMIs from computations to understand the blocking mechanism (see Fig. 5.). The authors state that finite sized objects cannot fully cover all surface sites by random, irreversible adsorption. This is also known from the packing of spheres in 3D.[273]

But packing can also be investigated with *ab initio* approaches. For MSA, strong adsorption on the NGS (Cu) could be computationally determined with DFT approaches while the GS (SiO_2) shows a large reaction barrier towards chemisorption.[87] The packing on the NGS was then derived by a systematic increase in coverage in the DFT computations. It was found that the adsorption

energy hardly changes up to full coverage, indicating a low steric hindrance for the adsorption even at high coverages. This DFT approach of determining coverage has been further applied to TMPS on NGS (SiO_2) in another computational work.[214] Here, a theoretical coverage limit of 4.2 SMIs nm^{-2} was deduced from a systematic increase in coverage. The advantage of *ab initio* methods for coverage determination is the possibility to analyze the underlying factors. Furthermore, it could be deduced that the coverage is limited by Pauli repulsion using a quantitative bonding analysis method: the pEDA (section 2.3.4).[143]

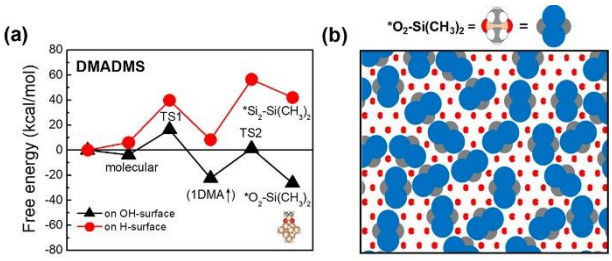

Fig. 14. (a) DFT-calculated reaction free energy diagram of bis(*N*,*N*-dimethylamino) dimethylsilane (DMADMS) adsorption on H−Si and SiO_2 surfaces. (b) configuration resulting from stochastic packing of DMADMS on the surface. Adapted reprint with permission from reference [71].

In contrast to these works on two dielectric surfaces, the modelling of AS-ALD on a dielectric surface (GS) vs. a metal surface (NGS) shows different signatures. As first investigated by Suh et al., in this case the SMI (3-hexyne) chemisorbs on the Cu surface while it physisorbs on the SiO_2 surface.[203] They termed this approach, which they had previously demonstrated for AS-CVD, "competitive adsorption".[264] The same difference in SMI bonding behavior has been found for aniline on SiO_2 (GS, physisorption) compared to Ru and Co (NGS, chemisorption) where - in addition - catalytic decomposition of the SMI on the metal surface increased the blocking ability.[159]

Blocking a metal surface and allowing growth on a dielectric surface is another target of AS-ALD: The dichotomy of physisorption and chemisorption of the SMIs has also been found useful here. For TMPS as SMI, Yarbrough et al. found chemisorption on SiO_2 (NGS) while physisorption was found on Cu (GS).[67] Here, the criterion of using the DFT-D3 component of the computed adsorption energy as indicator for a physisorbed species was introduced which had been introduced in surface science studies before.[272]

The resulting inhibitor layer might not be dense enough to achieve blocking after deposition. Several densification mechanisms have been studied computationally. Hydrolysis can be used to reduce the size of the SMI and have it pack more closely.[15,209] Condensation reactions were proposed for methoxysilane precursors to form siloxanes at the surface after hydrolyzing one methoxy group into an OH-group, albeit with a sizable barrier of ca. 130 $kJ \cdot mol^{-1}$.[67,214] Experiments did not show these condensation products yet.

What has hardly been done up to now is making use of the advantage of computational methods to screen a large number of inhibitor candidates to propose them for experimental AS-ALD investigations. While the general criteria for a good inhibitor have been outlined in several

studies,[46,47] the detailed chemical reactivity knowledge required to design an inhibitor and the many factors influencing this reactivity for a certain combination of GS/NGS make screening difficult. One recent study by the Shong group tested the ability of machine learning approaches to explore molecular design descriptors for precursors[246] It will need to be shown if the results help to improve experiments and if this approach can be applied successfully to inhibitor design as well.

3.4.2 Blocking mechanism

Since the beginning of AS-ALD research using inhibitors, the question about the blocking mechanism was explored. The main question here is thus how the inhibitor prevents the precursor from reacting with the surface. Already in the landmark work by Bent and co-workers,[64] the two major mechanisms were proposed that are still discussed today: steric blocking and chemical passivation (Fig. 5.).[206] Steric blocking is the physical blocking of the surface by a bulky tail group of an inhibitor (SMI or SAM, Fig. 4.). Chemical passivation means the chemical reaction of the inhibitor with the reactive groups at the surface that would otherwise engage in the ALD reaction with the precursor and/or co-reactant (Fig. 5.a).

For SAMs, as discussed in section 3.4.1.1, the blocking mechanism is clearly steric blocking. The difference in packing of similar SMIs was found, e.g., by Karasulu et al. to lead to more effective steric shielding.[208] Although diffusion through the SAM layer with a possible reaction with non-passivated surface groups has been hypothesized, there is no clear evidence yet. Thus, the discussion is focused in the following on SMIs.

Experimental work indicated already that both mechanisms are at hand in most SMIs, and some trends were discussed. For example, a near linear relationship between SMI size and nucleation delay was found,[208] but the limited number of three data points should be noted. Computational studies can shed more light on this question. For oxide surfaces, the chemical passivation of the reactive OH groups has been found crucial to achieve selectivity. But it was also found that some SMIs only cover approx. 50% of these surface hydroxyls. As discussed in section 3.4.1.2, there are several ways to increase SMI coverage. This was investigated systematically in a computational study for the SMI TMPS on SiO_2 and blocking mechanisms dependent on SMI coverage were found.[214] While at low SMI coverages, the precursor is not blocked at all, steric blocking is the major effect at high coverages. However, at medium coverages, there is a variant of the steric blocking effect, termed “reactivity reduction” (Fig. 5.d). In this case, the precursor can reach the surface and attach to the reactive surface groups, but it is not able to make ligand exchange reactions due to the limited space confined by the surrounding SMI layer. Thus, an unproductive desorption will take place eventually.

For Hacac, the question of blocking mechanisms has been investigated in detail from experimental as well as computational perspective by the Mackus and Sandoval groups.[74,113] They also compared Hacac to acetic acid (HAc) and 2,2,6,6-tetramethyl-3,5-heptanedione (Hthd) to better reveal the factors governing the contributions of the two mechanisms.[74] Their ALD experiments and spectroscopic investigations show that HAc and Hthd are the better SMIs for ALD of SiO_2 on

Al_2O_3 (Fig. 15.c). By a combination of DFT and RSA approaches, they find that on the one hand HAc benefits from its smaller size which leads to denser packed SMI layers via chemical passivation (Fig. 15.b). Hthd on the other hand benefits from its bulkiness leading to better steric blocking (Fig. 15.a). Finally, the authors compiled these insights into the conclusion that a good SMI either should target high chemical passivation or steric blocking. This leads to better selectivity than a precursor with a medium performance in both mechanisms. Further studies will be required to confirm this as a general conclusion, especially, since other studies conclude that a combination of steric blocking and chemical passivation should be targeted.[206]
This discrepancy is mainly a reflection of the lack of reliable data on the question of blocking mechanisms and hopefully more studies will appear addressing this in the future.

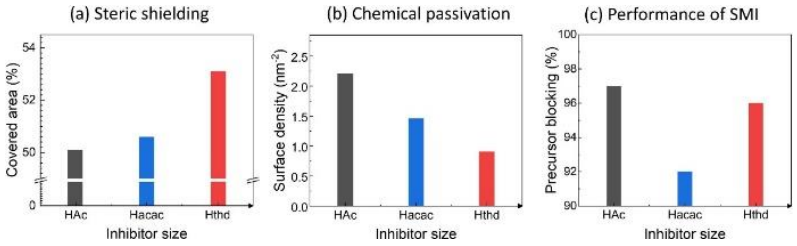

Fig. 15. (a) Covered area by small molecule inhibitors (SMIs) from random sequential adsorption (RSA), related to the steric shielding contribution. (b) Surface density of SMIs determined from RSA, a measure for chemical passivation. (c) Performance of SMIs for blocking based on experimental studies. Reprint with permission from reference [74].

An important parameter for the question of chemical passivation is the density of reactive groups at the surface which is rarely investigated experimentally.[74,249] This information is crucial for setting up suitable computational models correctly representing the experimentally observed reactive group density correctly (discussed in more detail in section 3.2). In combination with the knowledge of the theoretical coverage limit of an SMI, this gives an idea of how many reactive surface groups are left in the high-coverage limit.[206,214] The precursor can play a major role in the effectiveness of the blocking mechanism, especially w.r.t. decomposition reactions of the SMI layer and penetration which are discussed in the next section.

3.4.3 Selectivity-determining processes

As outlined in more detail above (section 1.4.4), there are four main mechanisms that lead to loss of selectivity in inhibitor-based AS-ALD: (i) penetration or (ii) decomposition of the inhibitor layer by the precursor, (iii) thermal decomposition of the inhibitors (including desorption) and (iv) overgrowth by nucleation on top of the inhibitor layer or growth over the interface to the GS (termed 'mushrooming')[69]. It is easily seen that the mechanisms (except iii) are tightly connected to the structure and chemical reactivity of the precursor. The general requirement for a good precursor are thus: it readily reacts with the GS but does not lift selectivity by decomposition, penetration or overgrowth of the inhibitor layer on the NGS. How have computational studies helped to reveal these factors?

3.4.3.1 Penetration of inhibitor layer

Selectivity is lifted through penetration by the precursor reaching reactive surface sites after diffusing through the inhibitor layer. Thus, the risk of penetration depends mostly on the density of the inhibitor layer and the size of the precursor. The factors governing the inhibitor density (i.e., surface coverage) have been discussed in section 3.4.2. Penetration risk is thereby affected twofold by the inhibitor density: (i) a higher density usually means more coverage of reactive surface groups (chemical passivation) and (ii) a more thorough blocking of the pathways to the surface (steric blocking).

Precursor size is typically discussed in terms of van-der-Waals volumes, leading to the assumption that small precursors like TMA show high risks of penetration.[71,159] This has been shown recently by computational analysis,[214] confirming the experimentally observed inability to achieve AS-ALD processes of Al_2O_3 using TMA. It was shown that TMA cannot only penetrate the inhibitor layer more effectively, but it is also more likely to react with reactive surface groups at the investigated SiO_2 surface (Fig. 18.). The larger triethylaluminum (TEA) shows the same thermodynamic driving force for penetration and adsorbing to the surface. However, the reaction with the surface OH-groups at medium coverages is governed by the reactivity-reduction mechanism (Fig. 5.d).

A very important aspect in the discussion of penetration is the reactivity of the remaining surface reactive groups towards the precursor. Reactive bridge oxygen (RBO) on the SiO_2 had been discussed before as potential nucleation sites for selectivity-lifting reactions.[250,274] In a computational study on ALD of Al_2O_3 on NGS SiO_2, RBOs are found to not be blocked by the SMI at medium densities of 2.5 SMIs nm^{-2} (Fig. 16.). TEA adsorbs on top of the SMI layer (this is the first step for overgrowth, see section 1.4.4) before penetrating the inhibitor layer with a low intralayer diffusion barrier ($\Delta E^{\ddagger}$ = 11 $kJ \cdot mol^{-1}$). It attaches to the RBO in an exothermic Lewis acid-Lewis base reaction (ΔE = -113 $kJ \cdot mol^{-1}$). The number in brackets in Fig. 16.a shows that the dispersion contribution to the bonding is the major factor up to this intermediate stage. This intermediate then readily converts into a surface-bonded TEA via a negligible barrier ($\Delta E^{\ddagger}$ = 3 $kJ \cdot mol^{-1}$) to a very stable and covalently bonded product (ΔE = -232 $kJ \cdot mol^{-1}$). Looking at the same process at an elevated SMI density of 3.4 SMIs nm^{-2}, the adsorption at the RBO turns into an endothermic reaction for both TMA and TEA highlighting again the crucial role of SMI surface coverage leading to steric blocking through adsorption prevention (Fig. 5.c). From this study it was concluded that a preceding water pulse removing the RBOs (Fig. 16.b) and creating more reactive OH-groups at the surface should be beneficial for creating a dense inhibitor layer.[275] Such an approach of increasing OH-density has already been used experimentally for a different ALD process.[276]

The effect of precursor size on selectivity has been investigated in several studies. Kim et al. presented an explanation for the often-observed high selectivity of AS-ALD when using DMAI as a precursor. In addition to the rather large vdW-volume of the precursor, it is present in dimerized form under typical ALD conditions which increases the efficiency of steric blocking.[160] A further study found the substitution of TMA by chlorinated precursors $Al(CH_3)_2Cl$ and $AlCl_3$ leading to

higher selectivity which was again explained via dimerization trends.[234] The role of precursor dimerization on selectivity has recently been investigated more systematically in two computational studies. One study investigated trends across a whole range of precursors with central elements B, Al, Ga and In and different ligand types using DFT methodology,[277] while the second study focused on high accuracy calculations using CCSD(T)/CBS quality calculations for Al-precursors eliminating most error sources and serving as benchmark data.[233]

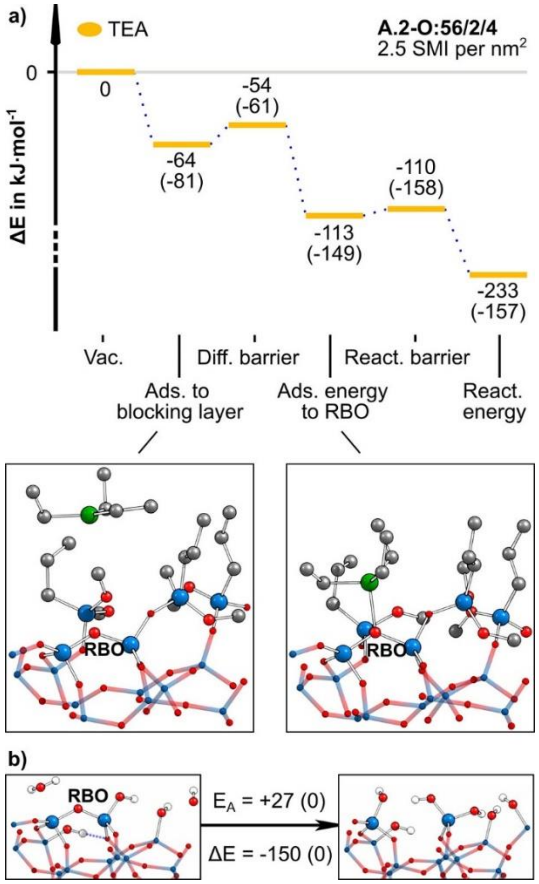

Fig. 16. Reactive bridge oxygen (RBO) opening reactions with triethylaluminum (TEA) and H_2O. (a) Reaction path of TEA. The reaction energies (ΔE) are given with dispersion contribution in parentheses (ΔE_{disp}). (b) Reaction of co-reactant water molecule with the RBO. All energies in kJ·mol^{-1}. Reprint with permission from reference [214].

Penetration has been investigated for other inhibitor approaches. With a molecular model and a combination of DFT and MD approaches, it was concluded that the precursor TMA physisorbs on the SAM layer and does not penetrate.[201] For thiol-based SAMs on Ge, the penetration by the co-reactant H_2O through defects in the SAM layer was found feasible. The thus generated nucleation sites on the surface can then initiate ALD growth.[278] This is in line with recent experimental findings of OH defects being responsible for the reactivity of the chemically closely related

H-Si(001).[249] Also for the CF_x inhibitor layer on silicon, the penetration of the co-reactant was found feasible but not for the precursor itself.[204]

3.4.3.2 Decomposition of inhibitor layers

Another way the precursor can diminish selectivity is by reacting with the inhibitor layer. This can either lead directly to unwanted growth nucleation or create defects in the layer which can then be used by further precursor molecules to initiate growth. Very early on, the computational investigations on SAM inhibitor layers focused on the question of decomposition of the tail group by the precursor. Xu and Musgrave found the interaction with the functionalized tail groups to be quite strong but the barriers for decomposition of hydrogen- or methyl-terminated SAMs to be too high to be overcome at ALD conditions in addition to having no thermodynamic driving force. They also showed that the trend of reaction and activation energies for tail groups follows the Hammond postulate (section 1.4.2). The authors concluded from varying the chain length in their model systems, that the interaction is very local and a long tail-group can be modelled with a simple ethyl group.[200] This knowledge has been used many years later in modelling TMA adsorption on an octadecylphosphonic acid (ODPA) SAM modelled by a propyl chain which led to similar findings.[201]

For SMI-based inhibitor layers, this research question has then been investigated for alkoxysilanes blocking SiO_2 first using a molecular model system. Low barriers of ca. 30 $kJ \cdot mol^{-1}$ were found for the attachment of TMA and TEA to a hydrolyzed methoxy-group at the TMPS precursor while the direct reaction with the methoxy groups of the SMI showed very high barriers.[67] Interaction with the co-reactant water had been investigated before showing that reaction with Al-CH_3 terminated surfaces is possible while high barriers are found for Si-CH_3 terminated surfaces.[71]

A comprehensive investigation of these decomposition reactions has been conducted later.[214] The different decomposition reactions possible by interaction of the precursor and the co-reactant with the inhibitor layer are summarized in Fig. 17..

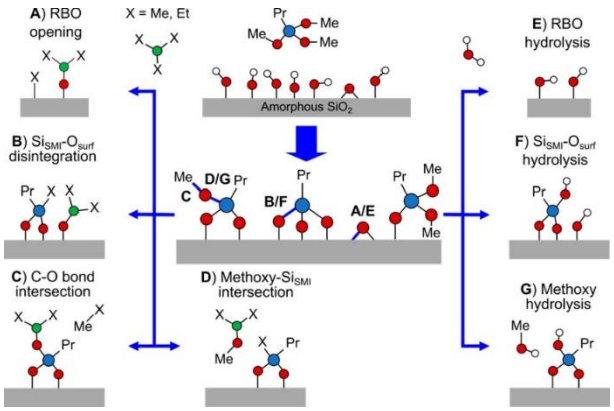

Fig. 17. Overview of possible decomposition reactions on trimethoxypropylsilane covered SiO_2 during ALD of Al_2O_3. Reprint with permission from reference [214].

It becomes clear that the chemical bonds of the SMI itself and the SMI-surface bonds can be attacked by the precursor or the co-reactant. For this system, the Si-O_{surf} bond is the most prone to be broken by the precursor, initiating unwanted ALD growth. Again, a dependence of the reactivity on the SMI layer density was found. While for an isolated SMI molecule (Fig. 18.a) at the surface, no difference between TMA and TEA was found in terms of the thermodynamic and kinetic signatures of the reaction (both show moderate barriers and strong thermodynamic driving force), at a realistic density of 2.5 SMIs per nm^2 the picture changes completely (Fig. 18.b). The precursors are more strongly bonded to the SMI-surface bond although the layer is denser. This can be explained by an increase in dispersion attraction. However, the activation energy more than doubles ($\Delta E^{\ddagger}$ = 217 kJ·mol^{-1} for TMA and 190 kJ·mol^{-1} for TEA) which essentially prohibits this reaction at typical ALD conditions. Thus, although the precursors adsorb, they cannot react. This is the essence of the concept of blocking by reactivity reduction (Fig. 5.d). When the SMI density is increased further to 3.4 SMI per nm^2, both precursors are blocked via adsorption prevention (Fig. 5.c). In Fig. 18.b, there is an additional reaction channel for TMA with a much lower barrier ($\Delta E^{\ddagger}$ = 92 kJ·mol^{-1}). Thus, it is proposed that the reason for the low selectivity of TMA is not the penetration of the layer but the ability to still react via ligand-exchange mechanisms in a sterically crowded environment.[214]

That the bonding mode of the inhibitor can play a crucial role for the decomposition reaction has been shown for Hacac. Here, the monodentate bonding configuration gets attacked by the precursor while the bidentate structure is inert.[113,206]

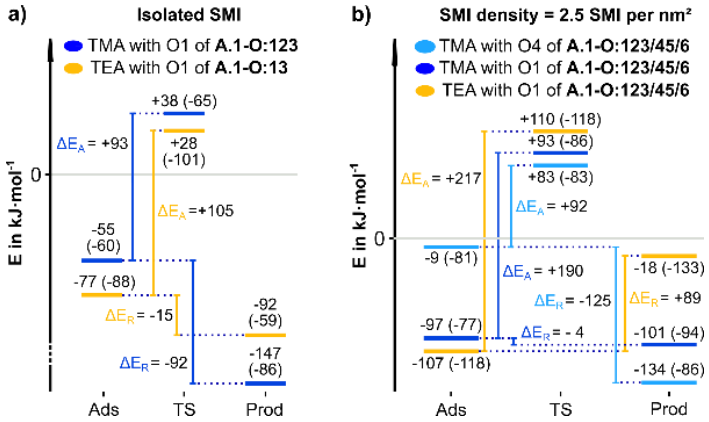

Fig. 18. Activation and reaction energies for the disintegration of the Si_{SMI} -O_{surf} bond with trimethylaluminum (TMA) and triethylaluminum (TEA) for (a) a single small molecule inhibitor (SMI) and (b) an inhibitor layer density of 2.5 SMIs/nm^2. Energies (in brackets dispersion contribution) are given with respect to the free reactants in kJ·mol^{-1}. Reprint with permission from reference [214].

3.4.3.3 Thermal decomposition of inhibitor layer and desorption of inhibitors

Aside from reactions with the precursor, the inhibitor layer itself can become defective. Either via thermal decomposition or via desorption of the inhibitor from the NGS. Desorption and

decomposition are known issues with SAM-based approaches for AS-ALD in experimental studies,[279] but have not been investigated computationally up to now. Physisorbed SMIs are usually desorbed during purging cycles and thus the discussion is focused on chemisorbed species. For Hacac, the previously mentioned monodentate bonding mode is prone to desorption as a function of purging time. A substantial theoretical desorption rate was deduced from the barrier towards desorption applying the Arrhenius equation.[113]

Thermal inhibitor decomposition was also investigated as a beneficial process to block two NGS with one SMI. Diethyl sulfide (DES) decomposes readily after adsorption on the Cu surface leaving both fragments (ethyl and thiolate) to block the surface. On the second NGS, SiO_2, the SMI shows a large barrier towards decomposition into endothermic products indicating a rare reaction event. Since the barrier towards desorption is lower than the first reaction barrier of decomposition, the SMI will more likely desorb. However, computations of the diffusion barrier showed that they are negligible for both SMI fragments resulting on the Cu surface. It was shown that recombinative desorption of the ethyl fragment as butane is likely while the thiolate fragment will remain to block the surface. For the blocking of SiO_2 with ethyl fragments, the high barriers for decomposition are overcome at elevated temperatures, in line with the experimental findings of good blocking on Cu and moderate blocking on SiO_2.[70] Cross-linking of SAM layers via extreme ultraviolet lithography (EUV) radiation was proposed by Wojtecki et al. as beneficial decomposition mechanism to increase blocking ability.[138]

3.4.3.4 Inhibitor layer overgrowth

The last mechanism to be discussed is ALD growth on top of the inhibitor layer. This necessitates nucleation via physisorbed or chemisorbed precursors interacting with the tail group of the inhibitor followed by regular ALD growth at this site (Fig. 7.d). This mechanism was studied quite often in computational AS-ALD literature and has first been investigated for SAM inhibitors. Xu and Musgrave first investigated this question and showed that non-alkyl SAM tail groups are prone to be nucleation sites for overgrowth while alkyl groups show very high barriers towards C-H bond cleavage.[200] Also Prinz et al. investigated this question and found very high barriers for the nucleation on alkyl-terminated SAMs.[181] Physisorption on the SAM layer was found as well,[201] which can lead to initiation of ALD growth.[202] The interaction of precursors with SMI-based inhibitors has been studied by many groups (RQ 3a in Tab. 1). Generally, it is assumed that physisorbed precursors are likely be purged away from the inhibitor layer before initiating growth.[67] If covalent bonding of the precursor is thermodynamically feasible and has a reasonable reaction barrier, this is deemed a very likely selectivity-lifting reaction. In several cases, the co-reactant H_2O is the more reactive species, especially for hydrolyzing ligands at the SMI.[214] As discussed above, this hydrolysis can also be beneficial and increase SMI density.[15]

3.5 ASD with activators

Only two computational studies focus on modelling of AS-ALD using activation approaches. In both cases, the modeling does not comprise the activation step itself, electron-beam induced

deposition (EBID), but instead focuses on the chemoselectivity of adsorption for the resulting surfaces.[88,219] Thus, as outlined above, the type of computational studies that is carried out parallels the modeling of intrinsically-selective AS-ALD. While modeling studies exist for plasma-based ALD,[196,280–286] none of these studies focusses on AS-ALD.

3.6 Connection to experiment

While computational modeling can provide insights into AS-ALD processes by itself, the crucial question is whether it can help understand experimental results and predict new avenues. The direct connection between *ab initio* computations and lab-scale experiments is difficult here since the direct computation of typical experimentally measured properties like growth rate, nucleation delays, or morphology is not possible. Instead, the connection between theoretical investigations on the atomic level and lab-scale experiments is mostly made via validating or revising hypotheses stemming from the experimental results.

Selectivity is an excellent property for the comparison between both worlds. Experimentally, the selectivity can be measured to quite a high precision (section 0). In the computations, the selectivity can be deduced from the ratio of barriers for reactions on GS and NGS, e.g., via an Arrhenius-type approach. When selectivity data is not available in a quantitative manner, the results of computations can be used in a qualitative sense ("precursor A reacts with GS and not with NGS in line with the observed ALD growth in the experiment").

However, a more direct connection between computational and lab experiments is desirable. This would allow better validation of the computational approaches and more direct feedback for experimental investigations to test new grounds. A typical way in *ab initio* theory is to connect via theoretical spectroscopy, i.e. the modeling of measurable spectroscopic quantities. However, this is rarely done up to now in AS-ALD modeling. Only one study modeled infrared spectroscopy results.[113] In contrast to surface science investigations, where the modeling of spectroscopic and imaging measurements is typically done,[183,269] there is room for development in AS-ALD research.

3.7 Beyond the atomistic picture

Ab initio data can also be used to feed multiscale models via the connection of kMC and MD simulations (Fig. 3.). This means that reaction thermodynamics and barriers can be fed into larger-scale methods. As outlined in section 2.6, this is far from trivial. Up to now, there is only one study combining DFT, MD, kMC and CFD approaches for AS-ALD modelling.[24] Typically, DFT results are fed into a stochastic model for coverage modeling. This is mostly done in a qualitative fashion, i.e. taking the most stable product or the vdW volume of the inhibitor from DFT modeling for the stochastic modeling. An approach that has only been applied once in AS-ALD modeling[157] is the actual usage of reaction barriers from DFT computations to feed a kMC model. This has been shown for ALD growth modelling to give insights into the atomistic processes.[287] In principle, machine learning approaches are also able to make the direct connection between *ab initio* modelling and large-scale properties, e.g., via learning from data (structures, energies, etc.)

and predicting new inhibitors or precursors for a certain application. However, data is quite scarce in AS-ALD and the approach has not been shown to be useful yet. For ALD, the current state-of-the-art is summarized in a recent book.[288] As outlined above, classical approaches for nucleation modeling are not discussed here since they have not been connected to *ab initio* modeling results.[94,97]

4 Challenges and perspectives

The chapters above outlined how computations have contributed to the field of AS-ALD up to now. However, several challenges and opportunities for the future emerge.

4.1 Moving to a dynamical picture

The vast majority of computations apply static DFT computations. However, several aspects of AS-ALD research would highly benefit from dynamic modeling. For example, the penetration of an inhibitor layer by a precursor is certainly not a static chemical reaction but will be highly influenced by the dynamic response of the layer to the incoming chemical species. Or the selectivity of inhibitor adsorption on GS and NGS, which is not only determined by kinetics and thermodynamics but would require modeling of adsorption probability for a full picture – similar to the experimental evaluation of sticking coefficients. The main reason that hardly any such studies are available is the prohibitive computational demand for the required AIMD methods to simulate long enough time scales (section 2.4). The development of machine-learned potentials could be a remedy here, enabling much more efficient computations.[289] Another option could be the usage of the upcoming efficient yet accurate semiempirical approaches like GFN2-xTB.[290]

4.2 Substrates under deposition conditions

Modeling nearly exclusively uses ideal surfaces to model substrates in AS-ALD. However, such an ideal surface barely exists under highly controlled UHV conditions, not to speak of the conditions in a typical ALD reactor. Thus, treating these non-ideal surface conditions is a way forward toward modeling of more realistic environments. This can include surface defects,[291] non-crystalline substrates,[214] and oxidized surfaces.[217] Every deviation from the ideal surface means a less ordered structure and, thus, a significant increase in modeling effort for the resulting larger unit cells in PBC computations. Furthermore, more information is required regarding the surface state under ALD conditions from experiments to set up more realistic computational models. What is not yet fully explored at the moment is considering the changing surface state under deposition conditions. While the initial inhibitor or precursor molecule sees a pristine surface, the next wave of adsorbates sees a precovered substrate. While this has been modeled in several coverage studies from a thermodynamic perspective, the influence on adsorption dynamics is still unknown.[80] Furthermore, the changing surface condition after the onset of the ALD process is not yet captured. What does the inhibited surface look like after 3, 5, or 10 pulses of ALD precursor?

4.3 Usage of machine learning tools

The era of data science is clearly still on the uprise and the first applications of methods derived from machine learning approaches entered the field of AS-ALD. However, the usage is yet scarce. Aside from the already mentioned possibility to use MLPs in dynamic modelling of selective deposition, ML approaches could also be used to reveal correlations of microscopic quantities computed by *ab initio* modelling with experimental observables like growth per cycle. Also, macroscopic properties like vapor pressure could be accessible via ML.[292] Modern ML techniques like active learning or reinforcement learning have not yet been applied to the field of AS-ALD. The major bottleneck here is the lack of comprehensive and accurate data sets to train reliable models on. This is a challenge for experiments as well as computational modeling and should ideally be approached together in the future. One important step here is the publication of research data associated with computational (and if possible, also with experimental) studies. Data availability statements are standard nowadays in most scientific journals. However, the deposition of data in publicly available repositories (e.g., Zenodo, NOMAD) is not yet common practice in AS-ALD.

4.4 Modelling spectroscopy

In many fields of chemistry, the connection between experiment and theory is made via the computation of spectroscopic quantities. This is underexplored in AS-ALD at the moment. Although several spectroscopic techniques are applied more or less routinely in in-situ experiments, modeling this data has rarely been done yet. Deriving infrared (IR) spectra or XPS shifts by computation could be a way to provide an assessment of the accuracy of computational modeling and a means to predict observables for modeling results.

4.5 Accuracy

AS-ALD modeling is nearly exclusively based on DFT computations. It is well-known that these efficient *ab initio* method has limited accuracy.[109] Furthermore, this accuracy can hardly be quantified intrinsically (exceptions are intrinsic error estimates in some functionals like BEEF-vdW[293]) and requires benchmarking to experimental data. However, these experimental data are hardly available. The second option for assessing the accuracy, the comparison to highly accurate wavefunction-based methods, is only available for the computation of molecular aspects of AS-ALD like the dimerization of precursors.[233] An option not yet well explored in AS-ALD modeling is the usage of more modern density functionals (e.g., the B97 family)[294], which promise an overall increase in accuracy. Also, the usage of converged computational parameters (e.g., basis sets and cluster sizes in cluster-based studies) will add to the increased accuracy of computational results. Besides the accuracy of the electronic energy computations, it is also necessary to have a look at the accuracy of thermodynamic modeling. For the calculation of Gibbs energies, it is important to consider ALD conditions in the derivation of correction terms.[233] Moreover, moving beyond the harmonic approximation is a challenging but potentially promising avenue here.

4.6 Concepts and design strategies

The question of optimal design strategies for inhibitors and precursors, particularly their combination for a given GS/NGS pair, remains unresolved. While some approaches exist, no general concept has yet emerged. Future efforts should focus on modeling a broader range of systems and critically assessing the factors influencing selectivity. A detailed understanding of these systems, such as through electronic structure analysis, is needed to uncover the principles governing growth and blocking. Currently, there is no consensus on which blocking mechanisms inhibitor-based approaches should prioritize. Both chemical passivation and steric blocking appear necessary for effective inhibition, but the optimal balance remains unclear. It is also unknown whether inhibitors should target both mechanisms simultaneously or maximize one for a given system. Since inhibitor layer decomposition is a key factor in selectivity reduction for AS-ALD, further studies are essential in this area.

4.7 Research questions in AS-ALD

The chemistry at the interface between GS and NGS, and its implications for selectivity-reducing reactions, remains largely unexplored. Similarly, nucleation and overgrowth of SMI layers have received limited attention. The targeted removal of inhibitor layers has yet to be addressed through computational studies. While molecular layer deposition has been used in an area-selective manner,[295] computational modeling offers further opportunities for insights beyond the previously discussed use of indicone as an inhibitor layer.[205] Publishing results that do not align with experiments could also provide valuable insights into the limitations of current modeling approaches, despite challenges in dissemination. For intrinsically selective AS-ALD, the influence of precursor dimerization remains unexamined, where differences in the reactivity of monomeric and dimeric forms could help distinguish between two surfaces, e.g., one able to open the dimer and the other not. The integration of density functional theory (DFT) with kinetic Monte Carlo (kMC) simulations is a promising yet unexplored approach. Additionally, while the penetration of precursors and inhibitors into self-assembled monolayer (SAM) layers has been briefly addressed, comprehensive computational investigations remain lacking.

4.8 Diffusion

Recently, the Delabie group showed that differences in surface diffusion can be used to achieve area-selective deposition.[296] Thereby, the diffusion length of the precursor is larger on the NGS. Hence, the precursor diffuses from the NGS to the GS where it is then deposited. The group applied rate-equation mean-field modeling approaches to explain the nucleation and growth in this regime. Surface diffusion for selective deposition has also been used by Klement et al. with the help of surface modification.[156] Notably, an atomistic picture of surface diffusion is possible using DFT or MD methods as has been applied successfully in fields like heterogeneous catalysis.[297] The transfer of these methods towards AS-ALD modelling promises to provide a more microscopic picture of the precursor-surface interaction that is ultimately responsible for the differences in diffusion length, allowing for a fine-tuning of diffusion processes and, thus, selectivity.

5 Conclusion

Ab initio modelling has left its mark in AS-ALD research already. It provides insights ranging from molecular aspects of inhibitor and precursor chemistry over the crucial question of surface chemistry determining the selectivity of the ALD process to the derivation of mechanisms and design principles. The major workhorse, density functional theory, delivers an efficient and accurate account of the essential chemical reactions in AS-ALD, providing thermodynamic and kinetic signatures. At the current stage, *ab initio* modelling is mainly used to explain experimental findings and give plausible hypotheses for the observed selectivity and reactivity. In the future, modelling will develop further to obtain predictions and insights, inspiring new experiments in AS-ALD. To this end, several necessary steps are outlined that require developments on the computational side, yet also an even stronger interaction between experimental and computational research in the field. It becomes clear that the limits of what computational approaches can deliver to the field of AS-ALD are far from being reached.

Acknowledgments
We thank Philipp Wellmann and Patrick Maue for critical feedback on the manuscript.

Abbreviations

General

ALD	atomic layer deposition
ALE	atomic layer etching
AS-ALD	area-selective atomic layer deposition
CVD	chemical vapor deposition
DDF	dissociated dimer fraction
EBID	electron-beam induced deposition
EUV	extreme ultraviolet lithography
FSAV	fully self-aligned via
GS	growth surface
NGS	non-growth surface
RBO	reactive bridge oxygen
RQ	research question
SAM	self-assembled monolayer
SMI	small molecule inhibitor
UHV	ultra-high vacuum

Computational methods

AI	artificial intelligence
AIM	atoms-in-molecules
AIMD	*ab initio* molecular dynamics

AO	atomic orbital
BEP	Bell-Evans-Polanyi principle
CBS	complete basis set
CC	coupled cluster
CFD	computational fluid dynamics
CI	configuration interaction
DF	density functional
DFT	density functional theory
DLPNO	domain localized pair natural orbitals
EDA	energy decomposition analysis
ESA	electronic structure analysis
FE	finite element
GC	group-contributions
GGA	generalized gradient approximation
HF	Hartree Fock
HPC	high-performance computing
kMC	kinetic Monte Carlo
KS	Kohn and Sham
LCAO	linear combination of atomic orbitals
LDA	local density approximation
MC	Monte Carlo
MD	molecular dynamics
ML	machine learning
MLP	machine learning potentials
MP*n*	Møller-Plesset perturbation theory of *n*-th order
MO	molecular orbital
PBC	periodic boundary conditions
pDOS	partial density of states
pEDA	energy decomposition analysis for extended systems
QMC	quantum Monte Carlo
QMDFF	quantum mechanically derived force fields
qq-TST	quasi-quantum transition state theory
QSPR	quantitative structure-property relationships
RRHO	rigid-rotor harmonic oscillator
RSA	random sequential adsorption
SCF	self-consistent field approach
TST	transition state theory

Ligands/SMIs

BDEAS	bis(diethylamino)silane
BDIPADS	1,2-bis(diisopropylamino)disilane

DES	diethyl sulfide
DEZ	diethyl zinc
DIPAS	di(isopropylamino)silane
DMADMS	bis(*N*,*N*-dimethylamino) dimethylsilane
DMATMS	(*N*,*N*-dimethylamino) trimethylsilane
DMDMS	dimethoxydimethylsilane
EBECH	(ethylbenzyl)(1-ethyl-1,4-cyclohexadienyl)
ET	ethanethiol
HAc	acetic acid
Hacac	acetylacetone
Hthd	2,2,6,6-tetramethyl-3,5-heptanedione
MSA	methylsulfonic acid
MTMS	methoxytrimethylsilane
ODPA	octadecylphosphonic acid
OTDS	octadecyltrichlorosilane
TBC	tert-butyl chloride
^{tbu2}DAD	1,4-di-tertbutyl-1,3-diazadiene
TDMAS	tris(dimethylamino)silane
TMES	trimethoxyethylsilane
tmhd	bis(2,2,6,6-tetramethyl-3,5-heptanedionato)
TMMS	trimethoxymethylsilane
TMPMCT	$Cp(CH_3)_5Ti(OMe)_3$
TMPS	trimethoxypropylsilane
TMS	trimethylsilyl

Precursors

Carish	dicarbonyl-bis(5-methyl-2,4-hexanediketonato)Ru(II)
DMAI	dimethylaluminum isopropoxide
EBECHRu	(ethylbenzyl)(1-ethyl-1,4-cyclohexadienyl)Ru(0)
TBTDMT	tert-butylimidotris(dimethylamino) tantulum
TDMAA	tris(dimethylamino)aluminum
TDMAHf	tetrakis(dimethylamino)hafnium
TDMAT	tetrakis(dimethylamino)titan
TEA	triethylaluminum
TEMAZ	$Zr[N(C_2H_5CH_3)]_4$
TMA	trimethylaluminum
T-Rudic	$Ru_2\{\mu^2\text{-}\eta^3\text{-}N(^tBu)\text{−}C(H)\text{−}C(^iPr)\}(CO)_6$
TRuST	tricarbonyl trimethylenemethane ruthenium

Spectroscopy

AES	Auger electron spectroscopy
EDS	energy-dispersive X-ray spectroscopy
FE-SEM	field emission electron microscopy
FTIR	Fourier-transform infrared spectroscopy
GIWAXS	grazing incidence wide angle X-ray scattering
IR	infrared spectroscopy

QCM	quartz crystal microbalance
QMS	quadrupole mass spectroscopy
RBS	Rutherford backscattering spectroscopy
SE	spectroscopy ellipsometry
TEM	transmission Electron Microscopy
WCA	water contact angle
XPS	X-ray photoelectron spectroscopy

Computational Codes

AMS	Amsterdam Modelling Suite
G03	Gaussian03
G16	Gaussian16
G98	Gaussian98
PWscf	Plane-wave self-consistent field
QE	Quantum Espresso
VASP	Vienna Ab Initio Simulation Package

References

[1] R. Clark, K. Tapily, K.-H. Yu, T. Hakamata, S. Consiglio, D. O'Meara, C. Wajda, J. Smith, G. Leusink, "Perspective: New process technologies required for future devices and scaling", *APL Mater.* **2018**, *6*, 058203, DOI: 10.1063/1.5026805.

[2] IEEE International Roadmap for Devices and Systems, "Executive Summary 2022," can be found under DOI: 10.60627/C13Z-V363, last accessed 17.12.2024, **2022**.

[3] H. J. Levinson, "High-NA EUV lithography: current status and outlook for the future", *Jpn. J. Appl. Phys.* **2022**, *61*, SD0803, DOI: 10.35848/1347-4065/ac49fa.

[4] M. Leskelä, M. Mattinen, M. Ritala, "Review Article: Atomic layer deposition of optoelectronic materials", *J. Vac. Sci. Technol. B* **2019**, *37*, 030801, DOI: 10.1116/1.5083692.

[5] M. Ritala, J. Niinistö, "Industrial Applications of Atomic Layer Deposition", *ECS Trans.* **2009**, *25*, 641–652, DOI: 10.1149/1.3207651.

[6] A. J. M. Mackus, A. A. Bol, W. M. M. Kessels, "The use of atomic layer deposition in advanced nanopatterning", *Nanoscale* **2014**, *6*, 10941–10960, DOI: 10.1039/C4NR01954G.

[7] H.-B.-R. Lee, S. F. Bent, "A Selective Toolbox for Nanofabrication", *Chem. Mater.* **2020**, *32*, 3323–3324, DOI: 10.1021/acs.chemmater.0c00838.

[8] A. J. M. Mackus, M. J. M. Merkx, W. M. M. Kessels, "From the Bottom-Up: Toward Area-Selective Atomic Layer Deposition with High Selectivity", *Chem. Mater.* **2019**, *31*, 2–12, DOI: 10.1021/acs.chemmater.8b03454.

[9] G. N. Parsons, R. D. Clark, "Area-Selective Deposition: Fundamentals, Applications, and Future Outlook", *Chem. Mater.* **2020**, *32*, 4920–4953, DOI: 10.1021/acs.chemmater.0c00722.

[10] H.-B.-R. Lee, "The Era of Atomic Crafting", *Chem. Mater.* **2019**, *31*, 1471–1472, DOI: 10.1021/acs.chemmater.9b00654.

[11] B. Macco, "Review Base at AtomicLimits," can be found under https://base.atomiclimits.com, last accessed 17.12.2024, **2024**.

[12] H. P. Chen, Y. H. Wu, H. Y. Huang, C. H. Tsai, S. K. Lee, C. C. Lee, T. H. Wei, H. C. Yao, Y. C. Wang, C. Y. Liao, H. K. Chang, C. W. Lu, W. S. Shue, M. Cao, in *2021 IEEE Int. Electron Devices Meet. IEDM*, **2021**, p. 22.1.1-22.1.4.

[13] A. Raley, J. Lee, J. T. Smith, X. Sun, R. A. Farrell, J. Shearer, Y. Xu, A. Ko, A. W. Metz, P. Biolsi, A. Devilliers, J. Arnold, N. Felix, "Self-aligned blocking integration demonstration for critical sub-30nm pitch Mx level patterning with EUV self-aligned double patterning", *Proc SPIE 10589 Adv. Etch Technol. Nanopatterning VII* **2018**, *105890L*, DOI: 10.1117/12.2297438, DOI 10.1117/12.2297438.

[14] H.-D. Yu, M. D. Regulacio, E. Ye, M.-Y. Han, "Chemical routes to top-down nanofabrication", *Chem. Soc. Rev.* **2013**, *42*, 6006–6018, DOI: 10.1039/c3cs60113g.

[15] C. T. Nguyen, E.-H. Cho, B. Gu, S. Lee, H.-S. Kim, J. Park, N.-K. Yu, S. Shin, B. Shong, J. Y. Lee, "Gradient area-selective deposition for seamless gap-filling in 3D nanostructures through surface chemical reactivity control", *Nat. Commun.* **2022**, *13*, 7597, DOI: 10.1038/s41467-022-35428-6.

[16] D. Solanki, C. He, Y. Lim, R. Yanagi, S. Hu, "Where Atomically Precise Catalysts, Optoelectronic Devices, and Quantum Information Technology Intersect: Atomic Layer Deposition", *Chem. Mater.* **2024**, *36*, 1013–1024, DOI: 10.1021/acs.chemmater.3c00589.

[17] Yury Koshtyal, Denis Olkhovskii, Aleksander Rumyantsev, M. Maximov, "Applications and Advantages of Atomic Layer Deposition for Lithium-Ion Batteries Cathodes: Review", *Batteries* **2022**, *8*, 184, DOI: 10.3390/batteries8100184.
[18] B. Gupta, Md. A. Hossain, A. Riaz, A. Sharma, D. Zhang, H. H. Tan, C. Jagadish, K. Catchpole, B. Hoex, S. Karuturi, "Recent Advances in Materials Design Using Atomic Layer Deposition for Energy Applications", *Adv. Funct. Mater.* **2022**, *32*, 2109105, DOI: 10.1002/adfm.202109105.
[19] H. Xu, M. K. Akbari, S. Kumar, F. Verpoort, S. Zhuiykov, "Atomic layer deposition – state-of-the-art approach to nanoscale hetero-interfacial engineering of chemical sensors electrodes: A review", *Sens. Actuators B-Chem.* **2021**, *331*, 129403, DOI: 10.1016/j.snb.2020.129403.
[20] A. Hossain, K. T. Khoo, X. Cui, G. K. Poduval, T. Zhang, X. Li, W. M. Li, B. Hoex, "Atomic layer deposition enabling higher efficiency solar cells: A review", **2020**, *2*, 204–226, DOI: 10.1016/j.nanoms.2019.10.001.
[21] K. Cao, J. Cai, X. Liu, R. Chen, R. Chen, "Review Article: Catalysts design and synthesis via selective atomic layer deposition", *J. Vac. Sci. Technol.* **2018**, *36*, 010801, DOI: 10.1116/1.5000587.
[22] R. A. Nye, K. Van Dongen, D. De Simone, H. Oka, G. N. Parsons, A. Delabie, "Enhancing Performance and Function of Polymethacrylate Extreme Ultraviolet Resists Using Area-Selective Deposition", *Chem. Mater.* **2023**, *35*, 2016–2026, DOI: 10.1021/acs.chemmater.2c03404.
[23] K. Seki, K. Saiki, "Transition from Reaction- to Diffusion-Limited Growth of Graphene by Chemical Vapor Deposition", *Cryst. Growth Des.* **2022**, *22*, 4396–4403, DOI: 10.1021/acs.cgd.2c00363.
[24] H. Wang, M. Tom, F. Ou, G. Orkoulas, P. D. Christofides, "Multiscale computational fluid dynamics modeling of an area-selective atomic layer deposition process using a discrete feed method", *Digit. Chem. Eng.* **2024**, *10*, 100140, DOI: 10.1016/j.dche.2024.100140.
[25] S. D. Elliott, "Atomic-scale simulation of ALD chemistry", *Semicond. Sci. Technol.* **2012**, *27*, 074008, DOI: 10.1088/0268-1242/27/7/074008.
[26] F. Grillo, J. A. Moulijn, M. T. Kreutzer, J. R. van Ommen, "Nanoparticle sintering in atomic layer deposition of supported catalysts: Kinetic modeling of the size distribution", *Catal. Today* **2018**, *316*, 51–61, DOI: 10.1016/j.cattod.2018.02.020.
[27] N. Cheimarios, D. To, G. Kokkoris, G. Memos, A. G. Boudouvis, "Monte Carlo and Kinetic Monte Carlo Models for Deposition Processes: A Review of Recent Works", *Front. Phys.* **2021**, *9*, 631918, DOI: 10.3389/fphy.2021.631918.
[28] J. R. Abelson, G. S. Girolami, "New strategies for conformal, superconformal, and ultrasmooth films by low temperature chemical vapor deposition", *J. Vac. Sci. Technol. Vac. Surf. Films* **2020**, *38*, 030802, DOI: 10.1116/6.0000035.
[29] M. Bonvalot, C. Vallée, C. Mannequin, M. Jaffal, R. Gassilloud, N. Possémé, T. Chevolleau, "Area selective deposition using alternate deposition and etch super-cycle strategies", *Dalton Trans.* **2022**, *51*, 442–450, DOI: 10.1039/D1DT03456A.
[30] G. Baek, H. L. Yang, G.-B. Park, J.-S. Park, "Review of molecular layer deposition process and application to area selective deposition via graphitization", *Jpn. J. Appl. Phys.* **2023**, *62*, SG0810, DOI: 10.35848/1347-4065/acc3a7.

[31] P. O. Oviroh, R. Akbarzadeh, D. Pan, R. A. M. Coetzee, T.-C. Jen, "New development of atomic layer deposition: processes, methods and applications", *Sci. Technol. Adv. Mater.* **2019**, *20*, 465–496, DOI: 10.1080/14686996.2019.1599694.
[32] R. A. Ovanesyan, E. A. Filatova, S. D. Elliott, D. M. Hausmann, D. C. Smith, S. Agarwal, "Atomic layer deposition of silicon-based dielectrics for semiconductor manufacturing: Current status and future outlook", *J. Vac. Sci. Technol. A* **2019**, *37*, 060904, DOI: 10.1116/1.5113631.
[33] K. Cao, J. M. Cai, R. Chen, "Inherently Selective Atomic Layer Deposition and Applications", *Chem. Mater.* **2020**, *32*, 2195–2207, DOI: 10.1021/acs.chemmater.9b04647.
[34] Esko Ahvenniemi, Andrew R. Akbashev, Saima Ali, Mikhael Bechelany, Maria Berdova, Stefan Boyadjiev, David C. Cameron, Rong Chen, Mikhail Chubarov, Veronique Cremers, Anjana Devi, Viktor Drozd, Liliya Elnikova, Gloria Gottardi, Kestutis Grigoras, Dennis M. Hausmann, Cheol Seong Hwang, Shih-Hui Jen, Tanja Kallio, Jaana Kanervo, Ivan Khmelnitskiy, Do Han Kim, Lev Klibanov, Yury Koshtyal, A. Outi I. Krause, Jakob Kuhs, Irina Kärkkänen, Marja-Leena Kääriäinen, Tommi Kääriäinen, Luca Lamagna, Adam A. Łapicki, Markku Leskelä, Harri Lipsanen, Jussi Lyytinen, Anatoly Malkov, Anatoly Malygin, Abdelkader Mennad, Christian Militzer, Jyrki Molarius, Małgorzata Norek, Çağla Özgit-Akgün, Mikhail Panov, Henrik Pedersen, Fabien Piallat, Georgi Popov, Riikka L. Puurunen, Geert Rampelberg, Robin H. A. Ras, Erwan Rauwel, Fred Roozeboom, Timo Sajavaara, Hossein Salami, Hele Savin, Nathanaelle Schneider, Thomas E. Seidel, Jonas Sundqvist, Dmitry B. Suyatin, Tobias Törndahl, J. Ruud van Ommen, Claudia Wiemer, Oili M. E. Ylivaara, Oksana Yurkevich, "Review Article: Recommended reading list of early publications on atomic layer deposition—Outcome of the 'Virtual Project on the History of ALD'", *J. Vac. Sci. Technol. A* **2017**, *35*, 010801, DOI: 10.1116/1.4971389.
[35] S. M. George, "Atomic Layer Deposition: An Overview", *Chem. Rev.* **2010**, *110*, 111–131, DOI: 10.1021/cr900056b.
[36] R. L. Puurunen, "Surface chemistry of atomic layer deposition: A case study for the trimethylaluminum/water process", *J. Appl. Phys.* **2005**, *97*, 121301, DOI: 10.1063/1.1940727.
[37] M. Leskelä, M. Ritala, "Atomic Layer Deposition Chemistry: Recent Developments and Future Challenges", *Angew. Chem. Int. Ed.* **2003**, *42*, 5548–5554, DOI: 10.1002/anie.200301652.
[38] R. W. Johnson, A. Hultqvist, S. F. Bent, "A brief review of atomic layer deposition: from fundamentals to applications", *Mater. Today* **2014**, *17*, 236–246, DOI: 10.1016/j.mattod.2014.04.026.
[39] G. Y. Fang, L. N. Xu, Y. Q. Cao, A. D. Li, "Theoretical design and computational screening of precursors for atomic layer deposition", *Coord. Chem. Rev.* **2016**, *322*, 94–103, DOI: 10.1016/j.ccr.2016.05.011.
[40] S. T. Barry, A. V. Teplyakov, F. Zaera, "The chemistry of inorganic precursors during the chemical deposition of films on solid surfaces", *Acc. Chem. Res.* **2018**, *51*, 800–809, DOI: 10.1021/acs.accounts.8b00012.
[41] J. A. Elliott, "Novel approaches to multiscale modelling in materials science", *Int. Mater. Rev.* **2011**, *56*, 207–225, DOI: 10.1179/1743280410y.0000000002.
[42] S. D. Elliott, "Predictive process design: a theoretical model of atomic layer deposition", *Comput. Mater. Sci.* **2005**, *33*, 20–25, DOI: 10.1016/j.commatsci.2004.12.032.

[43] S. D. Elliott, G. Dey, Y. Maimaiti, H. Ablat, E. A. Filatova, G. N. Fomengia, "Modeling mechanism and growth reactions for new nanofabrication processes by atomic layer deposition", *Adv. Mater.* **2016**, *28*, 5367–80, DOI: 10.1002/adma.201504043.
[44] D. Sibanda, S. T. Oyinbo, T.-C. Jen, "A review of atomic layer deposition modelling and simulation methodologies: Density functional theory and molecular dynamics", *Nanotechnol. Rev.* **2022**, *11*, 1332–1363, DOI: 10.1515/ntrev-2022-0084.
[45] C. B. Musgrave, in *At. Layer Depos. Nanostructured Mater.*, John Wiley & Sons, Ltd, **2011**, pp. 1–21.
[46] J. Yarbrough, A. B. Shearer, S. F. Bent, "Next generation nanopatterning using small molecule inhibitors for area-selective atomic layer deposition", *J. Vac. Sci. Technol. A* **2021**, *39*, 021002, DOI: 10.1116/6.0000840.
[47] A. Mameli, A. V. Teplyakov, "Selection Criteria for Small-Molecule Inhibitors in Area-Selective Atomic Layer Deposition: Fundamental Surface Chemistry Considerations", *Acc. Chem. Res.* **2023**, 2084–2095, DOI: 10.1021/acs.accounts.3c00221.
[48] R. Chen, E. Gu, K. Cao, J. Zhang, "Area Selective Deposition for Bottom-up Atomic-Scale Manufacturing", *Int. J. Mach. Tools Manuf.* **2024**, *199*, 104173, DOI: 10.1016/j.ijmachtools.2024.104173.
[49] M. Kim, J. Kim, S. Kwon, S. H. Lee, H. Eom, B. Shong, "Theoretical Design Strategies for Area-Selective Atomic Layer Deposition", *Chem. Mater.* **2024**, *36*, 5313–5324, DOI: 10.1021/acs.chemmater.3c03326.
[50] J. Kwon, M. Saly, M. D. Halls, R. K. Kanjolia, Y. J. Chabal, "Substrate Selectivity of (^{t}Bu-Allyl)Co(CO) $_3$ during Thermal Atomic Layer Deposition of Cobalt", *Chem. Mater.* **2012**, *24*, 1025–1030, DOI: 10.1021/cm2029189.
[51] Y. Li, Z. Qi, Y. Lan, K. Cao, Y. Wen, J. Zhang, E. Gu, J. Long, J. Yan, B. Shan, R. Chen, "Self-aligned patterning of tantalum oxide on Cu/SiO_2 through redox-coupled inherently selective atomic layer deposition", *Nat. Commun.* **2023**, *14*, 4493, DOI: 10.1038/s41467-023-40249-2.
[52] T. Parke, D. Silva-Quinones, G. T. Wang, A. V. Teplyakov, "The Effect of Surface Terminations on the Initial Stages of TiO_2 Deposition on Functionalized Silicon", *ChemPhysChem* **2023**, *24*, e202200724, DOI: 10.1002/cphc.202200724.
[53] R. C. Longo, S. McDonnell, D. Dick, R. M. Wallace, Y. J. Chabal, J. H. G. Owen, J. B. Ballard, J. N. Randall, K. Cho, "Selectivity of metal oxide atomic layer deposition on hydrogen terminated and oxidized Si(001)-(2×1) surface", *J. Vac. Sci. Technol. B Nanotechnol. Microelectron. Mater. Process. Meas. Phenom.* **2014**, *32*, 03D112, DOI: 10.1116/1.4864619.
[54] K. Cao, L. Shi, M. Gong, J. Cai, X. Liu, S. Chu, Y. Lang, B. Shan, R. Chen, "Nanofence Stabilized Platinum Nanoparticles Catalyst via Facet-Selective Atomic Layer Deposition", *Small* **2017**, *13*, 1700648, DOI: 10.1002/smll.201700648.
[55] R. Methaapanon, S. F. Bent, "Comparative Study of Titanium Dioxide Atomic Layer Deposition on Silicon Dioxide and Hydrogen-Terminated Silicon", *J. Phys. Chem. C* **2010**, *114*, 10498–10504, DOI: 10.1021/jp1013303.
[56] K. A. Perrine, A. V. Teplyakov, "Reactivity of selectively terminated single crystal silicon surfaces", *Chem. Soc. Rev.* **2010**, *39*, 3256, DOI: 10.1039/b822965c.
[57] S. E. Atanasov, B. Kalanyan, G. N. Parsons, "Inherent substrate-dependent growth initiation and selective-area atomic layer deposition of TiO_2 using 'water-free' metal-halide/metal

alkoxide reactants", *J. Vac. Sci. Technol. Vac. Surf. Films* **2016**, *34*, 01A148, DOI: 10.1116/1.4938481.
[58] B. Kalanyan, P. C. Lemaire, S. E. Atanasov, M. J. Ritz, G. N. Parsons, "Using Hydrogen To Expand the Inherent Substrate Selectivity Window During Tungsten Atomic Layer Deposition", *Chem. Mater.* **2016**, *28*, 117–126, DOI: 10.1021/acs.chemmater.5b03319.
[59] P. C. Lemaire, M. King, G. N. Parsons, "Understanding inherent substrate selectivity during atomic layer deposition: Effect of surface preparation, hydroxyl density, and metal oxide composition on nucleation mechanisms during tungsten ALD", *J. Chem. Phys.* **2017**, *146*, 052811, DOI: 10.1063/1.4967811.
[60] H. Nadhom, R. Boyd, P. Rouf, D. Lundin, H. Pedersen, "Area Selective Deposition of Metals from the Electrical Resistivity of the Substrate", *J. Phys. Chem. Lett.* **2021**, *12*, 4130–4133, DOI: 10.1021/acs.jpclett.1c00415.
[61] A. J. M. Mackus, J. J. L. Mulders, M. C. M. van de Sanden, W. M. M. Kessels, "Local deposition of high-purity Pt nanostructures by combining electron beam induced deposition and atomic layer deposition", *J. Appl. Phys.* **2010**, *107*, 116102, DOI: 10.1063/1.3431351.
[62] A. J. M. Mackus, S. A. F. Dielissen, J. J. L. Mulders, W. M. M. Kessels, "Nanopatterning by direct-write atomic layer deposition", *Nanoscale* **2012**, *4*, 4477, DOI: 10.1039/c2nr30664f.
[63] J. A. Singh, N. F. W. Thissen, W. H. Kim, H. Johnson, W. M. M. Kessels, A. A. Bol, S. F. Bent, A. J. M. Mackus, "Area-selective atomic layer deposition of metal oxides on noble metals through catalytic oxygen activation", *Chem. Mater.* **2018**, *30*, 663–670, DOI: 10.1021/acs.chemmater.7b03818.
[64] R. Chen, H. Kim, P. C. McIntyre, S. F. Bent, "Controlling area-selective atomic layer deposition of HfO_2 dielectric by self-assembled monolayers", *MRS Symp Proc* **2004**, *811*, D3.3, DOI: 10.1557/PROC-811-D3.3.
[65] M. Yan, Y. Koide, J. R. Babcock, P. R. Markworth, J. A. Belot, T. J. Marks, R. P. H. Chang, "Selective-area atomic layer epitaxy growth of ZnO features on soft lithography-patterned substrates", *Appl. Phys. Lett.* **2001**, *79*, 1709–1711, DOI: 10.1063/1.1402959.
[66] M. H. Park, Y. J. Jang, H. M. Sung-Suh, M. M. Sung, "Selective Atomic Layer Deposition of Titanium Oxide on Patterned Self-Assembled Monolayers Formed by Microcontact Printing", *Langmuir* **2004**, *20*, 2257–2260, DOI: 10.1021/la035760c.
[67] J. Yarbrough, F. Pieck, D. Grigjanis, I.-K. Oh, P. Maue, R. Tonner-Zech, S. F. Bent, "Tuning Molecular Inhibitors and Aluminum Precursors for the Area-Selective Atomic Layer Deposition of Al_2O_3", *Chem. Mater.* **2022**, *34*, 4646–4659, DOI: 10.1021/acs.chemmater.2c00513.
[68] A. Yanguas-Gil, J. A. Libera, J. W. Elam, "Modulation of the Growth Per Cycle in Atomic Layer Deposition Using Reversible Surface Functionalization", *Chem. Mater.* **2013**, *25*, 4849–4860, DOI: 10.1021/cm4029098.
[69] A. Mameli, M. J. M. Merkx, B. Karasulu, F. Roozeboom, W. M. M. Kessels, A. J. M. Mackus, "Area-Selective Atomic Layer Deposition of SiO_2 Using Acetylacetone as a Chemoselective Inhibitor in an ABC-Type Cycle", *ACS Nano* **2017**, *11*, 9303–9311, DOI: 10.1021/acsnano.7b04701.
[70] S. Zoha, F. Pieck, B. Gu, R. Tonner-Zech, H.-B.-R. Lee, "Organosulfide Inhibitor Instigated Passivation of Multiple Substrates for Area-Selective Atomic Layer Deposition of HfO2", *Chem. Mater.* **2024**, *36*, 2661–2673, DOI: 10.1021/acs.chemmater.3c02525.

[71] R. Khan, B. Shong, B. G. Ko, J. K. Lee, H. Lee, J. Y. Park, I.-K. Oh, S. S. Raya, H. M. Hong, K.-B. Chung, E. J. Luber, Y.-S. Kim, C.-H. Lee, W.-H. Kim, H.-B.-R. Lee, "Area-Selective Atomic Layer Deposition Using Si Precursors as Inhibitors", *Chem. Mater.* **2018**, *30*, 7603–7610, DOI: 10.1021/acs.chemmater.8b02774.
[72] S. K. Song, H. Saare, G. N. Parsons, "Integrated Isothermal Atomic Layer Deposition/Atomic Layer Etching Supercycles for Area-Selective Deposition of TiO_2", *Chem. Mater.* **2019**, *31*, 4793–4804, DOI: 10.1021/acs.chemmater.9b01143.
[73] S. M. George, "Mechanisms of Thermal Atomic Layer Etching", *Acc. Chem. Res.* **2020**, *53*, 1151–1160, DOI: 10.1021/acs.accounts.0c00084.
[74] P. Yu, M. J. M. Merkx, I. Tezsevin, P. C. Lemaire, D. M. Hausmann, T. E. Sandoval, W. M. M. Kessels, A. J. M. Mackus, "Blocking mechanisms in area-selective ALD by small molecule inhibitors of different sizes: Steric shielding versus chemical passivation", *Appl. Surf. Sci.* **2024**, *665*, 160141, DOI: 10.1016/j.apsusc.2024.160141.
[75] S. T. Barry, *Chemistry of Atomic Layer Deposition*, De Gruyter, **2021**.
[76] B. Kunert, K. Volz, J. Koch, W. Stolz, "Direct-band-gap Ga(NAsP)-material system pseudomorphically grown on GaP substrate", *Appl. Phys. Lett.* **2006**, *88*, 182108, DOI: 10.1063/1.2200758.
[77] K. Arts, S. Hamaguchi, T. Ito, K. Karahashi, H. C. M. Knoops, A. J. M. Mackus, W. M. M. Kessels, "Foundations of atomic-level plasma processing in nanoelectronics", *Plasma Sources Sci. Technol.* **2022**, *31*, DOI: 10.1088/1361-6595/ac95bc, DOI 10.1088/1361-6595/ac95bc.
[78] J. Amsler, P. N. Plessow, F. Studt, T. Bučko, "Anharmonic Correction to Free Energy Barriers from DFT-Based Molecular Dynamics Using Constrained Thermodynamic Integration", *J. Chem. Theory Comput.* **2023**, *19*, 2455–2468, DOI: 10.1021/acs.jctc.3c00169.
[79] G. Henkelman, A. Arnaldsson, H. Jónsson, "Theoretical calculations of CH_4 and H_2 associative desorption from Ni(111): Could subsurface hydrogen play an important role?", *J. Chem. Phys.* **2006**, *124*, 044706, DOI: 10.1063/1.2161193.
[80] L. Pecher, S. Schmidt, R. Tonner, "Modeling the Complex Adsorption Dynamics of Large Organic Molecules: Cyclooctyne on Si(001)", *J. Phys. Chem. C* **2017**, *121*, 26840–26850, DOI: 10.1021/acs.jpcc.7b09148.
[81] Y. Kaneda, R. A. Nye, E. A. Marques, S. Armini, A. Delabie, M. J. Van Setten, G. Pourtois, "A First-Principles Investigation of the Driving Forces Defining the Selectivity of TiO_2 Atomic Layer Deposition", *J. Phys. Chem. C* **2023**, *127*, 10303–10314, DOI: 10.1021/acs.jpcc.3c00965.
[82] A. Heyman, C. B. Musgrave, "A Quantum Chemical Study of the Atomic Layer Deposition of Al_2O_3 Using $AlCl_3$ and H_2O as Precursors", *J. Phys. Chem. B* **2004**, *108*, 5718–5725, DOI: 10.1021/jp049762x.
[83] H.-M. Kim, J.-H. Lee, S.-H. Lee, R. Harada, T. Shigetomi, S. Lee, T. Tsugawa, B. Shong, J.-S. Park, "Area-Selective Atomic Layer Deposition of Ruthenium Using a Novel Ru Precursor and H_2O as a Reactant", *Chem. Mater.* **2021**, *33*, 4353–4361, DOI: 10.1021/acs.chemmater.0c04496.
[84] W. L. Gladfelter, "Selective metalization by chemical vapor deposition", *Chem. Mater.* **1993**, *5*, 1372–1388, DOI: 10.1021/cm00034a004.
[85] S. McDonnell, R. C. Longo, O. Seitz, J. B. Ballard, G. Mordi, D. Dick, J. H. G. Owen, J. N. Randall, J. Kim, Y. J. Chabal, K. Cho, R. M. Wallace, "Controlling the Atomic Layer

Deposition of Titanium Dioxide on Silicon: Dependence on Surface Termination", *J. Phys. Chem. C* **2013**, *117*, 20250–20259, DOI: 10.1021/jp4060022.
[86] Y.-C. Li, K. Cao, Y.-X. Lan, J.-M. Zhang, M. Gong, Y.-W. Wen, B. Shan, R. Chen, "Inherently Area-Selective Atomic Layer Deposition of Manganese Oxide through Electronegativity-Induced Adsorption", *Molecules* **2021**, *26*, 3056, DOI: 10.3390/molecules26103056.
[87] J. Yarbrough, F. Pieck, A. B. Shearer, P. Maue, R. Tonner-Zech, S. F. Bent, "Area-Selective Atomic Layer Deposition of Al_2O_3 with a Methanesulfonic Acid Inhibitor", *Chem. Mater.* **2023**, *35*, 5963–5974, DOI: 10.1021/acs.chemmater.3c00904.
[88] A. Mameli, B. Karasulu, M. A. Verheijen, B. Barcones, B. Macco, A. J. M. Mackus, W. M. M. Kessels, F. Roozeboom, "Area-Selective Atomic Layer Deposition of ZnO by Area Activation Using Electron Beam-Induced Deposition", *Chem. Mater.* **2019**, *31*, 1250–1257, DOI: 10.1021/acs.chemmater.8b03165.
[89] N. E. Richey, C. De Paula, S. F. Bent, "Understanding chemical and physical mechanisms in atomic layer deposition", *J. Chem. Phys.* **2020**, *152*, 040902, DOI: 10.1063/1.5133390.
[90] J. Soethoudt, S. Crahaij, T. Conard, A. Delabie, "Impact of SiO_2 surface composition on trimethylsilane passivation for area-selective deposition", *J. Mater. Chem. C* **2019**, *7*, 11911–11918, DOI: 10.1039/C9TC04091A.
[91] M. J. M. Merkx, S. Vlaanderen, T. Faraz, M. A. Verheijen, W. M. M. Kessels, A. J. M. Mackus, "Area-Selective Atomic Layer Deposition of TiN Using Aromatic Inhibitor Molecules for Metal/Dielectric Selectivity", *Chem. Mater.* **2020**, *32*, 7788–7795, DOI: 10.1021/acs.chemmater.0c02370.
[92] J. Soethoudt, Y. Tomczak, B. Meynaerts, B. T. Chan, A. Delabie, "Insight into Selective Surface Reactions of Dimethylamino-trimethylsilane for Area-Selective Deposition of Metal, Nitride, and Oxide", *J. Phys. Chem. C* **2020**, *124*, 7163–7173, DOI: 10.1021/acs.jpcc.9b11270.
[93] M. J. M. Merkx, R. G. J. Jongen, A. Mameli, P. C. Lemaire, K. Sharma, D. M. Hausmann, W. M. M. Kessels, A. J. M. Mackus, "Insight into the removal and reapplication of small inhibitor molecules during area-selective atomic layer deposition of SiO_2", *J. Vac. Sci. Technol. A* **2021**, *39*, 012402, DOI: 10.1116/6.0000652.
[94] W. Xu, P. C. Lemaire, K. Sharma, R. J. Gasvoda, D. M. Hausmann, S. Agarwal, "Mechanism for growth initiation on aminosilane-functionalized SiO_2 during area-selective atomic layer deposition of ZrO_2", *J. Vac. Sci. Technol. A* **2021**, *39*, 032402, DOI: 10.1116/6.0000699.
[95] W. Xu, M. G. N. Haeve, P. C. Lemaire, K. Sharma, D. M. Hausmann, S. Agarwal, "Functionalization of the SiO_2 Surface with Aminosilanes to Enable Area-Selective Atomic Layer Deposition of Al_2O_3", *Langmuir* **2022**, *38*, 652–660, DOI: 10.1021/acs.langmuir.1c02216.
[96] K. Van Dongen, R. A. Nye, J. J. Clerix, C. Sixt, D. D. Simone, A. Delabie, "Aminosilane small molecule inhibitors for area-selective deposition: Study of substrate-inhibitor interfacial interactions", *J. Vac. Sci. Technol. A* **2023**, *41*, 032404, DOI: 10.1116/6.0002347.
[97] G. N. Parsons, "Functional model for analysis of ALD nucleation and quantification of area-selective deposition", *J. Vac. Sci. Technol. A* **2019**, *37*, 020911, DOI: 10.1116/1.5054285.
[98] F. Jensen, *Introduction to Computational Chemistry*, Wiley-VCH, **1999**.
[99] W. Koch, M. Holthausen, *A Chemist's Guide to Density Functional Theory*, John Wiley & Sons, Ltd, **2001**.

[100] A. D. Becke, "Perspective: Fifty years of density-functional theory in chemical physics", *J. Chem. Phys.* **2014**, *140*, 18A301, DOI: 10.1063/1.4869598.
[101] R. J. Maurer, C. Freysoldt, A. M. Reilly, J. G. Brandenburg, O. T. Hofmann, T. Bjorkman, S. Lebegue, A. Tkatchenko, in *Annu. Rev. Mater. Res.* (Ed.: D.R. Clarke), **2019**, pp. 1–30.
[102] P. Hohenberg, W. Kohn, "Inhomogeneous Electron Gas", *Phys. Rev.* **1964**, *136*, B864–B871.
[103] W. Kohn, L. J. Sham, "Self-Consistent Equations Including Exchange and Correlation Effects", *Phys. Rev.* **1965**, *140*, A1133–A1138.
[104] M. Kaupp, A. Wodyński, A. V. Arbuznikov, S. Fürst, C. J. Schattenberg, "Toward the Next Generation of Density Functionals: Escaping the Zero-Sum Game by Using the Exact-Exchange Energy Density", *Acc. Chem. Res.* **2024**, *57*, 1815–1826, DOI: 10.1021/acs.accounts.4c00209.
[105] D. P. Chong, O. V. Gritsenko, E. J. Baerends, "Interpretation of the Kohn–Sham orbital energies as approximate vertical ionization potentials", *J. Chem. Phys.* **2002**, *116*, 1760–1772, DOI: 10.1063/1.1430255.
[106] E. J. Baerends, "Density functional approximations for orbital energies and total energies of molecules and solids", *J. Chem. Phys.* **2018**, *149*, 054105, DOI: 10.1063/1.5026951.
[107] J. P. Perdew, K. Burke, M. Ernzerhof, "Generalized Gradient Approximation Made Simple", *Phys. Rev. Lett.* **1996**, *77*, 3865–3868, DOI: 10.1103/PhysRevLett.77.3865.
[108] L. Goerigk, S. Grimme, "A thorough benchmark of density functional methods for general main group thermochemistry, kinetics, and noncovalent interactions", *Phys. Chem. Chem. Phys.* **2011**, *13*, 6670–6688, DOI: 10.1039/C0CP02984J.
[109] L. Goerigk, A. Hansen, C. Bauer, S. Ehrlich, A. Najibi, S. Grimme, "A look at the density functional theory zoo with the advanced GMTKN55 database for general main group thermochemistry, kinetics and noncovalent interactions", *Phys. Chem. Chem. Phys.* **2017**, *19*, 32184–32215, DOI: 10.1039/c7cp04913g.
[110] N. Mardirossian, M. Head-Gordon, "Thirty years of density functional theory in computational chemistry: an overview and extensive assessment of 200 density functionals", *Mol. Phys.* **2017**, *115*, 2315–2372, DOI: 10.1080/00268976.2017.1333644.
[111] J. Wellendorff, T. L. Silbaugh, D. Garcia-Pintos, J. K. Norskov, T. Bligaard, F. Studt, C. T. Campbell, "A benchmark database for adsorption bond energies to transition metal surfaces and comparison to selected DFT functionals", *Surf. Sci.* **2015**, *640*, 36–44, DOI: 10.1016/j.susc.2015.03.023.
[112] T. Tchakoua, N. Gerrits, E. W. F. Smeets, G. J. Kroes, "SBH17: Benchmark Database of Barrier Heights for Dissociative Chemisorption on Transition Metal Surfaces", *J. Chem. Theory Comput.* **2023**, *19*, 245–270, DOI: 10.1021/acs.jctc.2c00824.
[113] M. J. M. Merkx, T. E. Sandoval, D. M. Hausmann, W. M. M. Kessels, A. J. M. Mackus, "Mechanism of Precursor Blocking by Acetylacetone Inhibitor Molecules during Area-Selective Atomic Layer Deposition of SiO_2", *Chem. Mater.* **2020**, *32*, 3335–3345, DOI: 10.1021/acs.chemmater.9b02992.
[114] A. J. Cohen, P. Mori-Sánchez, W. Yang, "Challenges for Density Functional Theory", *Chem. Rev.* **2012**, *112*, 289–320, DOI: 10.1021/cr200107z.
[115] K. R. Bryenton, A. A. Adeleke, S. G. Dale, E. R. Johnson, "Delocalization error: The greatest outstanding challenge in density-functional theory", *WIREs Comput. Mol. Sci.* **2023**, *13*, e1631, DOI: 10.1002/wcms.1631.

[116] S. Grimme, "Density functional theory with London dispersion corrections", *WIREs Comput. Mol. Sci.* **2011**, *1*, 211–228, DOI: 10.1002/wcms.30.
[117] P. Slavíček, R. Kalus, P. Paška, I. Odvárková, P. Hobza, A. Malijevský, "State-of-the-art correlated ab initio potential energy curves for heavy rare gas dimers: Ar_2, Kr_2, and Xe_2", *J. Chem. Phys.* **2003**, *119*, 2102–2119, DOI: 10.1063/1.1582838.
[118] S. Grimme, P. R. Schreiner, "Steric Crowding Can Stabilize a Labile Molecule: Solving the Hexaphenylethane Riddle", *Angew. Chem.-Int. Ed.* **2011**, *50*, 12639–12642, DOI: 10.1002/anie.201103615.
[119] S. Grimme, A. Hansen, J. G. Brandenburg, C. Bannwarth, "Dispersion-corrected mean-field electronic structure methods", *Chem. Rev.* **2016**, *116*, 5105–54, DOI: 10.1021/acs.chemrev.5b00533.
[120] R. Peverati, D. G. Truhlar, "Quest for a universal density functional: the accuracy of density functionals across a broad spectrum of databases in chemistry and physics", *Philos. Trans. R. Soc. -Math. Phys. Eng. Sci.* **2014**, *372*, 20120476, DOI: 10.1098/rsta.2012.0476.
[121] O. A. Vydrov, T. Van Voorhis, "Benchmark Assessment of the Accuracy of Several van der Waals Density Functionals", *J. Chem. Theory Comput.* **2012**, *8*, 1929–1934, DOI: 10.1021/ct300081y.
[122] S. Grimme, "Semiempirical GGA-type density functional constructed with a long-range dispersion correction", *J. Comput. Chem.* **2006**, *27*, 1787–1799, DOI: 10.1002/jcc.20495.
[123] S. Grimme, J. Antony, S. Ehrlich, H. Krieg, "A consistent and accurate *ab initio* parametrization of density functional dispersion correction (DFT-D) for the 94 elements H-Pu", *J. Chem. Phys.* **2010**, *132*, 154104, DOI: 10.1063/1.3382344.
[124] A. Tkatchenko, M. Scheffler, "Accurate Molecular Van Der Waals Interactions from Ground-State Electron Density and Free-Atom Reference Data", *Phys. Rev. Lett.* **2009**, *102*, 073005, DOI: 10.1103/PhysRevLett.102.073005.
[125] T. Helgaker, P. Jorgensen, J. Olsen, *Molecular Electronic-Structure Theory*, John Wiley & Sons, Ltd, **2000**.
[126] P. Borlido, T. Aull, A. W. Huran, F. Tran, M. A. L. Marques, S. Botti, "Large-Scale Benchmark of Exchange–Correlation Functionals for the Determination of Electronic Band Gaps of Solids", *J. Chem. Theory Comput.* **2019**, *15*, 5069–5079, DOI: 10.1021/acs.jctc.9b00322.
[127] L. Goerigk, H. Kruse, S. Grimme, "Benchmarking density functional methods against the S66 and S66x8 datasets for non-covalent interactions", *ChemPhysChem* **2011**, *12*, 3421–33, DOI: 10.1002/cphc.201100826.
[128] B. Doser, D. S. Lambrecht, J. Kussmann, C. Ochsenfeld, "Linear-scaling atomic orbital-based second-order Moller-Plesset perturbation theory by rigorous integral screening criteria", *J. Chem. Phys.* **2009**, *130*, 064107, DOI: 10.1063/1.3072903.
[129] S. A. Maurer, L. Clin, C. Ochsenfeld, "Cholesky-decomposed density MP2 with density fitting: Accurate MP2 and double-hybrid DFT energies for large systems", *J. Chem. Phys.* **2014**, *140*, 224112, DOI: 10.1063/1.4881144.
[130] J. Yang, W. F. Hu, D. Usvyat, D. Matthews, M. Schütz, G. K. L. Chan, "Ab initio determination of the crystalline benzene lattice energy to sub-kilojoule/mole accuracy", *Science* **2014**, *345*, 640–643, DOI: 10.1126/science.1254419.
[131] C. Riplinger, F. Neese, "An efficient and near linear scaling pair natural orbital based local coupled cluster method", *J. Chem. Phys.* **2013**, *138*, 034106, DOI: 10.1063/1.4773581.

[132] H.-J. Werner, A. Hansen, "Accurate Calculation of Isomerization and Conformational Energies of Larger Molecules Using Explicitly Correlated Local Coupled Cluster Methods in Molpro and ORCA", *J. Chem. Theory Comput.* **2023**, *19*, 7007–7030, DOI: 10.1021/acs.jctc.3c00270.
[133] G. Frenking, S. Shaik, Eds. , *The Chemical Bond*, Wiley-VCH, Weinheim, **2014**.
[134] N. Ashburn, X. Lang, S. Pandey, S. Wolf, S. Kramer, J. Smythe, G. Sandhu, C. Winter, A. C. Kummel, K. Cho, "Density functional theory study on reaction mechanisms of $Co(tbu_2DAD)_2$ for area selective-atomic layer deposition of Co films on metal surfaces", *J. Vac. Sci. Technol. A* **2023**, *41*, 052403, DOI: 10.1116/6.0002840.
[135] Y. Li, Y. Lan, K. Cao, J. Zhang, Y. Wen, B. Shan, R. Chen, "Surface Acidity-Induced Inherently Selective Atomic Layer Deposition of Tantalum Oxide on Dielectrics", *Chem. Mater.* **2022**, *34*, 9013–9022, DOI: 10.1021/acs.chemmater.2c00851.
[136] R. S. Mulliken, "Electronic Population Analysis on LCAO–MO Molecular Wave Functions I", *J. Chem. Phys.* **1955**, *23*, 1833–1840, DOI: 10.1063/1.1740588.
[137] M. Cho, N. Sylvetsky, S. Eshafi, G. Santra, I. Efremenko, J. M. L. Martin, "The Atomic Partial Charges Arboretum: Trying to See the Forest for the Trees", *ChemPhysChem* **2020**, *21*, 688–696, DOI: 10.1002/cphc.202000040.
[138] R. Wojtecki, J. Ma, I. Cordova, N. Arellano, K. Lionti, T. Magbitang, T. G. Pattison, X. Zhao, E. Delenia, N. Lanzillo, A. E. Hess, N. F. Nathel, H. Bui, C. Rettner, G. Wallraff, P. Naulleau, "Additive Lithography–Organic Monolayer Patterning Coupled with an Area-Selective Deposition", *ACS Appl. Mater. Interfaces* **2021**, *13*, 9081–9090, DOI: 10.1021/acsami.0c16817.
[139] R. Bader, *Atoms in Molecules: A Quantum Theory*, USA: Oxford University Press, **1994**.
[140] Y. Wen, Y. Lan, H. Li, Y. Li, K. Cao, F. Wu, R. Chen, B. Shan, "Nucleation Delay in Selective Atomic Layer Deposition: Density Functional Insights Coupled Numerical Nucleation Model", *J. Phys. Chem. C* **2024**, *128*, 9915–9925, DOI: 10.1021/acs.jpcc.4c01512.
[141] L. Zhao, M. Von Hopffgarten, D. M. Andrada, G. Frenking, "Energy decomposition analysis", *WIREs Comput. Mol. Sci.* **2018**, *8*, e1345, DOI: 10.1002/wcms.1345.
[142] E. Pastorczak, C. Corminboeuf, "Perspective: Found in translation: Quantum chemical tools for grasping non-covalent interactions", *J. Chem. Phys.* **2017**, *146*, 120901, DOI: 10.1063/1.4978951.
[143] M. Raupach, R. Tonner, "A periodic energy decomposition analysis method for the investigation of chemical bonding in extended systems", *J. Chem. Phys.* **2015**, *142*, 194105, DOI: 10.1063/1.4919943.
[144] L. Pecher, R. Tonner, "Deriving bonding concepts for molecules, surfaces, and solids with energy decomposition analysis for extended systems", *WIREs Comput. Mol. Sci.* **2019**, *9*, e1401, DOI: 10.1002/wcms.1401.
[145] P. Saalfrank, "Quantum Dynamical Approach to Ultrafast Molecular Desorption from Surfaces", *Chem. Rev.* **2006**, *106*, 4116–4159, DOI: 10.1021/cr0501691.
[146] D. Marx, J. Hutter, *Ab Initio Molecular Dynamics: Basic Theory and Advanced Methods*, Cambridge University Press, Cambridge, **2009**.
[147] X. Hu, J. Schuster, S. E. Schulz, "Multiparameter and Parallel Optimization of ReaxFF Reactive Force Field for Modeling the Atomic Layer Deposition of Copper", *J. Phys. Chem. C* **2017**, *121*, 28077–28089, DOI: 10.1021/acs.jpcc.7b09948.

[148] P. Schwerdtfeger, R. Tonner, G. E. Moyano, E. Pahl, "Towards J/mol Accuracy for the Cohesive Energy of Solid Argon", *Angew. Chem. Int. Ed.* **2016**, *55*, 12200–12205, DOI: 10.1002/anie.201605875.
[149] J. Behler, "Perspective: Machine learning potentials for atomistic simulations", *J. Chem. Phys.* **2016**, *145*, 170901, DOI: 10.1063/1.4966192.
[150] V. L. Deringer, M. A. Caro, G. Csányi, "Machine Learning Interatomic Potentials as Emerging Tools for Materials Science", *Adv. Mater.* **2019**, *31*, 1902765, DOI: 10.1002/adma.201902765.
[151] Y. Zuo, C. Chen, X. Li, Z. Deng, Y. Chen, J. Behler, G. Csányi, A. V. Shapeev, A. P. Thompson, M. A. Wood, S. P. Ong, "Performance and Cost Assessment of Machine Learning Interatomic Potentials", *J. Phys. Chem. A* **2020**, *124*, 731–745, DOI: 10.1021/acs.jpca.9b08723.
[152] K. Töpfer, L. I. Vazquez-Salazar, M. Meuwly, "Asparagus: A toolkit for autonomous, user-guided construction of machine-learned potential energy surfaces", *Comput. Phys. Commun.* **2025**, *308*, 109446, DOI: 10.1016/j.cpc.2024.109446.
[153] C. Verdi, F. Karsai, P. Liu, R. Jinnouchi, G. Kresse, "Thermal transport and phase transitions of zirconia by on-the-fly machine-learned interatomic potentials", *Npj Comput. Mater.* **2021**, *7*, 1–9, DOI: 10.1038/s41524-021-00630-5.
[154] A. Luchow, "Quantum Monte Carlo methods", *Wiley Interdiscip. Rev.-Comput. Mol. Sci.* **2011**, *1*, 388–402, DOI: 10.1002/wcms.40.
[155] J. J. Clerix, E. A. Marques, J. Soethoudt, F. Grillo, G. Pourtois, J. R. Van Ommen, A. Delabie, "Selectivity Enhancement for Ruthenium Atomic Layer Deposition in Sub-50 nm Nanopatterns by Diffusion and Size-Dependent Reactivity", *Adv. Mater. Interfaces* **2021**, *8*, 2100846, DOI: 10.1002/admi.202100846.
[156] P. Klement, D. Anders, L. Gümbel, M. Bastianello, F. Michel, J. Schörmann, M. T. Elm, C. Heiliger, S. Chatterjee, "Surface Diffusion Control Enables Tailored-Aspect-Ratio Nanostructures in Area-Selective Atomic Layer Deposition", *ACS Appl. Mater. Interfaces* **2021**, *13*, 19398–19405, DOI: 10.1021/acsami.0c22121.
[157] S. Yun, F. Ou, H. Wang, M. Tom, G. Orkoulas, P. D. Christofides, "Atomistic-mesoscopic modeling of area-selective thermal atomic layer deposition", *Chem. Eng. Res. Des.* **2022**, *188*, 271–286, DOI: 10.1016/j.cherd.2022.09.051.
[158] J. Li, I. Tezsevin, M. J. M. Merkx, J. F. W. Maas, W. M. M. Kessels, T. E. Sandoval, A. J. M. Mackus, "Packing of inhibitor molecules during area-selective atomic layer deposition studied using random sequential adsorption simulations", *J. Vac. Sci. Technol. A* **2022**, *40*, 062409, DOI: 10.1116/6.0002096.
[159] I. Tezsevin, J. F. W. Maas, M. J. M. Merkx, R. Lengers, W. M. M. Kessels, T. E. Sandoval, A. J. M. Mackus, "Computational Investigation of Precursor Blocking during Area-Selective Atomic Layer Deposition Using Aniline as a Small-Molecule Inhibitor", *Langmuir* **2023**, *39*, 4265–4273, DOI: 10.1021/acs.langmuir.2c03214.
[160] H. G. Kim, M. Kim, B. Gu, M. R. Khan, B. G. Ko, S. Yasmeen, C. S. Kim, S.-H. Kwon, J. Kim, J. Kwon, K. Jin, B. Cho, J.-S. Chun, B. Shong, H.-B.-R. Lee, "Effects of Al Precursors on Deposition Selectivity of Atomic Layer Deposition of Al_2O_3 Using Ethanethiol Inhibitor", *Chem. Mater.* **2020**, *32*, 8921–8929, DOI: 10.1021/acs.chemmater.0c02798.
[161] B. Gu, N. Le Trinh, C. T. Nguyen, S. Yasmeen, H. Gaiji, Y. Kang, H.-B.-R. Lee, "Computational Modeling of Physical Surface Reactions of Precursors in Atomic Layer

Deposition by Monte Carlo Simulations on a Home Desktop Computer", *Chem. Mater.* **2022**, *34*, 7635–7649, DOI: 10.1021/acs.chemmater.2c00854.
[162] B. Gu, S. Yasmeen, G.-H. Oh, I.-K. Oh, Y. Kang, H.-B.-R. Lee, "Si precursor-inhibitors for area selective deposition of Ru", *Appl. Surf. Sci.* **2024**, *669*, 160530, DOI: 10.1016/j.apsusc.2024.160530.
[163] N. M. Carroll, G. N. Parsons, "Stochastic lattice model for atomic layer deposition and area-selective deposition of metal oxides: Visualization and analysis of lateral overgrowth during area-selective deposition", *J. Vac. Sci. Technol. A* **2024**, *42*, 062411, DOI: 10.1116/6.0003838.
[164] B. W. J. Chen, L. Xu, M. Mavrikakis, "Computational Methods in Heterogeneous Catalysis", *Chem. Rev.* **2021**, *121*, 1007–1048, DOI: 10.1021/acs.chemrev.0c01060.
[165] H. Prats, F. Illas, R. Sayós, "General concepts, assumptions, drawbacks, and misuses in kinetic Monte Carlo and microkinetic modeling simulations applied to computational heterogeneous catalysis", *Int. J. Quantum Chem.* **2018**, *118*, e25518, DOI: 10.1002/qua.25518.
[166] A. H. Motagamwala, J. A. Dumesic, "Microkinetic Modeling: A Tool for Rational Catalyst Design", *Chem. Rev.* **2021**, *121*, 1049–1076, DOI: 10.1021/acs.chemrev.0c00394.
[167] J. Feder, "Random sequential adsorption", *J. Theor. Biol.* **1980**, *87*, 237–254, DOI: 10.1016/0022-5193(80)90358-6.
[168] E. L. Hinrichsen, J. Feder, T. Jøssang, "Geometry of random sequential adsorption", *J. Stat. Phys.* **1986**, *44*, 793–827, DOI: 10.1007/BF01011908.
[169] J. W. Evans, "Random and cooperative sequential adsorption", *Rev. Mod. Phys.* **1993**, *65*, 1281–1329, DOI: 10.1103/RevModPhys.65.1281.
[170] M. Hu, T. C. Hauger, B. C. Olsen, E. J. Luber, J. M. Buriak, "UV-Initiated Si–S, Si–Se, and Si–Te Bond Formation on Si(111): Coverage, Mechanism, and Electronics", *J. Phys. Chem. C* **2018**, *122*, 13803–13814, DOI: 10.1021/acs.jpcc.8b00910.
[171] M. Andersen, C. Panosetti, K. Reuter, "A Practical Guide to Surface Kinetic Monte Carlo Simulations", *Front. Chem.* **2019**, *7*, DOI: 10.3389/fchem.2019.00202, DOI 10.3389/fchem.2019.00202.
[172] M. Pineda, M. Stamatakis, "Kinetic Monte Carlo simulations for heterogeneous catalysis: Fundamentals, current status, and challenges", *J. Chem. Phys.* **2022**, *156*, 120902, DOI: 10.1063/5.0083251.
[173] A. B. Bortz, M. H. Kalos, J. L. Lebowitz, "A new algorithm for Monte Carlo simulation of Ising spin systems", *J. Comput. Phys.* **1975**, *17*, 10–18, DOI: 10.1016/0021-9991(75)90060-1.
[174] A. Bruix, J. T. Margraf, M. Andersen, K. Reuter, "First-principles-based multiscale modelling of heterogeneous catalysis", *Nat. Catal.* **2019**, *2*, 659–670, DOI: 10.1038/s41929-019-0298-3.
[175] J. A. Keith, V. Vassilev-Galindo, B. Cheng, S. Chmiela, M. Gastegger, K.-R. Müller, A. Tkatchenko, "Combining Machine Learning and Computational Chemistry for Predictive Insights Into Chemical Systems", *Chem. Rev.* **2021**, *121*, 9816–9872, DOI: 10.1021/acs.chemrev.1c00107.
[176] P. O. Dral, "Quantum Chemistry in the Age of Machine Learning", *J. Phys. Chem. Lett.* **2020**, 2336–2347, DOI: 10.1021/acs.jpclett.9b03664.

[177] J. Schmidt, M. R. G. Marques, S. Botti, M. A. L. Marques, "Recent advances and applications of machine learning in solid-state materials science", *Npj Comput. Mater.* **2019**, *5*, 36, DOI: 10.1038/s41524-019-0221-0.
[178] J. Behler, "Four Generations of High-Dimensional Neural Network Potentials", *Chem. Rev.* **2021**, *121*, 10037–10072, DOI: 10.1021/acs.chemrev.0c00868.
[179] A. Yanguas-Gil, J. W. Elam, "Machine learning and atomic layer deposition: Predicting saturation times from reactor growth profiles using artificial neural networks", *J. Vac. Sci. Technol. A* **2022**, *40*, 062408, DOI: 10.1116/6.0001973.
[180] Y. Widjaja, J. H. Han, C. B. Musgrave, "Quantum Chemical Study of Zirconium Oxide Deposition on the Si(100)−(2×1) Surface", *J. Phys. Chem. B* **2003**, *107*, 9319–9324, DOI: 10.1021/jp030257u.
[181] W. Lee, N. P. Dasgupta, O. Trejo, J.-R. Lee, J. Hwang, T. Usui, F. B. Prinz, "Area-Selective Atomic Layer Deposition of Lead Sulfide: Nanoscale Patterning and DFT Simulations", *Langmuir* **2010**, *26*, 6845–6852, DOI: 10.1021/la904122e.
[182] D. F. Tracey, B. Delley, D. R. McKenzie, O. Warschkow, "Molecular adsorption on silicon (001): A systematic evaluation of size effects in slab and cluster models", *AIP Adv.* **2013**, *3*, 042117, DOI: 10.1063/1.4802837.
[183] J. Heep, J.-N. Luy, C. Länger, J. Meinecke, U. Koert, R. Tonner, M. Dürr, "Adsorption of Methyl-Substituted Benzylazide on Si(001): Reaction Channels and Final Configurations", *J. Phys. Chem. C* **2020**, *124*, 9940–9946, DOI: 10.1021/acs.jpcc.0c01009.
[184] S. Bocharov, O. Dmitrenko, L. P. M. D. Leo, A. V. Teplyakov, "Azide Reactions for Controlling Clean Silicon Surface Chemistry: Benzylazide on Si(100)-2 x 1", *J Am Chem Soc* **2006**, *128*, 9300–9301.
[185] P. A. Cox, *The Electronic Structure and Chemistry of Solids*, Oxford Science Publications, **1987**.
[186] R. Hoffmann, *Solids and Surfaces - a Chemist's View of Bonding in Extended Structures*, VCH, New York, Weinheim, **1988**.
[187] R. Tonner, "Adsorption of Proline and Glycine on the TiO_2(110) Surface: A Density Functional Theory Study", *ChemPhysChem* **2010**, *11*, 1053–1061, DOI: 10.1002/cphc.200900902.
[188] J. Yoshinobu, "Physical properties and chemical reactivity of the buckled dimer on Si(100)", *Prog. Surf. Sci.* **2004**, *77*, 37–70, DOI: 10.1016/j.progsurf.2004.07.001.
[189] K. Ronnby, H. Pedersen, L. Ojamae, "Surface Structures from NH_3 Chemisorption in CVD and ALD of AlN, GaN, and InN Films", *J. Phys. Chem. C* **2022**, *126*, 5885–5895, DOI: 10.1021/acs.jpcc.2c00510.
[190] F. Tran, J. Stelzl, P. Blaha, "Rungs 1 to 4 of DFT Jacob's ladder: Extensive test on the lattice constant, bulk modulus, and cohesive energy of solids", *J. Chem. Phys.* **2016**, *144*, 204120, DOI: 10.1063/1.4948636.
[191] A. R. Bielinski, E. P. Kamphaus, L. Cheng, A. B. F. Martinson, "Resolving the Heat of Trimethylaluminum and Water Atomic Layer Deposition Half-Reactions", *J. Am. Chem. Soc.* **2022**, jacs.2c05460, DOI: 10.1021/jacs.2c05460.
[192] G. B. Damas, K. Ronnby, H. Pedersen, L. Ojamae, "Understanding indium nitride thin film growth under ALD conditions by atomic scale modelling: From the bulk to the In-rich layer", *Appl. Surf. Sci.* **2022**, *592*, 153290, DOI: 10.1016/j.apsusc.2022.153290.
[193] R. C. Longo, J. H. G. Owen, S. McDonnell, D. Dick, J. B. Ballard, J. N. Randall, R. M. Wallace, Y. J. Chabal, K. Cho, "Toward atomic-scale patterned atomic layer deposition:

Reactions of Al_2O_3 precursors on a Si(001) surface with mixed functionalizations", *J. Phys. Chem. C* **2016**, *120*, 2628–2641, DOI: 10.1021/acs.jpcc.5b09053.
[194] H. Pedersen, S. Elliott, "Studying chemical vapor deposition processes with theoretical chemistry", *Theor. Chem. Acc.* **2014**, *133*, 1–10, DOI: 10.1007/s00214-014-1476-7.
[195] J. Liu, R. Mullins, H. Lu, D. W. Zhang, M. Nolan, "Nucleation of Co and Ru Precursors on Silicon with Different Surface Terminations: Impact on Nucleation Delay", *J. Phys. Chem. C* **2023**, *127*, 13651–13658, DOI: 10.1021/acs.jpcc.3c02933.
[196] J. Liu, H. Lu, D. W. Zhang, M. Nolan, "Reaction Mechanism of the Metal Precursor Pulse in Plasma-Enhanced Atomic Layer Deposition of Cobalt and the Role of Surface Facets", *J. Phys. Chem. C* **2020**, *124*, 11990–12000, DOI: 10.1021/acs.jpcc.0c02976.
[197] D. Zanders, J. Liu, J. Obenlueneschloss, C. Bock, D. Rogalla, L. Mai, M. Nolan, S. T. Barry, A. Devi, "Cobalt Metal ALD: Understanding the Mechanism and Role of Zinc Alkyl Precursors as Reductants for Low-Resistivity Co Thin Films", *Chem. Mater.* **2021**, *33*, 5045–5057, DOI: 10.1021/acs.chemmater.1c00877.
[198] G. Y. Fang, L. N. Xu, J. Ma, A. D. Li, "Theoretical Understanding of the Reaction Mechanism of SiO_2 Atomic Layer Deposition", *Chem. Mater.* **2016**, *28*, 1247–1255, DOI: 10.1021/acs.chemmater.5b04422.
[199] X. Zhang, Z. Zhou, R. Xu, J. Guo, L. Xu, Y. Ding, H. Xiao, X. Li, A. Li, G. Fang, "Reaction mechanism of nickel sulfide atomic layer deposition using bis(N,N'-di-tert-butylacetamidinato)nickel(II) and hydrogen sulfide", *Phys. Chem. Chem. Phys. - PCCP* **2023**, *25*, 13465–13473, DOI: 10.1039/d2cp05450g.
[200] Y. Xu, C. B. Musgrave, "A DFT Study of the Al_2O_3 Atomic Layer Deposition on SAMs: Effect of SAM Termination", *Chem. Mater.* **2004**, *16*, 646–653, DOI: 10.1021/cm035009p.
[201] S. Seo, B. C. Yeo, S. S. Han, C. M. Yoon, J. Y. Yang, J. Yoon, C. Yoo, H. Kim, Y. Lee, S. J. Lee, J.-M. Myoung, H.-B.-R. Lee, W.-H. Kim, I.-K. Oh, H. Kim, "Reaction Mechanism of Area-Selective Atomic Layer Deposition for Al_2O_3 Nanopatterns", *ACS Appl. Mater. Interfaces* **2017**, *9*, 41607–41617, DOI: 10.1021/acsami.7b13365.
[202] S. Patwardhan, D. H. Cao, G. C. Schatz, A. B. F. Martinson, "Atomic Layer Deposition Nucleation on Isolated Self-Assembled Monolayer Functional Groups: A Combined DFT and Experimental Study", *ACS Appl. Energy Mater.* **2019**, *2*, 4618–4628, DOI: 10.1021/acsaem.8b02202.
[203] T. Suh, Y. Yang, H. W. Sohn, R. A. DiStasio, J. R. Engstrom, "Area-selective atomic layer deposition enabled by competitive adsorption", *J. Vac. Sci. Technol. Vac. Surf. Films* **2020**, *38*, 062411, DOI: 10.1116/6.0000497.
[204] W.-H. Kim, K. Shin, B. Shong, L. Godet, S. F. Bent, "Atomic Layer Deposition of Pt on the Surface Deactivated by Fluorocarbon Implantation: Investigation of the Growth Mechanism", *Chem. Mater.* **2020**, *32*, 9696–9703, DOI: 10.1021/acs.chemmater.0c03372.
[205] S. Lee, M. Kim, G. Baek, H. Kim, T. N. V. Tran, D. Gwak, K. Heo, B. Shong, J.-S. Park, "Thermal Annealing of Molecular Layer-Deposited Indicone Toward Area-Selective Atomic Layer Deposition", *ACS Appl. Mater. Interfaces* **2020**, *12*, 43212–43221, DOI: 10.1021/acsami.0c10322.
[206] M. J. M. Merkx, A. Angelidis, A. Mameli, J. Li, P. C. Lemaire, K. Sharma, D. M. Hausmann, W. M. M. Kessels, T. E. Sandoval, A. J. M. Mackus, "Relation between Reactive Surface Sites and Precursor Choice for Area-Selective Atomic Layer Deposition Using Small Molecule Inhibitors", *J. Phys. Chem. C* **2022**, *126*, 4845–4853, DOI: 10.1021/acs.jpcc.1c10816.

[207] M. Tom, H. Wang, F. Ou, G. Orkoulas, P. D. Christofides, "Machine Learning Modeling and Run-to-Run Control of an Area-Selective Atomic Layer Deposition Spatial Reactor", *Coatings* **2024**, *14*, 38, DOI: 10.3390/coatings14010038.
[208] B. Karasulu, F. Roozeboom, A. Mameli, "High-Throughput Area-Selective Spatial Atomic Layer Deposition of SiO_2 with Interleaved Small Molecule Inhibitors and Integrated Back-Etch Correction for Low Defectivity", *Adv. Mater.* **2023**, *35*, 2301204, DOI: 10.1002/adma.202301204.
[209] C. T. Nguyen, E.-H. Cho, N. L. Trinh, B. Gu, M. Lee, S. Lee, J.-Y. Lee, Y. Kang, H.-B.-R. Lee, "Area-Selective Deposition of Ruthenium Using Homometallic Precursor-inhibitor", *Chem. Mater.* **2023**, *35*, 5331–5340, DOI: 10.1021/acs.chemmater.3c00525.
[210] J. Kim, C. Yeon, D.-H. Cho, J. Jung, B. Shong, "Enhancement of Conformality of Silicon Nitride Thin Films by ABC-Type Atomic Layer Deposition", *Adv. Electron. Mater.* **2023**, 2300722, DOI: 10.1002/aelm.202300722.
[211] M. J. M. Merkx, I. Tezsevin, P. Yu, T. Janssen, R. H. G. M. Heinemans, R. J. Lengers, J.-R. Chen, C. J. Jezewski, S. B. Clendenning, W. M. M. Kessels, T. E. Sandoval, A. J. M. Mackus, "In situ formation of inhibitor species through catalytic surface reactions during area-selective atomic layer deposition of TaN", *J. Chem. Phys.* **2024**, *160*, 204701, DOI: 10.1063/5.0207496.
[212] J. Lee, J. Oh, J. Kim, H. Oh, B. Shong, W.-H. Kim, "Area-selective atomic layer deposition of Ru thin films by chemo-selective inhibition of alkyl aldehyde molecules on nitride surfaces", *Appl. Surf. Sci.* **2024**, 160099, DOI: 10.1016/j.apsusc.2024.160099.
[213] L. A. Ogunfowora, I. Singh, N. Arellano, T. G. Pattison, T. Magbitang, K. Nguyen, B. Ransom, K. Lionti, S. Nguyen, T. Topura, E. Delenia, M. Sherwood, B. M. Savoie, R. Wojtecki, "Reactive Vapor-Phase Inhibitors for Area-Selective Depositions at Tunable Critical Dimensions", *ACS Appl. Mater. Interfaces* **2024**, *16*, 5268–5277, DOI: 10.1021/acsami.3c14821.
[214] P. P. Wellmann, F. Pieck, R. Tonner-Zech, "An Atomistic Picture of Buildup and Degradation Reactions in Area-Selective Atomic Layer Deposition with a Small Molecule Inhibitor", *Chem. Mater.* **2024**, *36*, 7343–7361, DOI: 10.1021/acs.chemmater.4c01269.
[215] S. Zoha, F. Pieck, B. Gu, R. Tonner-Zech, H.-B.-R. Lee, "Organosulfide Inhibitor Instigated Passivation of Multiple Substrates for Area-Selective Atomic Layer Deposition of HfO_2", *Chem. Mater.* **2024**, *36*, 2661–2673, DOI: 10.1021/acs.chemmater.3c02525.
[216] E.-H. Cho, D. Kong, I. Cho, Y. Leem, Y. M. Lee, M. Kim, C. T. Nguyen, J. Y. Lee, B. Shong, H.-B.-R. Lee, "Area-Selective Atomic Layer Deposition of Ruthenium via Reduction of Interfacial Oxidation", *Chem. Mater.* **2024**, *36*, 8663–8672, DOI: 10.1021/acs.chemmater.4c01133.
[217] A. B. Shearer, F. Pieck, J. Yarbrough, A. Werbrouck, R. Tonner-Zech, S. F. Bent, "Role of Molecular Orientation: Comparison of Nitrogenous Aromatic Small Molecule Inhibitors for Area-Selective Atomic Layer Deposition", *Chem. Mater.* **2024**, DOI: in print, DOI in print.
[218] J. Lu, B. Liu, N. P. Guisinger, P. C. Stair, J. P. Greeley, J. W. Elam, "First-Principles Predictions and in Situ Experimental Validation of Alumina Atomic Layer Deposition on Metal Surfaces", *Chem. Mater.* **2014**, *26*, 6752–6761, DOI: 10.1021/cm503178j.
[219] A. Mameli, Y. Kuang, M. Aghaee, C. K. Ande, B. Karasulu, M. Creatore, A. J. M. Mackus, W. M. M. Kessels, F. Roozeboom, "Area-Selective Atomic Layer Deposition of In_2O_3:H Using a μ-Plasma Printer for Local Area Activation", *Chem. Mater.* **2017**, *29*, 921–925, DOI: 10.1021/acs.chemmater.6b04469.

[220] J. Cai, J. Zhang, K. Cao, M. Gong, Y. Lang, X. Liu, S. Chu, B. Shan, R. Chen, "Selective Passivation of Pt Nanoparticles with Enhanced Sintering Resistance and Activity toward CO Oxidation via Atomic Layer Deposition", *ACS Appl. Nano Mater.* **2018**, *1*, 522–530, DOI: 10.1021/acsanm.7b00026.
[221] Y. Wen, J. Cai, J. Zhang, J. Yang, L. Shi, K. Cao, R. Chen, B. Shan, "Edge-Selective Growth of MCp_2 (M = Fe, Co, and Ni) Precursors on Pt Nanoparticles in Atomic Layer Deposition: A Combined Theoretical and Experimental Study", *Chem. Mater.* **2019**, *31*, 101–111, DOI: 10.1021/acs.chemmater.8b03168.
[222] J. Lee, J.-M. Lee, H. Oh, C. Kim, J. Kim, D. H. Kim, B. Shong, T. J. Park, W.-H. Kim, "Inherently Area-Selective Atomic Layer Deposition of SiO_2 Thin Films to Confer Oxide Versus Nitride Selectivity", *Adv. Funct. Mater.* **2021**, *31*, 2102556, DOI: 10.1002/adfm.202102556.
[223] C.-Y. Chou, W.-H. Lee, C.-P. Chuu, T.-A. Chen, C.-H. Hou, Y.-T. Yin, T.-Y. Wang, J.-J. Shyue, L.-J. Li, M.-J. Chen, "Atomic Layer Nucleation Engineering: Inhibitor-Free Area-Selective Atomic Layer Deposition of Oxide and Nitride", *Chem. Mater.* **2021**, *33*, 5584–5590, DOI: 10.1021/acs.chemmater.1c00823.
[224] J.-M. Lee, J. Lee, H. Oh, J. Kim, B. Shong, T. J. Park, W.-H. Kim, "Inhibitor-free area-selective atomic layer deposition of SiO_2 through chemoselective adsorption of an aminodisilane precursor on oxide versus nitride substrates", *Appl. Surf. Sci.* **2022**, *589*, 152939, DOI: 10.1016/j.apsusc.2022.152939.
[225] C.-Y. Chou, C.-L. Mo, C.-P. Chuu, T.-Y. Wang, C.-C. Huang, C.-H. Hou, C.-H. Chuang, Y.-S. Jiang, J.-J. Shyue, M.-J. Chen, "Inhibitor-Free Area-Selective Atomic Layer Deposition with Feature Size Down to Nearly 10 nm", *Chem. Mater.* **2023**, *35*, 1107–1115, DOI: 10.1021/acs.chemmater.2c03046.
[226] J. C. Jones, E. P. Kamphaus, J. R. Guest, A. U. Mane, L. Cheng, A. B. F. Martinson, "Site-Selective Atomic Layer Deposition at Thermally Generated Surface Oxygen Vacancies on Rutile TiO_2", *Chem. Mater.* **2023**, *35*, 2857–2863, DOI: 10.1021/acs.chemmater.2c03679.
[227] E. P. Kamphaus, J. C. Jones, N. Shan, A. B. F. Martinson, L. Cheng, "Site-Selective Atomic Layer Deposition on Rutile TiO_2: Selective Hydration as a Route to Target Point Defects", *J. Phys. Chem. C* **2023**, *127*, 1397–1406, DOI: 10.1021/acs.jpcc.2c06992.
[228] Z. Qi, H. Li, K. Cao, E. Gu, Y. Wen, J. Long, B. Shan, R. Chen, "Area Selective Deposition of Ru on W/SiO_2 Nanopatterns via Sequential Reactant Dosing and Thermal Defect Correction", *Chem. Mater.* **2024**, *36*, 8133–8140, DOI: 10.1021/acs.chemmater.4c00475.
[229] Y. Lee, S. Seo, A. B. Shearer, A. Werbrouck, H. Kim, S. F. Bent, "HfO2 Area-Selective Atomic Layer Deposition with a Carbon-Free Inhibition Layer", *Chem. Mater.* **2024**, DOI: 10.1021/acs.chemmater.3c03161, DOI 10.1021/acs.chemmater.3c03161.
[230] S. E. Potts, W. M. M. Kessels, "Energy-enhanced atomic layer deposition for more process and precursor versatility", *Coord. Chem. Rev.* **2013**, *257*, 3254–3270, DOI: 10.1016/j.ccr.2013.06.015.
[231] A. W. Laubengayer, W. F. Gilliam, "The Alkyls of the Third Group Elements I Vapor Phase Studies of the Alkyls of Aluminum, Gallium and Indium", *J. Am. Chem. Soc.* **1941**, *63*, 477–479, DOI: 10.1021/ja01847a031.
[232] M. B. Smith, "The monomer−dimer equilibria of liquid aluminum alkyls", *J. Organomet. Chem.* **1972**, *46*, 31–49, DOI: 10.1016/S0022-328X(00)90473-X.
[233] P. Maue, É. Chantraine, F. Pieck, R. Tonner-Zech, "Accurately computed dimerization fraction of ALD precursors and their impact on surface reactivity in area-selective atomic

layer deposition", **2024**, DOI: 10.26434/chemrxiv-2024-x3n3k, DOI 10.26434/chemrxiv-2024-x3n3k.
[234] I.-K. Oh, T. E. Sandoval, T.-L. Liu, N. E. Richey, S. F. Bent, "Role of Precursor Choice on Area-Selective Atomic Layer Deposition", *Chem. Mater.* **2021**, *33*, 3926–3935, DOI: 10.1021/acs.chemmater.0c04718.
[235] R. A. Adomaitis, "Estimating the thermochemical properties of trimethylaluminum for thin-film processing applications", *J. Vac. Sci. Technol. A* **2018**, *36*, 050602, DOI: 10.1116/1.5045342.
[236] M. Kim, S. Kim, B. Shong, "Adsorption of dimethylaluminum isopropoxide (DMAI) on the Al_2O_3 surface: a machine-learning potential study", *J. Sci. Adv. Mater. Devices* **2024**, *9*, 100754, DOI: 10.1016/j.jsamd.2024.100754.
[237] S. Monaghan, J. C. Greer, S. D. Elliott, "Thermal decomposition mechanisms of hafnium and zirconium silicates at the atomic scale", *J. Appl. Phys.* **2005**, *97*, 114911, DOI: 10.1063/1.1926399.
[238] M. B. E. Griffiths, Z. S. Dubrawski, G. Bačić, A. Japahuge, J. D. Masuda, T. Zeng, S. T. Barry, "Controlling the Thermal Stability and Volatility of Organogold(I) Compounds for Vapor Deposition with Complementary Ligand Design", *Eur. J. Inorg. Chem.* **2019**, *2019*, 4927–4938, DOI: 10.1002/ejic.201901087.
[239] A. Zydor, S. D. Elliott, "Thermal Stability of Precursors for Atomic Layer Deposition of TiO_2, ZrO_2, and HfO_2: An Ab Initio Study of α-Hydrogen Abstraction in Bis-cyclopentadienyl Dimethyl Complexes", *J. Phys. Chem. A* **2010**, *114*, 1879–1886, DOI: 10.1021/jp9072608.
[240] A. Devi, "'Old Chemistries' for new applications: Perspectives for development of precursors for MOCVD and ALD applications", *Coord. Chem. Rev.* **2013**, *257*, 3332–3384, DOI: 10.1016/j.ccr.2013.07.025.
[241] F. Gharagheizi, A. Eslamimanesh, P. Ilani-Kashkouli, A. H. Mohammadi, D. Richon, "QSPR molecular approach for representation/prediction of very large vapor pressure dataset", *Chem. Eng. Sci.* **2012**, *76*, 99–107, DOI: 10.1016/j.ces.2012.03.033.
[242] H. Matsukawa, M. Kitahara, K. Otake, "Estimation of pure component parameters of PC-SAFT EoS by an artificial neural network based on a group contribution method", *Fluid Phase Equilibria* **2021**, *548*, 113179, DOI: 10.1016/j.fluid.2021.113179.
[243] S. Grimme, "A General Quantum Mechanically Derived Force Field (QMDFF) for Molecules and Condensed Phase Simulations", *J. Chem. Theory Comput.* **2014**, *10*, 4497–4514, DOI: 10.1021/ct500573f.
[244] A. Odinokov, W.-J. Son, A. Yakubovich, J. Y. Park, Y. Jung, "Ab Initio Prediction of Vapor Pressure for Diverse Atomic Layer Deposition Precursors", *J. Chem. Theory Comput.* **2024**, *20*, 6144–6151, DOI: 10.1021/acs.jctc.3c01416.
[245] F. Zaera, "Mechanisms of surface reactions in thin solid film chemical deposition processes", *Coord. Chem. Rev.* **2013**, *257*, 3177–3191, DOI: 10.1016/j.ccr.2013.04.006.
[246] T. T. Ngoc Van, C. Kim, H. Lee, J. Kim, B. Shong, "Machine learning-based exploration of molecular design descriptors for area-selective atomic layer deposition (AS-ALD) precursors", *J. Mol. Model.* **2024**, *30*, 10, DOI: 10.1007/s00894-023-05806-y.
[247] A. Groß, *Theoretical Surface Science - A Microscopic Perspective*, Springer, Berlin, Heidelberg, **2009**.

[248] Á. Morales-García, F. Viñes, J. R. B. Gomes, F. Illas, "Concepts, models, and methods in computational heterogeneous catalysis illustrated through CO conversion", *WIREs Comput. Mol. Sci.* **2021**, *11*, e1530, DOI: 10.1002/wcms.1530.
[249] J.-W. J. Clerix, G. Dianat, A. Delabie, G. N. Parsons, "In situ analysis of nucleation reactions during $TiCl_4/H_2O$ atomic layer deposition on SiO_2 and H-terminated Si surfaces treated with a silane small molecule inhibitor", *J. Vac. Sci. Technol. A* **2023**, *41*, 032406, DOI: 10.1116/6.0002493.
[250] H. Saare, G. Dianat, G. N. Parsons, "Comparative In Situ Study of the Initial Growth Trends of Atomic Layer-Deposited Al_2O_3 Films", *J. Phys. Chem. C* **2022**, *126*, 7036–7046, DOI: 10.1021/acs.jpcc.2c01033.
[251] X. Qu, D. Yan, R. Li, J. Cen, C. Zhou, W. Zhang, D. Lu, K. Attenkofer, D. J. Stacchiola, M. S. Hybertsen, E. Stavitski, M. Liu, "Resolving the Evolution of Atomic Layer-Deposited Thin-Film Growth by Continuous In Situ X-Ray Absorption Spectroscopy", *Chem. Mater.* **2021**, *33*, 1740–1751, DOI: 10.1021/acs.chemmater.0c04547.
[252] V. Vandalon, W. M. M. Kessels, "Revisiting the growth mechanism of atomic layer deposition of Al_2O_3: A vibrational sum-frequency generation study", *J Vac Sci Technol A* **2017**, *35*, 15, DOI: 10.1116/1.4993597.
[253] L. T. Zhuravlev, "The surface chemistry of amorphous silica Zhuravlev model", *Colloids Surf. Physicochem. Eng. Asp.* **2000**, *173*, 1–38, DOI: 10.1016/S0927-7757(00)00556-2.
[254] P. Rosenow, R. Tonner, "Extent of hydrogen coverage of Si(001) under chemical vapor deposition conditions from ab initio approaches", *J. Chem. Phys.* **2016**, *144*, 204706, DOI: 10.1063/1.4952603.
[255] G. M. Repa, L. A. Fredin, "Predicting Electronic Structure of Realistic Amorphous Surfaces", *Adv. Theory Simul.* **2023**, *6*, 2300292, DOI: 10.1002/adts.202300292.
[256] A. S. Sandupatla, K. Alexopoulos, M.-F. Reyniers, G. B. Marin, "DFT Investigation into Alumina ALD Growth Inhibition on Hydroxylated Amorphous Silica Surface", *J. Phys. Chem. C* **2015**, *119*, 18380–18388, DOI: 10.1021/acs.jpcc.5b05261.
[257] G. Kresse, J. Furthmüller, "Efficiency of ab-initio total energy calculations for metals and semiconductors using a plane-wave basis set", *Comput. Mater. Sci.* **1996**, *6*, 15–50, DOI: 10.1016/0927-0256(96)00008-0.
[258] G. Kresse, J. Furthmüller, "Efficient iterative schemes for *ab initio* total-energy calculations using a plane-wave basis set", *Phys. Rev. B* **1996**, *54*, 11169–11186, DOI: 10.1103/PhysRevB.54.11169.
[259] G. Kresse, J. Hafner, "Ab initio molecular dynamics for liquid metals", *Phys. Rev. B* **1993**, *47*, 558–561, DOI: 10.1103/PhysRevB.47.558.
[260] G. Kresse, J. Hafner, "*Ab initio* molecular-dynamics simulation of the liquid-metal–amorphous-semiconductor transition in germanium", *Phys. Rev. B* **1994**, *49*, 14251–14269, DOI: 10.1103/PhysRevB.49.14251.
[261] M. J. Frisch, G. W. Trucks, H. B. Schlegel, G. E. Scuseria, M. A. Robb, J. R. Cheeseman, G. Scalmani, V. Barone, G. A. Petersson, H. Nakatsuji, X. Li, M. Caricato, A. V. Marenich, J. Bloino, B. G. Janesko, R. Gomperts, B. Mennucci, H. P. Hratchian, J. V. Ortiz, A. F. Izmaylov, J. L. Sonnenberg, D. Williams-Young, F. Ding, F. Lipparini, F. Egidi, J. Goings, B. Peng, A. Petrone, T. Henderson, D. Ranasinghe, V. G. Zakrzewski, J. Gao, N. Rega, G. Zheng, W. Liang, M. Hada, M. Ehara, K. Toyota, R. Fukuda, J. Hasegawa, M. Ishida, T. Nakajima, Y. Honda, O. Kitao, H. Nakai, T. Vreven, K. Throssell, J. A. Montgomery Jr., J. E. Peralta, F. Ogliaro, M. J. Bearpark, J. J. Heyd, E. N. Brothers, K. N. Kudin, V. N.

Staroverov, T. A. Keith, R. Kobayashi, J. Normand, K. Raghavachari, A. P. Rendell, J. C. Burant, S. S. Iyengar, J. Tomasi, M. Cossi, J. M. Millam, M. Klene, C. Adamo, R. Cammi, J. W. Ochterski, R. L. Martin, K. Morokuma, O. Farkas, J. B. Foresman, D. J. Fox, "Gaussian 16", **2016**,.

[262] E. Aprà, E. J. Bylaska, W. A. de Jong, N. Govind, K. Kowalski, T. P. Straatsma, M. Valiev, H. J. J. van Dam, Y. Alexeev, J. Anchell, V. Anisimov, F. W. Aquino, R. Atta-Fynn, J. Autschbach, N. P. Bauman, J. C. Becca, D. E. Bernholdt, K. Bhaskaran-Nair, S. Bogatko, P. Borowski, J. Boschen, J. Brabec, A. Bruner, E. Cauët, Y. Chen, G. N. Chuev, C. J. Cramer, J. Daily, M. J. O. Deegan, T. H. Dunning, M. Dupuis, K. G. Dyall, G. I. Fann, S. A. Fischer, A. Fonari, H. Früchtl, L. Gagliardi, J. Garza, N. Gawande, S. Ghosh, K. Glaesemann, A. W. Götz, J. Hammond, V. Helms, E. D. Hermes, K. Hirao, S. Hirata, M. Jacquelin, L. Jensen, B. G. Johnson, H. Jónsson, R. A. Kendall, M. Klemm, R. Kobayashi, V. Konkov, S. Krishnamoorthy, M. Krishnan, Z. Lin, R. D. Lins, R. J. Littlefield, A. J. Logsdail, K. Lopata, W. Ma, A. V. Marenich, J. Martin del Campo, D. Mejia-Rodriguez, J. E. Moore, J. M. Mullin, T. Nakajima, D. R. Nascimento, J. A. Nichols, P. J. Nichols, J. Nieplocha, A. Otero-de-la-Roza, B. Palmer, A. Panyala, T. Pirojsirikul, B. Peng, R. Peverati, J. Pittner, L. Pollack, R. M. Richard, P. Sadayappan, G. C. Schatz, W. A. Shelton, D. W. Silverstein, D. M. A. Smith, T. A. Soares, D. Song, M. Swart, H. L. Taylor, G. S. Thomas, V. Tipparaju, D. G. Truhlar, K. Tsemekhman, T. Van Voorhis, Á. Vázquez-Mayagoitia, P. Verma, O. Villa, A. Vishnu, K. D. Vogiatzis, D. Wang, J. H. Weare, M. J. Williamson, T. L. Windus, K. Woliński, A. T. Wong, Q. Wu, C. Yang, Q. Yu, M. Zacharias, Z. Zhang, Y. Zhao, R. J. Harrison, "NWChem: Past, present, and future", *J. Chem. Phys.* **2020**, *152*, 184102, DOI: 10.1063/5.0004997.

[263] J. J. Clerix, A. Sanz-Matias, S. Armini, J. N. Harvey, A. Delabie, "Structural Phases of Alkanethiolate Self-Assembled Monolayers ($C_{1–12}$) on Cu[100] by Density Functional Theory", *J. Phys. Chem. C* **2020**, *124*, 3802–3811, DOI: 10.1021/acs.jpcc.9b08206.

[264] T. Suh, Y. Yang, P. Zhao, K. U. Lao, H.-Y. Ko, J. Wong, R. A. DiStasio, J. R. Engstrom, "Competitive Adsorption as a Route to Area-Selective Deposition", *ACS Appl. Mater. Interfaces* **2020**, *12*, 9989–9999, DOI: 10.1021/acsami.9b22065.

[265] F. S. Minaye Hashemi, C. Prasittichai, S. F. Bent, "Self-Correcting Process for High Quality Patterning by Atomic Layer Deposition", *ACS Nano* **2015**, *9*, 8710–8717, DOI: 10.1021/acsnano.5b03125.

[266] D. K. Schwartz, "Mechanisms and kinetics of self-assembled monolayer formation", *Annu. Rev. Phys. Chem.* **2001**, *52*, 107–137, DOI: 10.1146/annurev.physchem.52.1.107.

[267] S. R. Kachel, B. P. Klein, J. M. Morbec, M. Schöniger, M. Hutter, M. Schmid, P. Kratzer, B. Meyer, R. Tonner, J. M. Gottfried, "Chemisorption and Physisorption at the Metal/Organic Interface: Bond Energies of Naphthalene and Azulene on Coinage Metal Surfaces", *J. Phys. Chem. C* **2020**, *124*, 8257–8268, DOI: 10.1021/acs.jpcc.0c00915.

[268] B. P. Klein, N. J. van der Heijden, S. R. Kachel, M. Franke, C. K. Krug, K. K. Greulich, L. Ruppenthal, P. Müller, P. Rosenow, S. Parhizkar, F. C. Bocquet, M. Schmid, W. Hieringer, R. J. Maurer, R. Tonner, C. Kumpf, I. Swart, J. M. Gottfried, "Molecular Topology and the Surface Chemical Bond: Alternant Versus Nonalternant Aromatic Systems as Functional Structural Elements", *Phys. Rev. X* **2019**, *9*, 011030, DOI: 10.1103/PhysRevX.9.011030.

[269] Z. Ruan, J. Schramm, J. B. Bauer, T. Naumann, H. F. Bettinger, R. Tonner-Zech, J. M. Gottfried, "Synthesis of Tridecacene by Multistep Single-Molecule Manipulation", *J. Am. Chem. Soc.* **2024**, *146*, 3700–3709, DOI: 10.1021/jacs.3c09392.

[270] H.-B.-R. Lee, S. F. Bent, in *At. Layer Depos. Nanostructured Mater.*, John Wiley & Sons, Ltd, **2011**, pp. 193–225.
[271] C. Vericat, M. E. Vela, G. Benitez, P. Carro, R. C. Salvarezza, "Self-assembled monolayers of thiols and dithiols on gold: new challenges for a well-known system", *Chem. Soc. Rev.* **2010**, *39*, 1805–1834, DOI: 10.1039/B907301A.
[272] L. Pecher, R. Tonner, "Precursor States of Organic Adsorbates on Semiconductor Surfaces are Chemisorbed and Immobile", *ChemPhysChem* **2017**, *18*, 34–38, DOI: 10.1002/cphc.201601129.
[273] S. Cooper, A. Robles-Navarro, O. R. Smits, P. Schwerdtfeger, "From Hard to Soft Dense Sphere Packings: The Cohesive Energy of Barlow Structures Using Exact Lattice Summations for a General Lennard-Jones Potential", *J. Phys. Chem. Lett.* **2024**, *15*, 8387–8392, DOI: 10.1021/acs.jpclett.4c01986.
[274] S. Monaghan, J. C. Greer, S. D. Elliott, "Atomic scale model interfaces between high-*k* hafnium silicates and silicon", *Phys. Rev. B* **2007**, *75*, 245304, DOI: 10.1103/PhysRevB.75.245304.
[275] P. P. Wellmann, F. Pieck, R. Tonner-Zech, "An Atomistic Picture of Buildup and Degradation Reactions in Area-Selective Atomic Layer Deposition with a Small Molecule Inhibitor", *Chem. Mater.* **2024**, *36*, 7343–7361, DOI: 10.1021/acs.chemmater.4c01269.
[276] R. Jones, G. D'Acunto, P. Shayesteh, I. Pinsard, F. Rochet, F. Bournel, J.-J. Gallet, A. Head, J. Schnadt, "Operando study of HfO_2 atomic layer deposition on partially hydroxylated Si(111)", *J. Vac. Sci. Technol. A* **2024**, *42*, 022404, DOI: 10.1116/6.0003349.
[277] M. Kim, B. Shong, "Dimerization equilibrium of group 13 precursors for vapor deposition of thin films", *Comput. Theor. Chem.* **2024**, 114953, DOI: 10.1016/j.comptc.2024.114953.
[278] S. Garvey, A. Serino, M. B. Maccioni, J. D. Holmes, M. Nolan, N. Draeger, E. Gurer, B. Long, "Towards Ge-based electronic devices: Increased longevity of alkanethiol-passivated Ge(100) in low humidity environments", *Thin Solid Films* **2022**, *759*, 139466, DOI: 10.1016/j.tsf.2022.139466.
[279] H.-B.-R. Lee, M. N. Mullings, X. Jiang, B. M. Clemens, S. F. Bent, "Nucleation-Controlled Growth of Nanoparticles by Atomic Layer Deposition", *Chem. Mater.* **2012**, *24*, 4051–4059, DOI: 10.1021/cm3014978.
[280] T. Iwao, T.-H. Yang, G. S. Hwang, P. L. G. Ventzek, "Microkinetic based growth and property modeling of plasma enhanced atomic layer deposition silicon nitride thin film", *J. Vac. Sci. Technol. A* **2023**, *41*, 032410, DOI: 10.1116/6.0002499.
[281] J. Liu, H. Lu, D. W. Zhang, M. Nolan, "Self-limiting nitrogen/hydrogen plasma radical chemistry in plasma-enhanced atomic layer deposition of cobalt", *Nanoscale* **2022**, *14*, 4712–4725, DOI: 10.1039/d1nr05568b.
[282] Y. Lee, S. Seo, T. Nam, H. Lee, H. Yoon, S. Sun, I.-K. Oh, S. Lee, B. Shong, J. H. Seo, J. H. Seok, H. Kim, "Growth mechanism and electrical properties of tungsten films deposited by plasma-enhanced atomic layer deposition with chloride and metal organic precursors", *Appl. Surf. Sci.* **2021**, *568*, 150939, DOI: 10.1016/j.apsusc.2021.150939.
[283] S. Lee, M. Kim, G. Mun, J. Ko, H.-I. Yeom, G.-H. Lee, B. Shong, S.-H. K. Park, "Effects of Al Precursors on the Characteristics of Indium–Aluminum Oxide Semiconductor Grown by Plasma-Enhanced Atomic Layer Deposition", *ACS Appl. Mater. Interfaces* **2021**, *13*, 40134–40144, DOI: 10.1021/acsami.1c11304.

[284] J.-H. Kim, T. N. V. Tran, J. Oh, S.-M. Bae, S. I. Lee, B. Shong, J.-H. Hwang, "Plasma-enhanced atomic layer deposition of hafnium silicate thin films using a single source precursor", *Ceram. Int.* **2020**, *46*, 10121–10129, DOI: 10.1016/j.ceramint.2020.01.002.
[285] G. N. Fomengia, M. Nolan, S. D. Elliott, "First principles mechanistic study of self-limiting oxidative adsorption of remote oxygen plasma during the atomic layer deposition of alumina", *Phys. Chem. Chem. Phys.* **2018**, *20*, 22783–22795, DOI: 10.1039/c8cp03495h.
[286] E. A. Filatova, D. Hausmann, S. D. Elliott, "Understanding the Mechanism of SiC Plasma-Enhanced Chemical Vapor Deposition (PECVD) and Developing Routes toward SiC Atomic Layer Deposition (ALD) with Density Functional Theory", *ACS Appl. Mater. Interfaces* **2018**, *10*, 15216–15225, DOI: 10.1021/acsami.8b00794.
[287] M. Shirazi, S. D. Elliott, "Atomistic kinetic Monte Carlo study of atomic layer deposition derived from density functional theory", *J. Comput. Chem.* **2014**, *35*, 244–259, DOI: 10.1002/jcc.23491.
[288] O. Adeleke, S. Karimzadeh, T.-C. Jen, *Machine Learning-Based Modelling in Atomic Layer Deposition Processes*, CRC Press, **2023**.
[289] B. Focassio, L. P. M. Freitas, G. R. Schleder, "Performance Assessment of Universal Machine Learning Interatomic Potentials: Challenges and Directions for Materials' Surfaces", *ACS Appl. Mater. Interfaces* **2024**, DOI: 10.1021/acsami.4c03815, DOI 10.1021/acsami.4c03815.
[290] C. Bannwarth, S. Ehlert, S. Grimme, "GFN2-xTB—An Accurate and Broadly Parametrized Self-Consistent Tight-Binding Quantum Chemical Method with Multipole Electrostatics and Density-Dependent Dispersion Contributions", *J. Chem. Theory Comput.* **2019**, *15*, 1652–1671, DOI: 10.1021/acs.jctc.8b01176.
[291] J.-N. Luy, R. Tonner, "Organic Functionalization at the Si(001) Dimer Vacancy Defect – Structure, Bonding and Reactivity", *J. Phys. Chem. C* **2021**, *125*, 5635–5646, DOI: 10.1021/acs.jpcc.1c00262.
[292] V. V. Santana, C. M. Rebello, L. P. Queiroz, A. M. Ribeiro, N. Shardt, I. B. R. Nogueira, "PUFFIN: A path-unifying feed-forward interfaced network for vapor pressure prediction", *Chem. Eng. Sci.* **2024**, *286*, 119623, DOI: 10.1016/j.ces.2023.119623.
[293] J. Wellendorff, K. T. Lundgaard, A. Mogelhoj, V. Petzold, D. D. Landis, J. K. Norskov, T. Bligaard, K. W. Jacobsen, "Density functionals for surface science: Exchange-correlation model development with Bayesian error estimation", *Phys. Rev. B* **2012**, *85*, 235149, DOI: Artn 235149 Doi 10.1103/Physrevb.85.235149.
[294] A. D. Becke, "Density-functional thermochemistry V Systematic optimization of exchange-correlation functionals", *J. Chem. Phys.* **1997**, *107*, 8554–8560, DOI: 10.1063/1.475007.
[295] C. Zhang, M. Vehkamäki, M. Pietikäinen, M. Leskelä, M. Ritala, "Area-Selective Molecular Layer Deposition of Polyimide on Cu through Cu-Catalyzed Formation of a Crystalline Interchain Polyimide", *Chem. Mater.* **2020**, DOI: 10.1021/acs.chemmater.0c00898, DOI 10.1021/acs.chemmater.0c00898.
[296] F. Grillo, J. Soethoudt, E. A. Marques, L. de Martín, K. Van Dongen, J. R. van Ommen, A. Delabie, "Area-Selective Deposition of Ruthenium by Area-Dependent Surface Diffusion", *Chem. Mater.* **2020**, *32*, 9560–9572, DOI: 10.1021/acs.chemmater.0c02588.
[297] L. Bonati, D. Polino, C. Pizzolitto, P. Biasi, R. Eckert, S. Reitmeier, R. Schlögl, M. Parrinello, "The role of dynamics in heterogeneous catalysis: Surface diffusivity and N_2 decomposition on Fe(111)", *Proc. Natl. Acad. Sci.* **2023**, *120*, e2313023120, DOI: 10.1073/pnas.2313023120.